AN ABSTRACT OF THE THESIS OF

Robert Lawrence Swanson (Name) for the Ph. D. (Degree)

in Oceanography (Major) presented on December 17, 1970 (Date)

Title: SOME ASPECTS OF CURRENTS IN LONG ISLAND SOUND

Abstract approved: Redacted for Privacy

Current observations were obtained at three locations forming a cross section along 70°34'W longitude in Long Island Sound. Fifteen days of data were selected from each series so that nearly simultaneous observations were used in the analysis.

Elementary statistics were computed for the data prior to performing a least squares tidal current analysis. Eight tidal current constituents were fitted in two cases and nine in the remaining instance. Constituent current ellipses were constructed along with the average ellipses.

Using the constituents previously computed, the tidal current was predicted for the period of observations. These values were subtracted from the observed current, generating a residual current series. Spectra were computed for each directional component along with cross spectra between the north and east components and also

between corresponding components at each of the three different locations. Coherence square and phase relationships also accompanied the latter.

An attempt was also made to correlate wind and the residual current by means of cross spectra. However, lack of sufficient wind data prevented a meaningful analysis.

The natural period of oscillation of Long Island Sound was estimated by Defant's method of seiche analysis for a bay. This value was used in the equations for a cooscillating system and a comparison was made between the computed and observed amplitudes of the tide. The mean percent error for numerous locations throughout the Sound was 7.1%. Comparison was also made between the maximum flows computed from the above equations and some observed values. The maximum percent error was 24% in an ebbing direction.

Some Aspects of Currents in Long Island Sound

by

Robert Lawrence Swanson

A THESIS

submitted to

Oregon State University

in partial fulfillment of
the requirements for the
degree of

Doctor of Philosophy

June 1971

APPROVED:

Redacted for Privacy

Professor of Oceanography
In Charge of Major

Redacted for Privacy

Chairman of Department of Oceanography

Redacted for Privacy

Dean of Graduate School

Date thesis is presented December 17, 1970

Typed by Marcia Griffin for Robert Lawrence Swanson

ACKNOWLEDGEMENT

The Environmental Science Services Administration, Coast and Geodetic Survey, sponsored my work at Oregon State University and I am extremely grateful for the wonderful opportunity which they gave me for continuing my education.

I would like to express my appreciation to Dr. June G. Pattullo for her inspiration and guidance throughout my educational program at Oregon State University.

I wish to extend my gratitude to Dr. Robert L. Smith for his continued assistance, and to Dr. Fred L. Ramsey for his efforts in furthering my limited knowledge of spectral techniques.

Also, I am indebted to the remainder of my committee which includes Dr. Donald Guthrie, Mr. John Seaders and Dr. R. E. Dimick. Thanks to Miss Frances Mayhugh who typed the several draft copies of this paper.

Lastly, a hearty thanks to my wife, Dana, for her consistent needling to complete my work on the project.

TABLE OF CONTENTS

LIST OF TABLES

LIST OF FIGURES

SOME ASPECTS OF CURRENTS IN LONG ISLAND SOUND

CHAPTER 1. INTRODUCTION

This study developed from a project, undertaken by the Coast and Geodetic Survey, to update and supplement the then existing tidal current information in Long Island and Block Island Sounds. The project represents a turning point in tidal current investigations as performed by the Coast and Geodetic Survey. Prior to 1965 most current investigations had been done on an intermittent basis. However, in the late 1950's, with the acquisition of the USC&GSS MARMER, areal surveys were commenced at least on a small scale. None, however, approached the magnitude of that proposed for those two extremely important bodies of water. Even though the budget was still extremely limited, purchase of some new equipment permitted collection of longer time series of current speed and direction at greater frequencies. Because of the self recording capability of this equipment, greater synoptic coverage was possible when coordinated with traditional manually recorded current meter systems. Simultaneously with the new and improved field techniques introduced throughout the project automated data handling and processing of current data were undertaken. Thus, a thoroughness and flexibility of circulatory investigation was initiated through this work in Long Island and Block Island Sounds. With each year since 1965, new and

vital additions have been made to the standard procedures, always keeping in mind the ever increasing desire for more and higher quality tidal current data needed for understanding and management of our nation's estuaries.

From 1965 through 1967, currents were measured at one hundred and fifty-six locations throughout Long Island Sound, Block Island Sound, the Peconic Bays, and the Housatonic, Connecticut, and Thames Rivers. The current meters were located at fifteen feet below the surface. Often additional meters were suspended at one-half and five-sixths the charted depths. Surface currents were measured at all locations, but subsurface currents were measured only at specially selected sites. The length of observation at the individual sites varied between one hundred hours, fifteen days, and thirty days.

For the most part, Roberts Radio Current Meters and Richardson-type Geodyne Current Meters, Model A-100, were used on the project. In addition, the TICUS System, specially designed for the Coast and Geodetic Survey by the Geodyne Division of EG&G International, was used in 1967. This tidal current survey system consisted of an internally recording magnetic tape current meter which also had the capability of telemetering the data to a console located ashore or aboard a ship.

All field operations were conducted by the officers and men

of the USC&GSS MARMER.

The semidiurnal current in Long Island Sound is the dominating horizontal motion. Anyone who has traversed The Race at maximum current is well aware of the high speeds and turbulent conditions occurring roughly every 6 1/4 hours. However, there are many lesser current phenomena that have not been previously described in this particular embayment. Modern science and technology have provided instruments and mathematical techniques for measuring, analyzing, and displaying more detailed current information.

Oceanographers are now in a position to take advantage of this recently acquired know-how to study currents more rigorously, provided sufficient and reliable data are obtained.

If a short series (fifteen or thirty days) of tidal or tidal current information is subjected to a traditional harmonic analysis, only a few of the periodic tidal motions can be distinguished in the data. These major tidal motions account for most of the variance of the data series. Many additional phenomena are undoubtedly disguised in the records. Seiche and inertial periods can be approximated by numerical methods and elementary theory. The periods of the minor tidal constituents such as overtides and compound tides are known. Spectral techniques can be used as a basis for assessing the importance of many of these frequencies. Using cross spectral techniques, inferences can be made regarding the relationship of

the current at different locations, and the relationship of the current and various driving mechanisms such as wind and barometric pressure.

The examination of several current records by the approach mentioned in the previous paragraph was undertaken as the objective of this disquisition. As is often the case, however, difficulty arises when attempting to accomplish specific goals using data from an undertaking designed for other purposes. More current data were available than could be evaluated by this investigator considering the time and financial framework provided. A slightly different distribution of current observations in time and space might have been more advantageous. Meteorological data that were accessible were not as complete as was desired and in the long run proved to be of limited value.

CHAPTER 2. LITERATURE SURVEY

Long Island Sound is generally defined as being that body of water bounded by the northern coast of Long Island on the south and the New York and Connecticut shoreline on the north. The eastern end of the Sound can be visualized as a line connecting Watch Hill Point in Rhode Island to Orient Point on Long Island. The western entrance is considered to be through the section connecting Throgs Neck with Willets Point.

Block Island Sound is adjacent to Long Island Sound on the east. The northern boundary is the Rhode Island coastline to Point Judith. On the east the limits are defined as being from Point Judith along the western edge of Block Island. The southern limit is the Long Island shoreline including the Peconic Bays to Montauk Point thence to the southwest point of Block Island (LeLacheur and Sammons, 1932).

Long Island Sound is undoubtedly one of the most extensively used bodies of water in the United States. It has played an important role as a navigable waterway for several centuries. As a consequence, it is only natural that industry has developed throughout the years in certain areas along its shoreline. The fishing industry has also exploited the resources provided in this waterway. The Sound has served as a playground for millions. On a summer weekend it

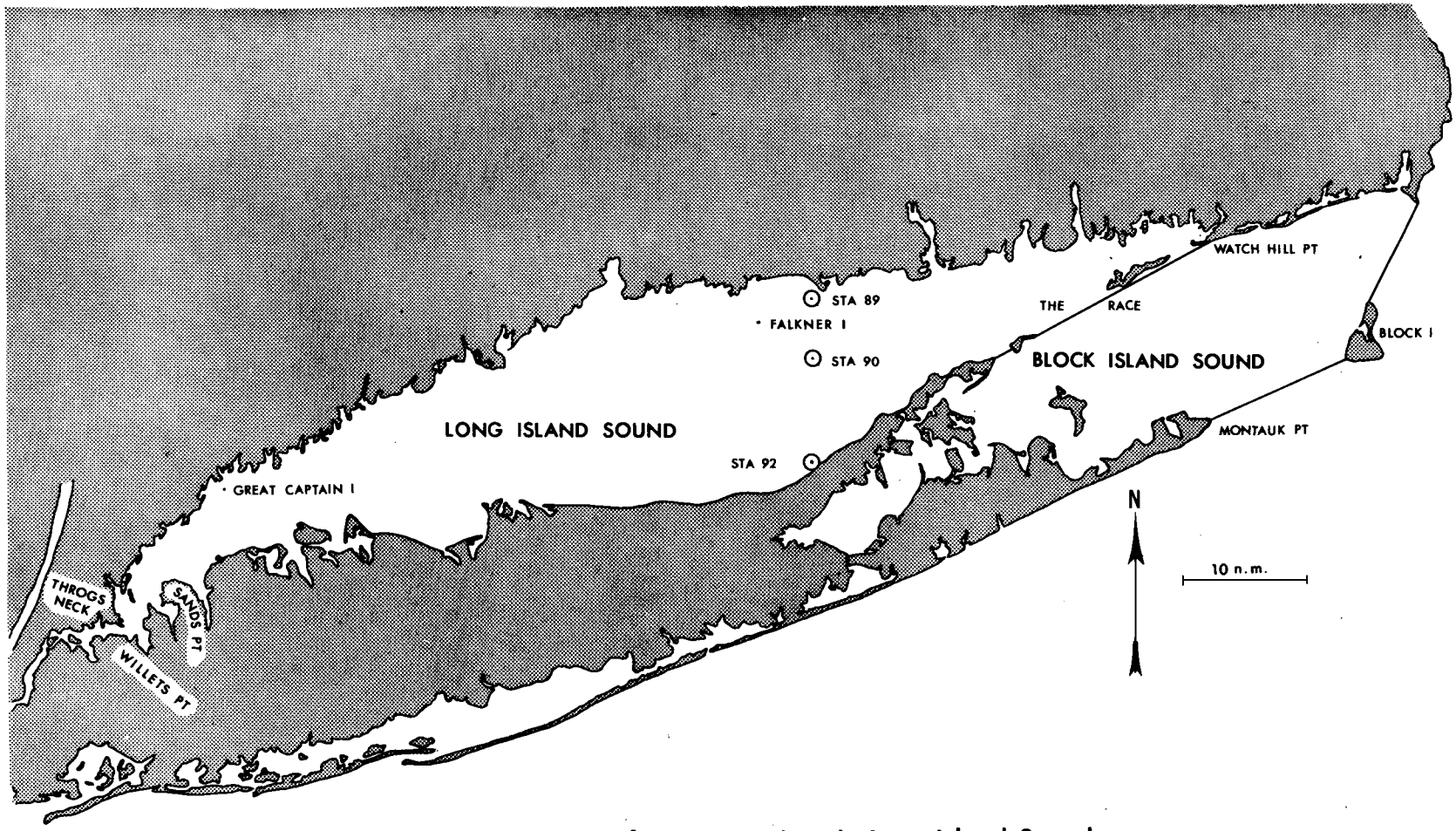

Figure 1. Location of current stations in Long Island Sound.

is difficult to travel in the Sound because of the thousands of power-boating, sailing, and fishing enthusiasts. Unfortunately, this same body of water serves as a sewer for these same people and for millions more.

It is interesting to note that as much as people use Long Island Sound there is little oceanographic data available, even though some of the earliest studies of estuarine environments probably were done in this area. Tidal observations are on record for Fort Schuyler, New York, at the western end of the Sound as early as August 1837. At the eastern end of Long Island Sound, tidal observations were made in the vicinity of New London Harbor Light in 1839 (LeLacheur and Sammons, 1932).

Current observations were taken as early as 1845 near Race Rock Light by G. S. Blake of the Coast and Geodetic Survey. He used a "current pole" a description of which has apparently been lost with time. From his tabulation of the data the depth of observation is recorded as nine feet, which would imply that the pole was eighteen feet in length (the procedure is to take half the pole length as the depth of observation). His observations were carried out over a period of a day and a half. The first extensive investigation of currents was undertaken a year later in 1846 and 1847. J. R. Goldsborough, also of the Coast and Geodetic Survey, used a surface float for short series of observations throughout the Sound. He

collected data at some twenty-four locations, a considerable undertaking for the times.

Since these early observations, numerous tidal and current data have been collected over the years by a variety of techniques. Tidal heights have been observed using staffs and continuously recording gages. Currents have been measured by pole, float, Price meters, and even the tilt of navigational buoys.

The results have led to the calculation of tidal and tidal current parameters used for prediction in the Tide Tables, Tidal Current Tables, and Tidal Current Charts. Results have also been tabulated and summarized in the Coast and Geodetic Survey publication by LeLacheur and Sammons (1932).

Other physical oceanographic data such as temperature and salinity are considerably more sparse. Most of this information comes from cruises of the Woods Hole Oceanographic Institution from January 1946 to January 1947. Using their data, Riley has perhaps contributed more to our understanding of the physical oceanography of Long Island Sound than any other individual, see for example Riley (1952).

R. G. Williams has written a review of the literature concerning Block Island Sound, which is adjacent to Long Island Sound on the east. Much of the information, however, also refers to Long Island Sound, and certainly his bibliography is the most comprehensive

at this time (Williams, 1967).

Long Island Sound is a semi-enclosed body of water with the tides and tidal currents characterized by a strong semi-diurnal period. The tide moves up the Atlantic Ocean and into Block Island Sound as a progressive wave (Redfield, 1950). In the vicinity of The Race at the eastern entrance to Long Island Sound, the progressive wave appears to have its characteristics changed to that of a standing wave (Riley, 1952). The tidal wave is modified by the natural frequency of the basin in such a way that the Sound can be considered a cooscillating tidal basin (Defant, 1961). The embayment tends to oscillate at its natural frequency with the semi-diurnal tidal wave serving as a forcing function at the mouth of the system.

Such a system should be characterized by a minimum tidal range and maximum tidal current at its mouth, and a maximum tidal range with no horizontal current at the closed end (Defant, 1961). The time of high tide should occur simultaneously throughout. Long Island Sound tends to have these characteristics but like most natural phenomena it does not strictly follow the simplified theory. In the first place, Long Island Sound does not conform to the model. There is a small opening at the western end of the Sound (the East River) so that there is a horizontal exchange of water where the model has none. The range of tide near The Race is about 2.5 feet while at the

western end of the Sound, at Throgs Neck, the range is about 7.2 feet. Current speeds at The Race approach five knots and decrease toward the west. Since there is a small outlet at the western end, there is no location of no horizontal motion as required in the rectilinear model. The maximum current does appear to be a minimum in the proximity of Sands Point, according to the Tidal Current Chart (United States Coast and Geodetic Survey, 1958).

The times of high water do not occur simultaneously throughout the Sound but have a tendency to be later as one progresses to the west. Redfield (1950) attributes this phenomenon to damping within the channel.

CHAPTER 3. THE DATA AND ITS PREPARATION

Current Data

Four current stations were selected for analysis primarily because they formed a set of practically simultaneous data over a north-south cross section of Long Island Sound. Each station had a minimum length of observation of fifteen days. Surface data at fifteen feet was the only data collected.

All four stations were observed using the Model A-100 single-ended Geodyne Current Meter. The meter was suspended from a 120-inch boat-shaped Roberts radio current buoy. The buoy was anchored using a Danforth anchor with 1/4-inch stainless steel cable. A scope of 3:1 was used on the anchor cable. Charted depths were used for determining the scope.

The current stations were located approximately five miles apart across the Sound on longitude $70^{o}34'$W. Exact positions information can be obtained from Table I.

The current stations used in this paper were numbers 89, 90, 91, and 92 in the project and will be identified in this manner.

The photographic Geodyne meter records on 16 mm film, with only a relative time actually being recorded on the film. It is essential that absolute time be referenced to some distinctive mark that can be identified on the film. This was accomplished by having the

savonious rotor taped prior to installation and then spinning the rotor rapidly during the installation. On the film this instantaneous increase in speed of rotation of the rotor is clearly visible. The reverse procedure is done on removal of the meter from the water. In this case, the rotor is again spun rapidly and then taped. Thus, there is a time check before and after the series of observations.

Speeds in Long Island Sound were expected to be as great as five knots (kts.). Consequently, inclination of the meter with the vertical was expected. Tilt of the meter was indicated on the film by means of a light pulse in five degree intervals. This is done by means of a mercury switch attached to the camera drive motor (Geodyne, n. d.). The inclinometer system is far from foolproof and the mercury switch has a history of malfunction. With tilt of the meter, the plates between which the savonious rotor is mounted tend to create a turbulent condition in the vicinity of the rotor, which could adversely affect its speed of rotation.

In order to overcome the problem of excessive tilt, the Engineering Division of the Coast and Geodetic Survey designed a bridle for suspension of the meter. The bridle consists of a brass collar which is located near the center of drag of the meter. Rocker arms are attached to the collar and are free to rotate in a vertical plane. Brass chain is then attached to the arms which leads around both

ends of the meter attaching to a length of cable which then supports the remainder of the meter string. The meter then will remain in a vertical position in the direction of flow with currents less than four kts., provided the current is distributed evenly over the length of the meter. Transverse tilt, however, becomes a problem when speeds exceed or equal 1.7 kts. (Swanson and Kerley, 1970).

One obvious objection to the system is that the chain will create additional turbulence in the vicinity of the rotor and vane. This is undoubtedly true but in this particular survey surface currents only were measured. As a result, no extraneous hardware was near the rotor and vane.

Geodyne Corporation claims an accuracy of the savonious rotor of 0.05 kts. at speeds less than one kt. and not greater than 0.1 kts. when the speed exceeds one kt. With a tilt of the savonious rotor the error caused in the recorded data is 3% at 5^{o}, 6% at 10^{o}, 12% at 20^{o}, and 20% at 30^{o}.

Direction is determined by an internal magnetic compass, which is referenced to a vane follower that orients itself to the path of the current. Resolution of both the compass and the vane is 2.8^{o} (Geodyne, n. d.).

Data was collected at each station every ten minutes over a fifty second interval throughout the period of observations. Speed was determined by counting rotor revolutions while direction was

determined by averaging instantaneous values recorded every 2-1/2 seconds during the fifty second interval. The specifics regarding each station are in Table I.

Station 89 operated satisfactorily throughout the period of observations. Numerous problems were encountered at the three remaining sites. Autumn storms were frequent from Labor Day weekend through the remainder of September.

Station 90 was found several miles off position on September 16. Maximum velocities in the ebb and flood directions were plotted separately against time. The data appear to follow two continuous curves except at apparent breaks near 1800 September 14. Easterly and northeasterly winds as high as 33 kts. were recorded at Falkner Island on that date and the following day. Data were assumed to be acceptable until 1600 September 14.

Data from station 91 was totally unacceptable and was rejected. This points out the problem of using internally recording equipment which cannot be interrogated while it is operating. Apparently the timer did not function properly, as the film did not have the correct number of frames exposed for the time the meter was in the water. So many frames were missing that reconstruction was impossible. Station 91 will not be considered elsewhere in this report.

Table I. Pertinent Mooring Information

Station	89	90	91	92
Latitude	41°14.22'N	41°09.80'N	41°05.35'N	41°01.68'N
Longitude	72°34.00'W	72°34.17'W	72°34.10'W	72°34.22'W
Meter Depth Below Surface (feet)	15	15	15	15
Sounded Depth (feet)	41	94	71	51
Time Zone	60°W	60°W	60°W	60°W
Date of Installation	Sept. 2, 1966	Aug. 24, 1966	Sept. 7, 1966	Aug. 24, 1966
First Good Data Frame	1340	1410	1330	1240
Date Removed	Sept. 19, 1966	Sept. 26, 1966	Sept. 22, 1966	See text
Last Good Data Frame	1300	0820	1420	See text
Time Check	2 min slow	12 min 45 sec slow	8 min slow Data unuseable	8 min slow

Station 92 ran without incident for twenty-nine days. It was observed at the proper location on September 22 at 1300 and was due to be retrieved on the following day. On the evening of September 22 another autumn storm blew up and the buoy broke free of its anchorage. The buoy and meter were found the following day on the beach at Duck Pond Point, Long Island. Internally, the meter was not damaged. The timer was found to be eight minutes slow.

Using the three stations 89, 90, and 92 it was decided to continue the investigation proposed in the introduction of this paper. Fifteen days of observation were selected so that the best possible overlap in time could be made.

Consequently, the following time series were selected:

Station 89	1600 September 2	-	1600 September 17
Station 90	1600 August 30	-	1600 September 14
Station 92	1600 September 2	-	1600 September 17

It was assumed that time lost on each meter was a linear function. The maximum time lost over a fifteen-day interval was about eight minutes on station 90. The loss on the other two meters was considerably less over fifteen days. As a result, it was decided not to adjust the data for time but to consider all data points to be evenly spaced at ten-minute intervals.

The film from each current meter was spot-checked for accuracy of both speed and direction. The film was read as suggested in the Geodyne instruction manual. The original printout of the data

as processed by automated techniques at Geodyne was accepted if the speed was within 0.05 kts. and direction was within 10^{o} as determined from scanning the film. Considerable disagreement was found with the printout. The Geodyne printout often indicated speed values of 0.51 and 0.76 kts. These occurred in such a manner that large isolated jumps appeared in the data. These jumps were found not to exist on the original film record and were apparently a result of processing procedures.

Initial examination of the data indicated that there was an apparent distortion in the records at low velocities. This is to be expected because of the relative motion of the current meter and the water due to the surface buoy being free to float about its anchored position (Paquette, 1963).

Any buoy will oscillate around a point near the place where the anchor cable is attached to the buoy. This type of motion is known as yawing. The buoy will also tend to "swing" about the anchor. Additional movement of the buoy will be caused as the anchor cable is alternately relaxed and tightened as a result of nonuniform current and wind forces. In shallow depths (100 meters) using small surface vessels, all of these motions have been found to be insignificant in currents on the order of one kt. (Paquette, 1963).

Paquette has also investigated the effect of slack and elasticity in a mooring similar to the type used by the Coast and Geodetic

Survey. In his investigation a scope of 3:1 was used in 300 feet of water. It was found that shortly after slack water (in a reversing current) when the elastic extension had been relaxed, the buoy was free to move with the current and the relative current was near zero. Consequently, a slack period of abnormal duration appears in the data. The speed then increases rapidly as the slack in the anchor cable is taken up (Paquette, 1963). A sketch of the distortion of the tidal current curve due to the movement, the elasticity, and slack in the anchor cable is shown in Figure 2.

My data indicated distortions near slack water which were of a slightly different nature than that previously mentioned. This is probably caused by the fact that the buoy began to drift back toward the anchor before slack, causing an increase in the relative current. When slack actually occurred the buoy continued to drift, possibly because of strain on the cable, or wind causing a relative current which was highly variable, depending on the conditions. A speed of zero was rarely found in the data and a jump from flood to ebb and conversely was more noticeable by a change in direction.

An attempt was made to adjust the zero crossings. Each current record had on its speed curve some transitions through slack that appeared to follow an ideal sinusoidal curve. A straight line approximation for the speed through these apparently good zero crossings fits very well for about thirty minutes before and after slack.

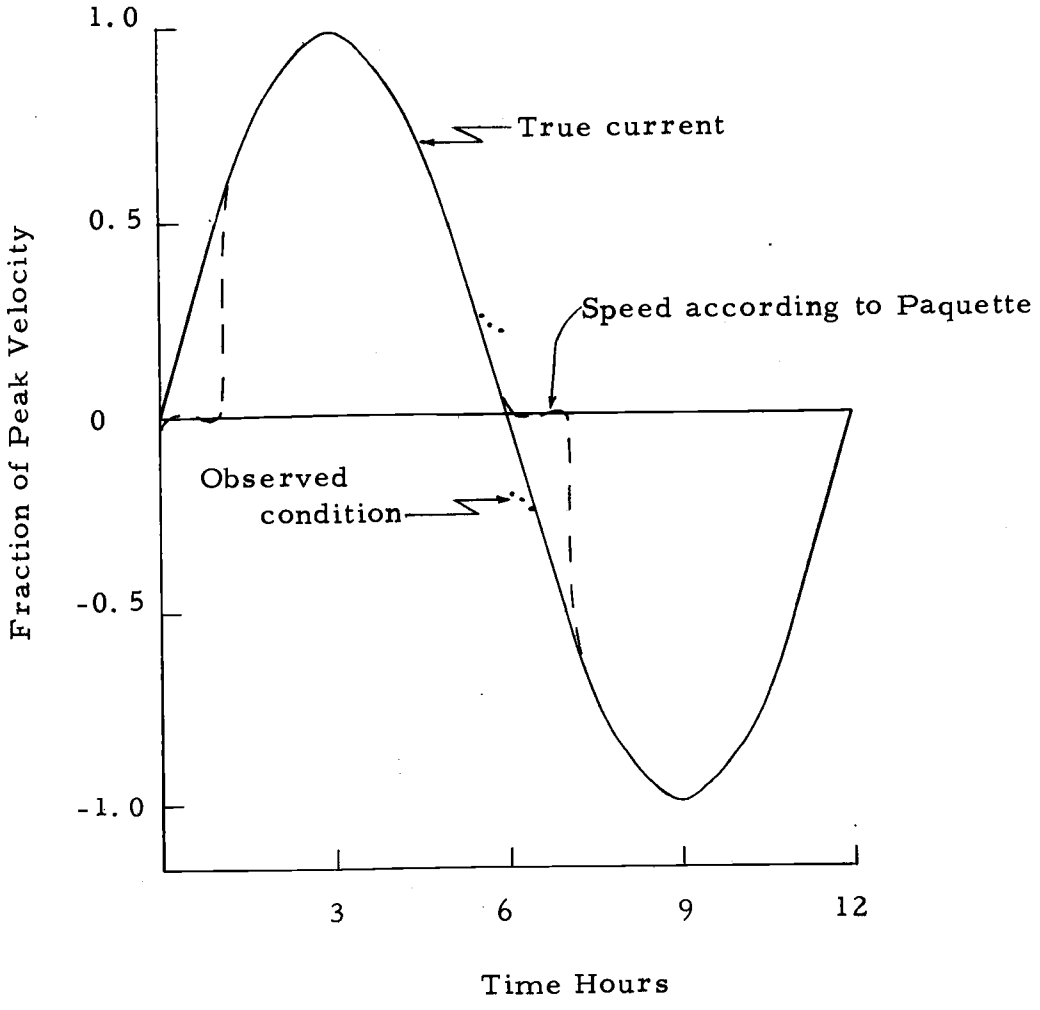

Figure 2. Distortion of a tidal current time series due to motion of the surface float.

The acceleration through these slack periods could be calculated simply by the formula:

$$\text{acceleration} = \frac{\Delta \text{ speed}}{\Delta \text{ time}} \quad .$$

The maximum speeds before and after the slack period were also recorded.

A plot of the data was made showing acceleration versus range in current speed, between maximum ebb and flood for the good zero crossings. A least square line was plotted through the data points. This then gave an estimate for the slope of the current curve (acceleration) passing through each slack water as a function of the maximum speed before and after the slack water in question.

Supposedly, the current meter should be recording nearly true current speed after the buoy has reached its maximum displacement from the anchored position. This position is a function of the scope of the anchor cable, the type of cable, and current velocity.

It is important to be able to approximate the time at which the meter will commence recording good data. If this can be estimated, then a limit can be made for rejecting supposedly inaccurate data near slack water.

It was assumed that the anchor cable was taut, forming a straight line rather than an approximate catenary. This is not a bad assumption for depths of 100 feet or less.

With knowledge of the depth and scope, the horizontal displacement of the buoy from the anchor could be computed. The acceleration of the current, and therefore the buoy (assuming the buoy drifts with the speed of the current) was known from above. Using the equation:

$$\text{horizontal displacement} = \text{initial speed} \times \text{time} + 1/2 \text{ acceleration} \times (\text{time})^2$$

the time for the buoy to move from directly over the anchor to its extended position could be calculated. The initial speed was assumed zero at slack water (this is when the buoy should be nearly over the anchor). At the depths in question, the drift of the buoy should have been completed well within the linear portion of the current curve (speed as a function of time).

The following information was known at this point:

1. The time at which the buoy reached its extended position as referenced to slack water, and
2. The velocity of the current at the time the buoy reached its extended position.

For the depths in which these current buoys were anchored, the time it took for the buoy to reach its extended position from the anchor (using the above assumptions) was in the vicinity of ten to twenty-five minutes after slack. If the true shape of the catenary of

the anchor cable had been known, the time would have been slightly less. The meter, however, sampled every ten minutes; therefore the assumption that the anchor cable was taut would cause an error no greater than one data point on each side of slack water.

The estimated slope can be visually fitted to the remaining portion of the speed curve. Data can then be picked off for the appropriate times during the very low speeds.

This procedure was time-consuming. It would have been much easier to sketch in a curve. However, one never knows how much data should be rejected or how much of the curve should be sketched. With this method a minimum of data was rejected throughout the record.

A numerical example is included in Appendix I.

Wind Data

Wind speed and direction (Appendix II) were obtained from the U. S. Coast Guard Lighthouse Station on Falkner Island. The wind data was collected approximately 99 feet above mean low water. The data was collected every three hours Greenwich mean time. To convert the observations to eastern daylight savings time (the time zone used for referencing current observations) four hours were subtracted from the time of each wind reading.

CHAPTER 4. BASIC CURRENT STATISTICS

Prior to any detailed analysis of the data, a number of calculations were performed in order to help obtain a better feeling for the numbers involved.

The distribution of the current observations was desired. In order to do this, the magnetic compass card was subdivided into five degree segments using 2-1/2, 7-1/2, --- 357-1/2 as the subdivisions. The number of current vectors in each segment was tabulated, as was the magnitude of each vector. From this the mean magnitude of the vectors within each interval was found, along with the relative frequency of the vectors lying in the same interval. Here relative frequency is defined as:

$$\text{relative frequency} = 100 \times \frac{\text{number of observations within interval}}{\text{total number of observations}} \qquad (4\text{-}1)$$

(Li, 1957).

There are some interesting aspects presented by the plots of relative frequency and average speed as shown in Figures 3, 4, and 5. The most obvious is that the interval of greatest directional frequency was also the direction interval of the maximum vector mean. Data from station 90 are more evenly distributed in both speed and

Figure 3. Average current speed and relative frequency of direction as a function of direction - station 89.

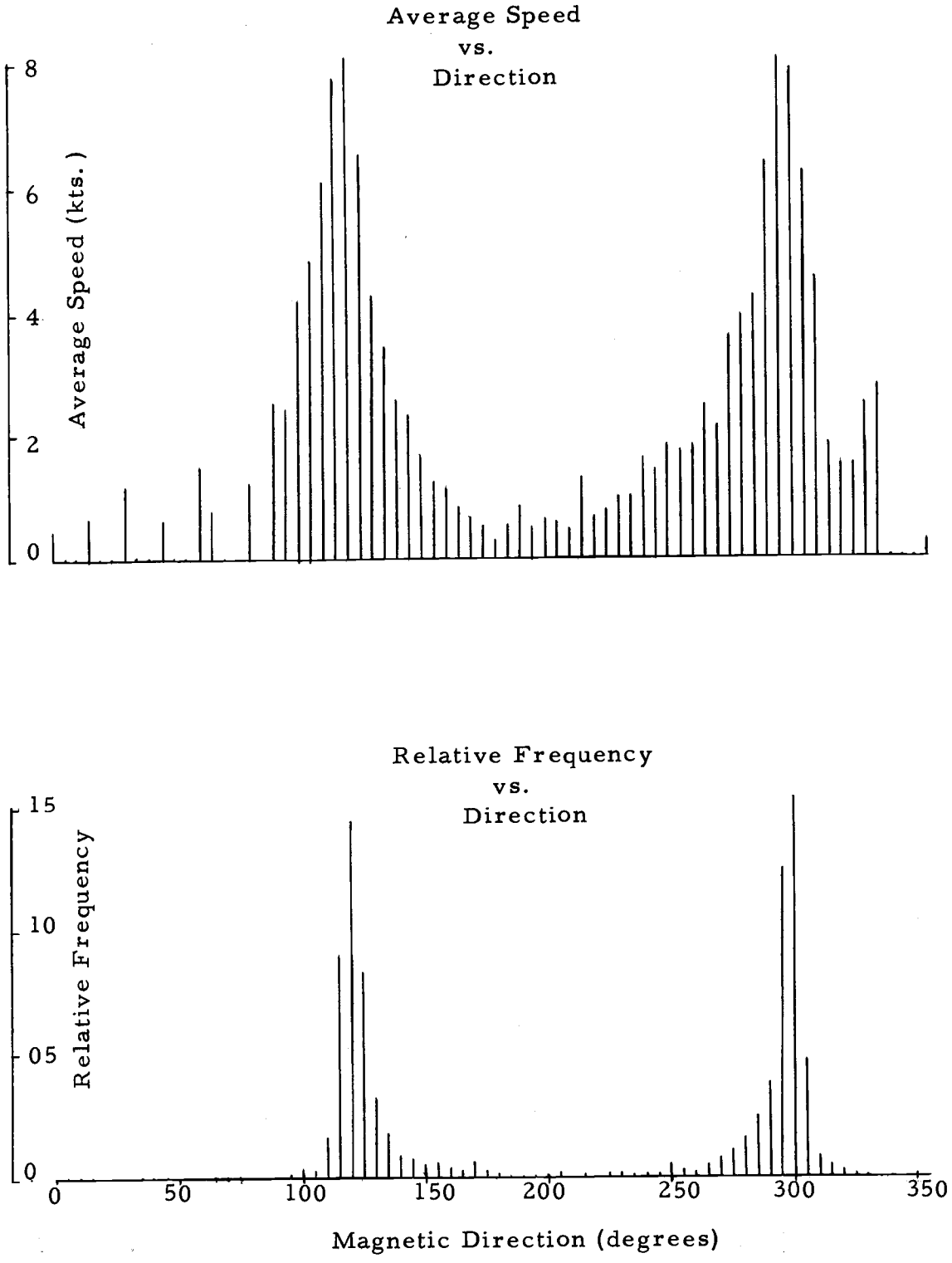

Figure 4. Average current speed and relative frequency of direction as a function of direction - station 90.

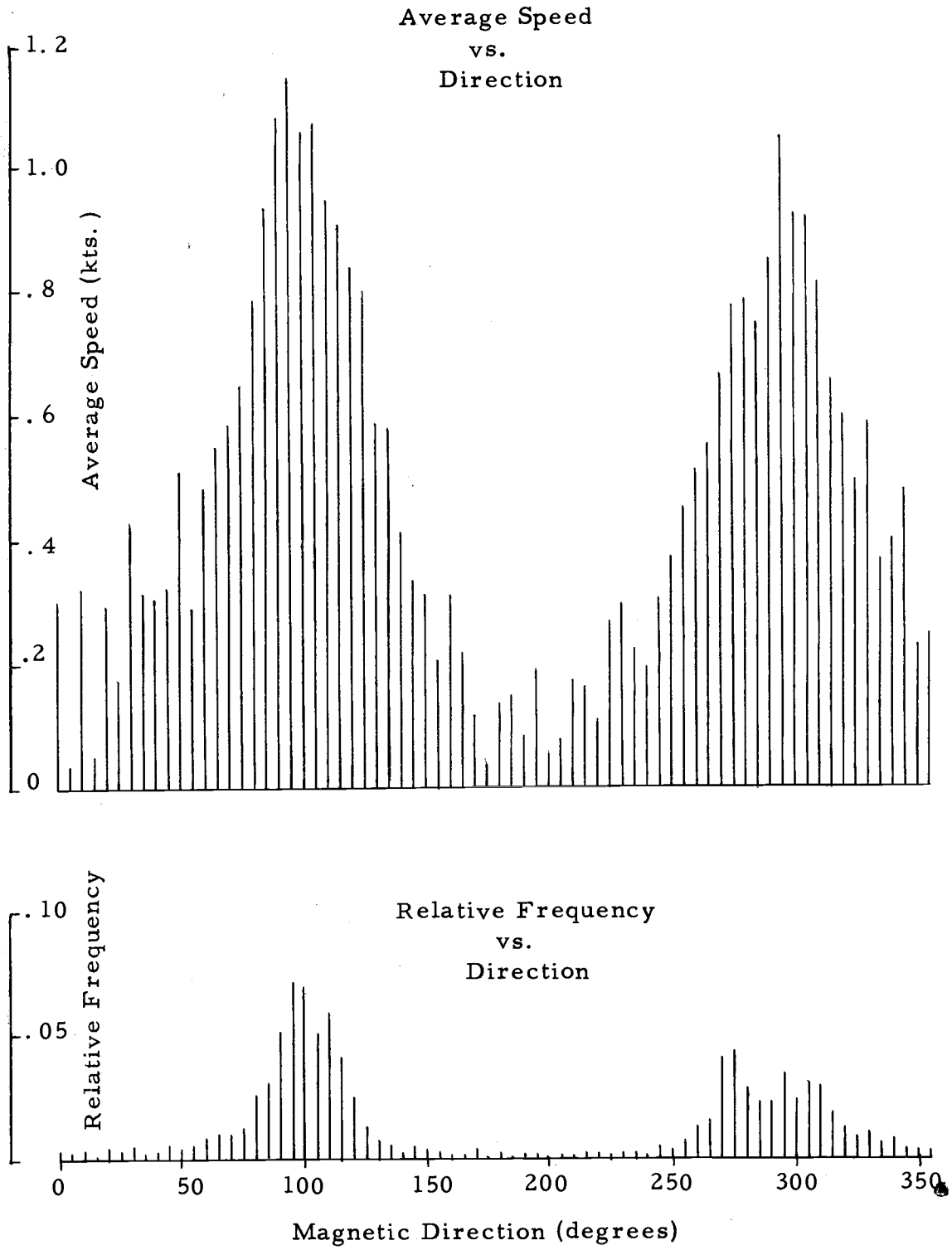

Figure 5. Average current speed and relative frequency of direction as a function of direction - station 92.

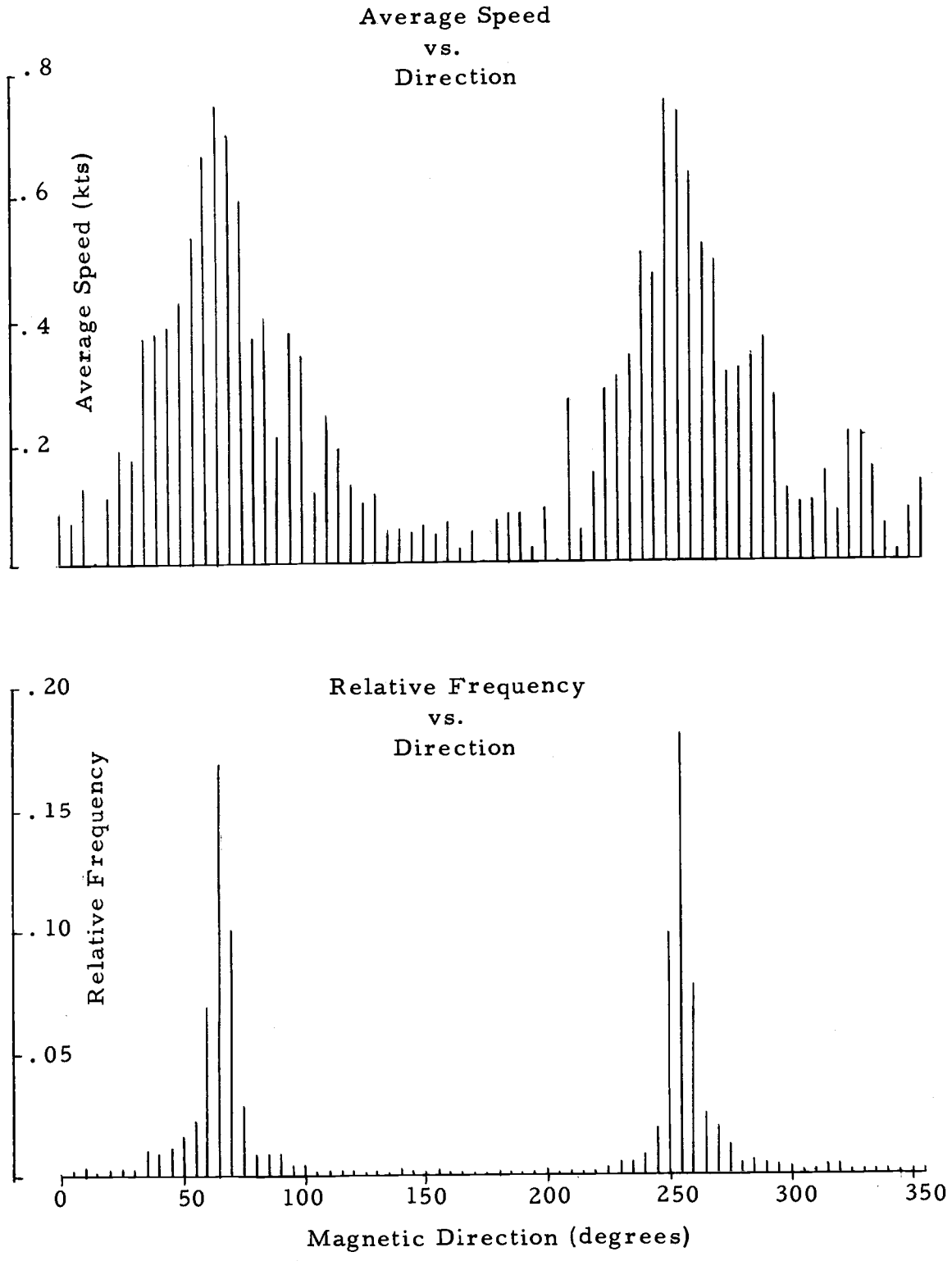

relative frequency of occurrence around the compass. An obvious inference is that this can be associated with the greater distance from the shore, where rotary currents are anticipated. Maximum speeds are greater near the center of the Sound at this cross section. The maximum average speeds occur in an ebbing direction around 095° magnetic and are on the order of 1.14 knots. The maximum average flood speed is 1.04 knots in a direction of 290° magnetic. Thus, the current must turn though 195°, if in a clockwise direction, from maximum ebb to a maximum flood.

Stations 89 and 92 are conspicuous because of the maximum average speeds and high relative frequency being centered around a very small range in direction. Both also have their two peaks for all practical purposes 180° apart. Station 89 is unique in that there are few observations occurring from 340° clockwise to 085° magnetic.

In order to appraise the nature of the data, the current vectors were divided into northerly and easterly magnetic components. The means and variances of each component of the three stations were then calculated. The sample mean is defined as

$$\bar{x} = \sum_{i=1}^{n} \frac{x_i}{n} \tag{4-2}$$

and the variance as

$$s^2 = \sum_{i=1}^{n} \frac{(x_i - \bar{x})^2}{n} = \sum_{i=1}^{n} \frac{x_i^2}{n} - \bar{x}^2 \tag{4-3}$$

The x_i's are the individual samples from the population and n is the total number of samples (Hogg and Craig, 1965). Table 2 contains these statistics.

Using the inequality

$$|\bar{x}| < 1.96\sqrt{\frac{s^2}{n}}$$

as a definition of small (Hogg and Craig, 1960) it is observed from Table II that the mean flows are significantly different from zero with the exception of the easterly components of stations 89 and 92.

In the center there was a flow out of the Sound at the surface to the east. Riley (1952) found a similar eastward flow in the same general location. Averaged over a tidal cycle his results show the net surface drift to be on the order of 3 cm/sec. This study, averaged over twenty-nine tidal cycles, indicated a net drift of nearly 10 cm/sec.

There was a slight tendency at the inshore stations to have a drift toward the center of the Sound at this particular cross section. These drifts were not found in Riley's investigation.

The variance indicates that most of the variability about the mean lies in the east-west direction or along the axis of Long Island Sound. This certainly is evidenced by examination of the relative frequency diagrams. The variance in the northerly direction is the greatest at station 89, which, from the average speed diagram, has

Table II. Mean and Variance of the Northerly and Easterly Components of Current Velocity

Station No.	Easterly Component			Northerly Component		
	Mean* (knots)	Variance $(\text{knots})^2$	$1.96\sqrt{\frac{s^2}{n}}$	Mean** (knots)	Variance $(\text{knots})^2$	$1.96\sqrt{\frac{s^2}{n}}$
89	-0.001	0.378	0.026	-0.027	0.115	0.014
90	0.190	0.641	0.034	0.028	0.093	0.013
92	-0.023	0.390	0.026	0.050	0.056	0.010

Sample size n = 2160

* + is East

** + is North

maximum velocities centered more toward north and south than 90 or 92.

The basic statistical data presented in this section certainly indicates that the predominating flow is characteristic of tidal currents.

CHAPTER 5. TIDAL CURRENT ANALYSIS

Fitting of Tidal Frequencies

Tidal currents are the predominating horizontal motions in Long Island Sound. Any description of the current regime in the Sound must therefore include that portion of the spectrum associated with the tidal frequencies.

A least squares program for tidal analysis of randomly-spaced data was used to fit a sinusoid of the form

$$Z_o + A_i \cos n_i t + B_i \sin n_i t \qquad (5\text{-}1)$$

to the north and east components of the current. In this equation Z_o represents the mean of the data series and shows in which direction the current predominates. The A's and B's are the coefficients of sines and cosines and the n's the speeds of the tidal current constituents of interest (Zetler et al. 1965). The normal equations were formed and solved by Gauss-Seidel iteration yielding the coefficients of the sines and cosines.

The amplitude and phase of each constituent at time t = 0, were then computed as indicated below.

$$\text{Amplitude} = (A_i^2 + B_i^2)^{1/2} \qquad (5\text{-}2)$$

$$\text{Phase} = \text{Tan}^{-1} \frac{Bi}{Ai} \qquad (5\text{-}3)$$

Over a short record the selection of tidal constituents is limited. The Coast and Geodetic Survey recommends analyzing harmonically for K_1, O_1, M_2 and S_2, M_4, M_6, M_8 with a series of less than twenty-nine days (Schureman, 1941). See Appendix III for definition of constituents. This basic series for tidal currents can be expanded if Rayleigh's test is used for determining the separation of frequencies in a least square analysis. Two constituents can be separated if

$$\left|\sigma_1 - \sigma_{1+1}\right| 2N > 1 \qquad (5\text{-}4)$$

where σ_1, σ_{1+1} are the frequencies in question and 2N+1 is the number of hourly observations in the series (Godin, 1967). For fifteen days of observations

$$2N+1 = 360. \qquad (5\text{-}5)$$

Godin's pair arrangements of frequencies to be tested are used for the most part.

Using Rayleigh's criteria, all the frequencies in Table 3 can be satisfactorily separated for the fifteen-day series of observations.

Eight constituents were originally selected for analysis. These were the ones listed in Table III, with the exception of the S_4 constituent. The percent variance remaining (see Results and Conclusions) for each of the three sets of data were compared (Table VI). The percent variance remaining in the northern component of station

Table III. Test for Frequency Selection

Name	Frequency cycles/hour	Pair Arrangement	$\lvert\sigma_1 - \sigma_{1+1}\rvert$	$\lvert\sigma_1 - \sigma_{1+1}\rvert 2N$
S_2	0.08333			
M_2	0.08051	S_2, M_2	0.00282	1.012
μ_2	0.07769	M_2, μ_2	0.00282	1.012
K_1	0.04178	μ_2, K_1	0.03591	12.892
O_1	0.03873	K_1, O_1	0.00305	1.095
M_4	0.16102	S_2, M_4	0.07769	27.891
S_4	0.16666	M_4, S_4	0.00564	2.025
M_6	0.24153	S_4, M_6	0.07847	4.630
M_8	0.32205	M_6, M_8	0.08052	4.751

90, using the eight constituents, was 31.6, almost three times that of station 92 which had the next greatest percent variance remaining. The spectra on the residual current series (see Chapter 6) of station 90 had a large peak at the quarter diurnal frequency, even though M_4 had been used in the analysis. In an attempt to reduce the remaining percent variance, S_4 was added to the original list of eight constituents for station 90. Use of the additional constituent reduced the percent variance remaining to 28.61. This reduced the spectral peak on the east component by nearly half, although it remained significant. The peak on the north component, however, was significantly reduced. No effort was made to include S_4 in the analysis of the two remaining stations.

The solutions for the constants of equation (5-1) are tabulated below. The constants A_1 and B_1 refer to the east-west components and A_2 and B_2 the north-south components.

Table V shows the amplitude and phase for each constituent for north and east components after having been computed from equations (5-2) and (5-3). The nontidal effect Z_o is also indicated.

The Constituent Tidal Current Ellipses

In confined bodies of water, tidal currents usually can be considered as reversing currents. That is, the currents flood primarily in a given direction and alternately ebb in the opposite direction.

Table IV. Computed Constants, Amplitudes and Phases for Each Constituent

Constituent / Station		M_2	S_2	K_1	O_1	μ_2	M_4	M_6	M_8	S_4
					EAST-WEST					
89	A_1 Kts	0.827	0.156	-0.008	0.017	-0.088	0.002	-0.025	-0.004	---
	B_1 Kts	0.017	-0.033	0.026	-0.014	0.128	-0.012	-0.060	0.006	---
90	A_1 Kts	0.650	0.197	-0.001	-0.008	0.181	0..026	0.019	-0.004	-0.016
	B_1 Kts	-0.850	0.045	0.047	-0.003	-0.001	0.045	-0.001	-0.014	0.018
92	A_1 Kts	0.782	0.127	-0.006	0.029	-0.019	0.012	-0.012	0.004	---
	B_1 Kts	0.345	0.044	0.043	-0.005	0.052	-0.005	-0.027	0.012	---
								+East		
					NORTH-SOUTH					
Station		M_2	S_2	K_1	O_1	μ_2	M_4	M_6	M_8	S_4
89	A_2 Kts	-0.451	-0.067	-0.001	-0.010	0.047	0.032	-0.001	0.008	---
	B_2 Kts	-0.049	0.014	-0.020	0.012	-0.061	0.010	0.038	-0.011	---
90	A_2 Kts	-0.311	-0.105	0.024	0.015	-0.013	0.050	-0.007	-0.011	0.019
	B_2 Kts	0.114	-0.019	-0.045	0.035	-0.010	-0.035	0.015	-0.042	0.019
92	A_2 Kts	0.294	0.054	0.001	0.006	-0.021	0.022	0.005	0.000	---
	B_2 Kts	0.091	0.022	0.013	-0.015	0.026	-0.004	-0.001 + North	-0.011	---

Table IV. Continued

Constituent / Station		NORTH-SOUTH COMPONENT									
		M_2	S_2	K_1	O_1	μ_2	M_4	M_6	M_8	S_4	Z_o
	AMP										+North
89	Kts	0.454	0.069	0.020	0.016	0.077	0.034	0.038	0.014	----	-0.028
	PH										
	Mag	186.1°	168.1°	266.1°	131.1°	307.6°	17.5°	91.3°	306.3°	----	
	AMP										
90	Kts	0.331	0.107	0.051	0.038	0.017	0.061	0.017	0.043	0.026	0.027
	PH										
	Mag	159.8°	190.5°	297.6°	66.3°	216.5°	325.5°	115.7°	255.4°	44.7°	
	AMP										
92	Kts	0.308	0.058	0.013	0.017	0.033	0.023	0.006	0.011	----	0.051
	PH										
	Mag	17.2°	21.9°	83.5°	292.8°	123.7°	350.6°	349.5°	268.9°	----	

Station		EAST-WEST COMPONENT									
		M_2	S_2	K_1	O_1	μ_2	M_4	M_6	M_8	S_4	Z_o
	AMP										+East
89	Kts	0.827	0.160	0.027	0.022	0.156	0.013	0.065	.007	----	-0.001
	PH										
	Mag	1.2°	347.9°	107.8°	320.3°	124.3°	278.7°	247.5°	123.9°	----	
	AMP										
90	Kts	1.070	0.202	0.047	0.009	0.181	0.051	0.019	0.015	0.024	0.191
	PH										
	Mag	307.4°	12.8°	91.6°	200.3°	359.7°	60.2°	357.6°	255.6°	132.7°	
	AMP										
92	Kts	0.855	0.134	0.043	0.030	0.055	0.013	0.030	0.013	----	-0.023
	PH										
	Mag	23.8°	19.0°	98.6°	350.2°	110.2°	336.7°	245.0°	73.4°	----	

Due to the earth's rotation, tidal currents in unconfined bodies of water tend to be rotary. Both speed and direction vary with the locus of the velocity vectors usually describing an ellipse (United States Coast and Geodetic Survey, 1950).

Long Island Sound, in the central portion, is far from being restricted, and it should be expected that rotary currents do exist. It is possible to construct the constituent tidal ellipses by letting

$$u = A_1 \cos nt + B_1 \sin nt \qquad (5\text{-}6)$$
$$v = A_2 \cos nt + B_2 \sin nt$$

represent the east and north components of the motion respectively. The notation is identical to that previously given.

Squaring and summing the two above equations yields the square of the velocity at any moment

$$\begin{aligned} W^2 &= (A_1 \cos nt + B_1 \sin nt)^2 + (A_2 \cos nt + B_2 \sin nt)^2 \\ &= (A_1^2 + A_2^2)\cos^2 nt + (B_1^2 + B_2^2)\sin^2 nt \\ &\quad + (A_1 B_1 + A_2 B_2)\cos nt \sin nt. \end{aligned} \qquad (5\text{-}7)$$

Manipulating the above expression using trigonometric identities eventually leads to expressions for W_1 and W_2, the maximum and minimum speeds of the tidal ellipse. These expressions are derived by Doodson (1966) who relates them to angles θ_1 and θ_2. These angles, measured clockwise from the east, give the orientation of

Table V. Parameters for Tidal Ellipses

	Constituent / Parameter	M_2	S_2	K_1	O_1	μ_2	M_4	M_6	M_8	S_4
STATION 89	W_1 Kts	0.94	0.17	0.03	0.03	0.17	0.03	0.07	0.02	---
	θ_1 Deg	331.3°	156.7°	323.8°	144.8°	333.6°	93.8°	150.8°	296.9°	---
	W_2 Kts	0.03	0.00	0.01	0.00	0.00	0.01	0.01	0.00	---
	θ_2 Deg	241.3°	66.8°	413.8°	234.8°	243.6°	183.8°	60.8°	206.9°	---
	Phase Deg	2.32°	167.9°	100.2°	137.3°	125.0°	18.9°	73.3°	125.8°	---
	Rotation	CW	CW	CCW	CCW	CW	CCW	CW	CW	---
STATION 90	W_1 Kts	1.11	0.23	0.07	0.04	0.18	0.06	0.02	0.05	0.03
	θ_1 Deg	165.0°	332.1°	312.5°	99.3°	175.8°	283.0°	143.6°	251.0°	80.2°
	W_2 Kts	0.17	0.00	0.02	0.01	0.01	0.05	0.01	0.00	0.02
	θ_2 Deg	75.0°	422.1°	222.5°	9.3°	85.8°	193.0°	233.6°	161.0°	350.2°
	Phase Deg	129.8°	12.3°	105.6°	64.8°	180.0°	134.7°	154.2°	75.4°	53.6°
	Rotation	CW	CCW	CW	CW	CW	CW	CCW	CW	CW

Table V. Continued

Constituent / Parameter		M_2	S_2	K_1	O_1	μ_2	M_4	M_6	M_8	S_4
STATION 92	W_1 Kts	0.91	0.15	0.04	0.03	0.06	0.03	0.03	0.02	---
	θ_1 Deg	19.7°	23.5°	16.2°	200.8°	30.3°	239.8°	177.2°	319.0°	---
	W_2 Kts	0.03	0.00	0.00	0.01	0.01	0.00	0.01	0.00	---
	θ_2 Deg	289.7°	113.5°	286.2°	110.8°	120.3°	329.8°	267.2°	219.0°	---
	Phase Deg	23.0°	19.5°	97.4°	161.0°	115.0°	167.0°	64.5°	80.1°	---
	Rotation	CW	CCW	CW	CW	CCW	CCW	CCW	CW	---

the maximum and minimum axes of the tidal ellipse. The direction of the rotation is clockwise if

$$\theta_2 - \theta_1 = -90^o$$

and counterclockwise, if

$$\theta_2 - \theta_1 = 90^o.$$

(Doodson, 1966)

Figures 6 through 10 show the magnitudes and orientation of the various constituent tidal ellipses. The phases of station 90 as listed in Table V are not comparable to those of stations 89 and 92 since the beginning of the series of station 90 commenced three days before the other two series. The tidal ellipses shown for station 90 indicate the position of the tidal current vector at 1600 September 2, 1966, for comparison purposes.

The Average Tidal Current Ellipses

In addition to the constituent tidal current ellipses, the average tidal current ellipses have been estimated by averaging of semidiurnal constituent hours over the period of observations. These are shown in Figure 11. The times indicated on the ellipse are referenced to maximum ebbs at each station. Station 90 has its maximum ebb 20 minutes before maximum ebb at The Race (which is the reference

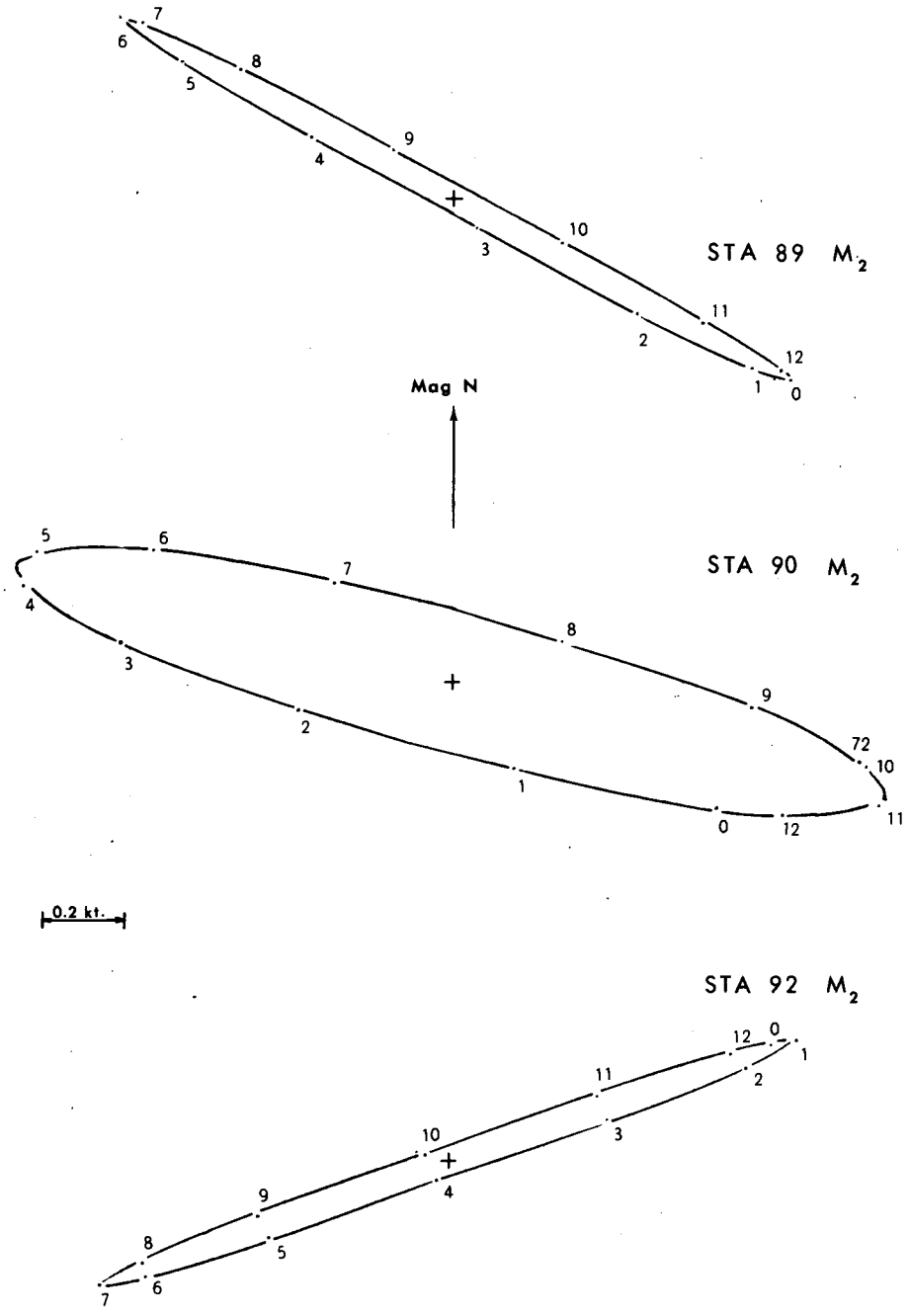

Figure 6. Constituent tidal current ellipses, (M_2).

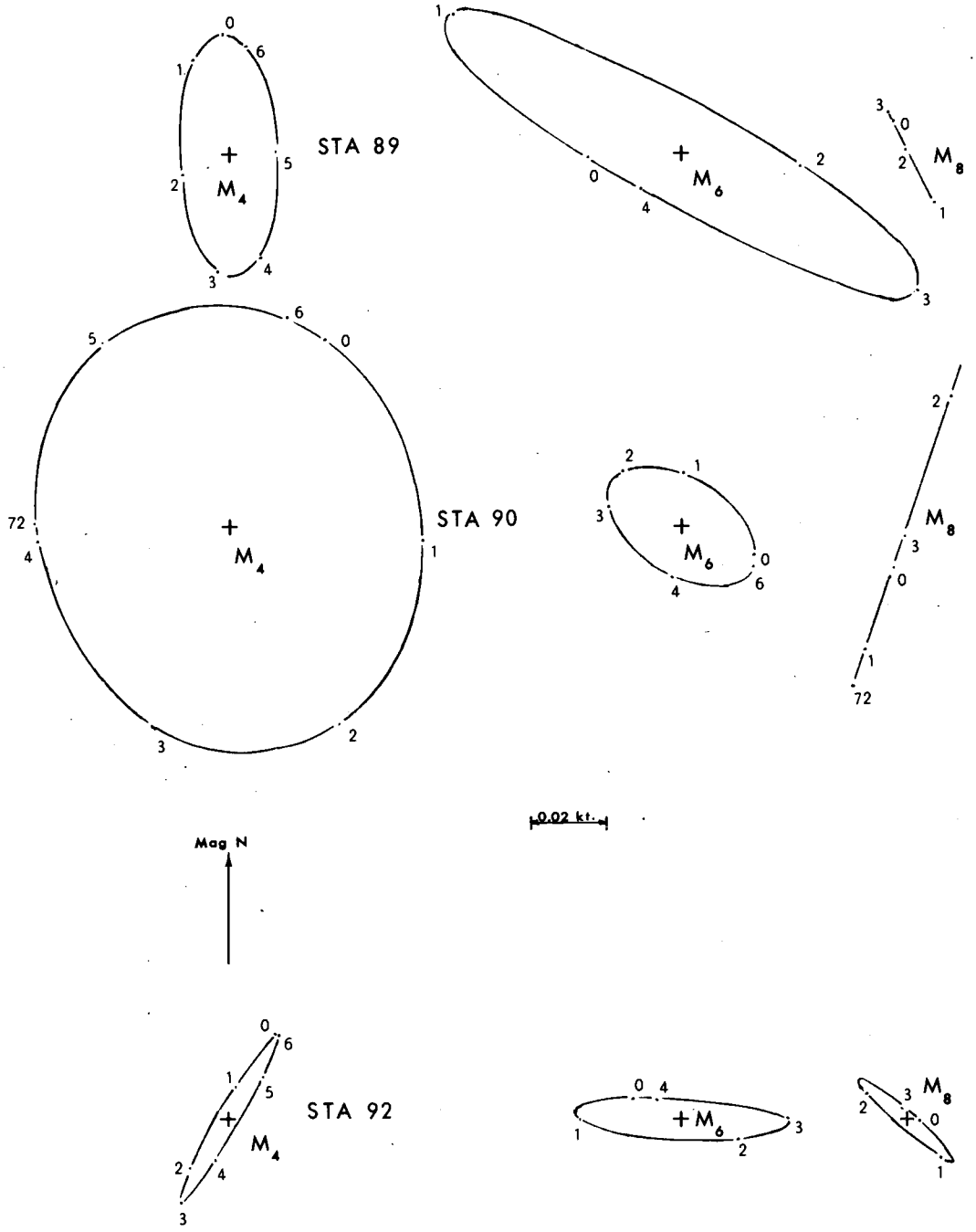

Figure 7. Constituent tidal current ellipses, (M_4, M_6, M_8).

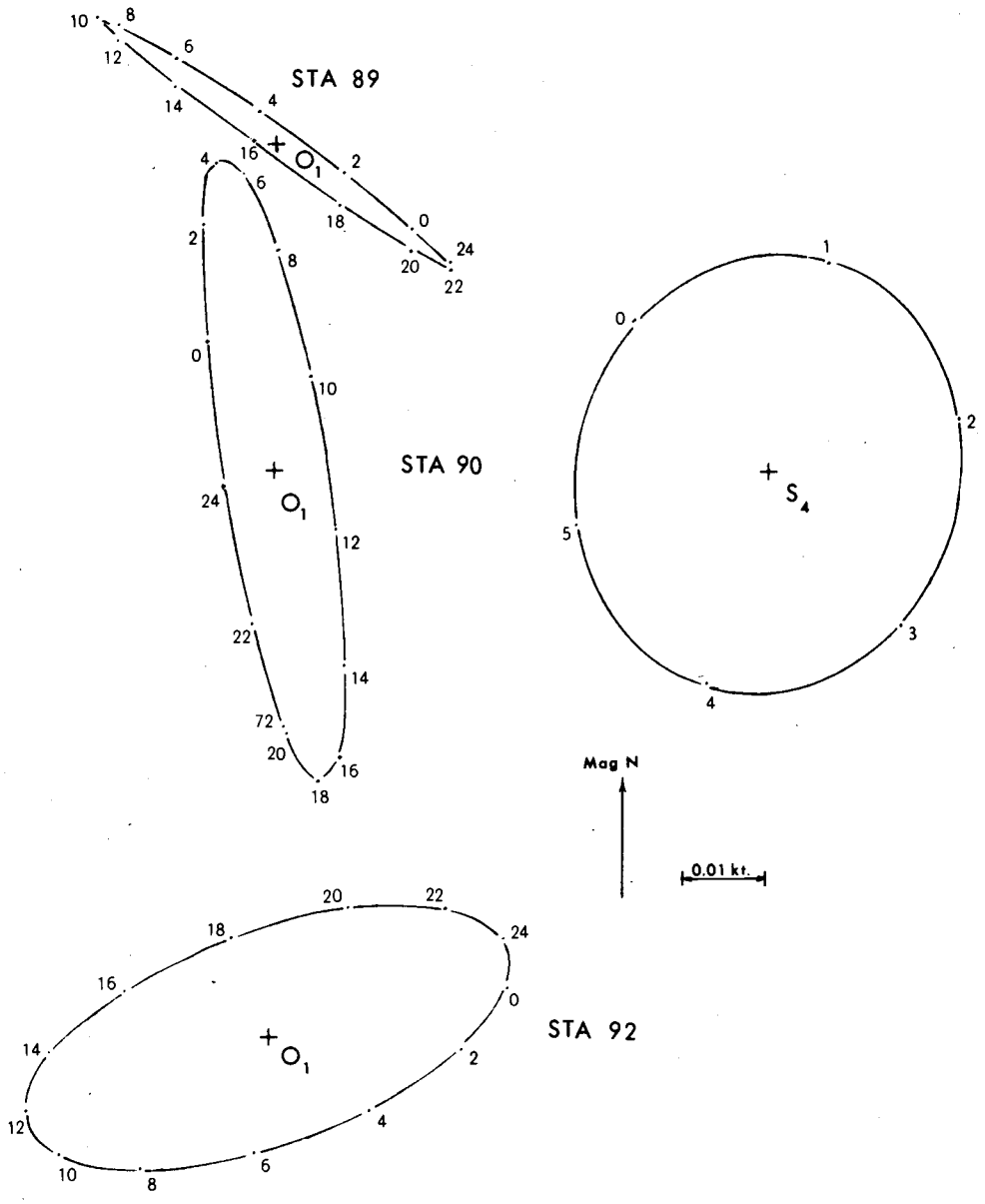

Figure 8. Constituent tidal current ellipses, (O_1, S_4).

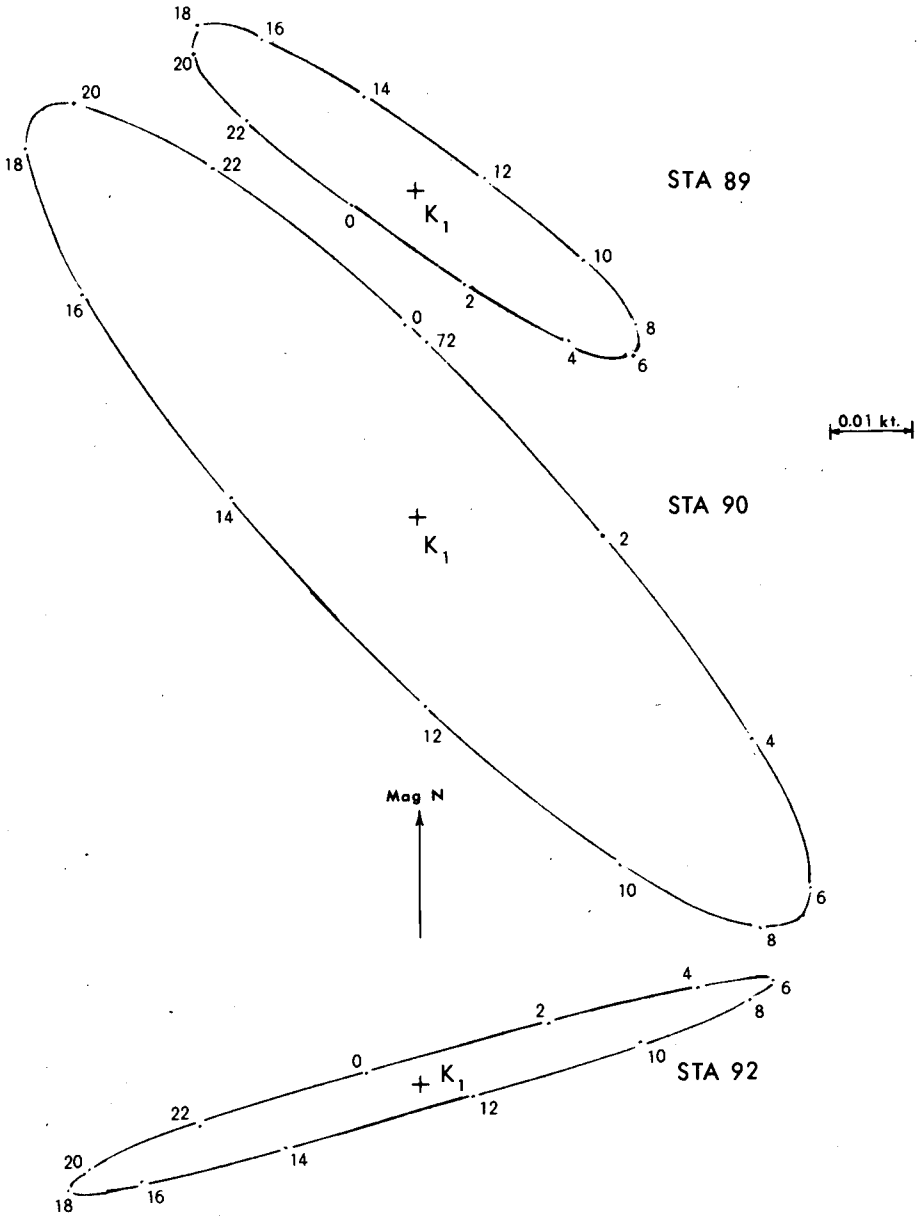

Figure 9. Constituent tidal current ellipses, (K_1).

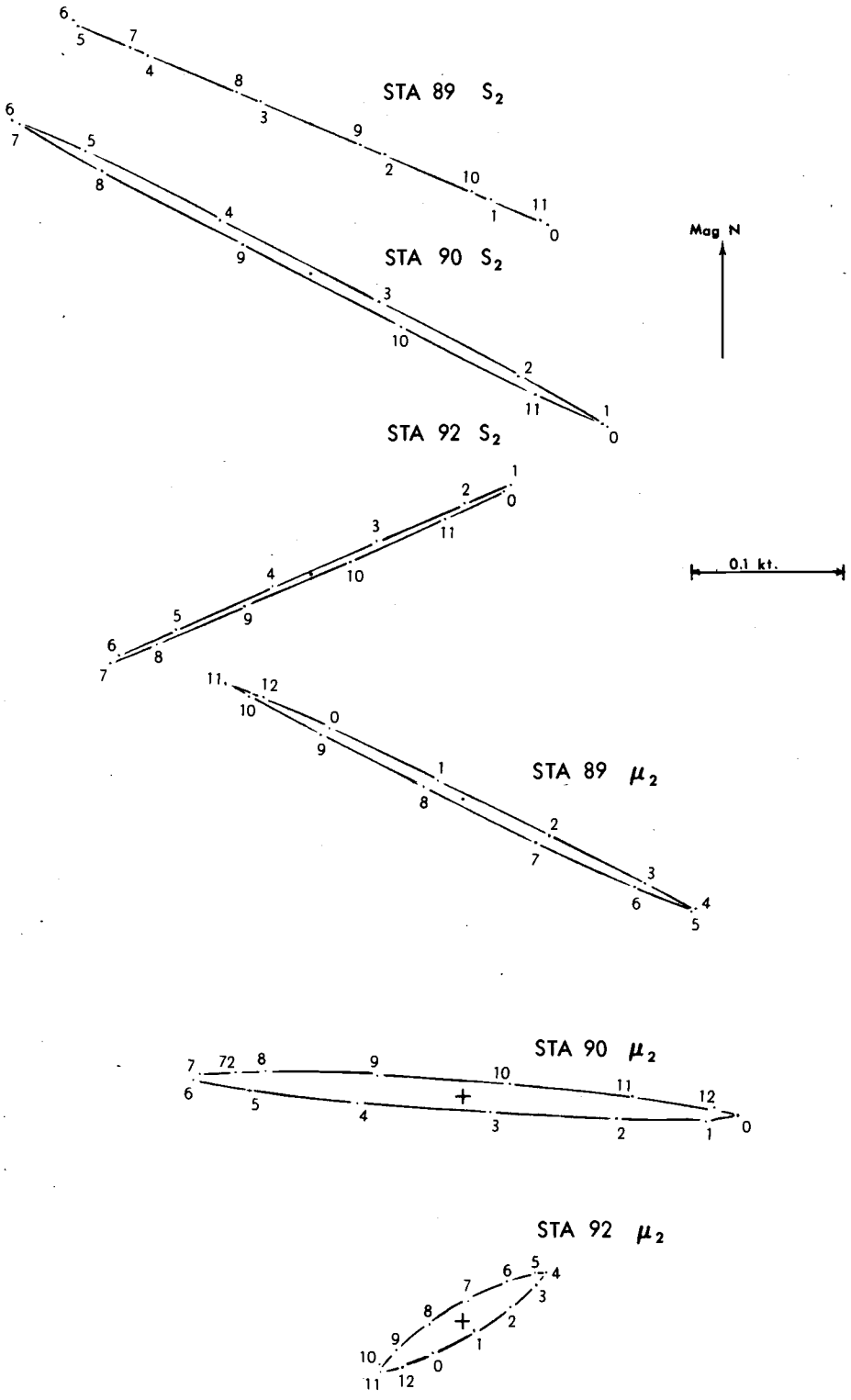

Figure 10. Constituent tidal current ellipses, (S_2,μ_2).

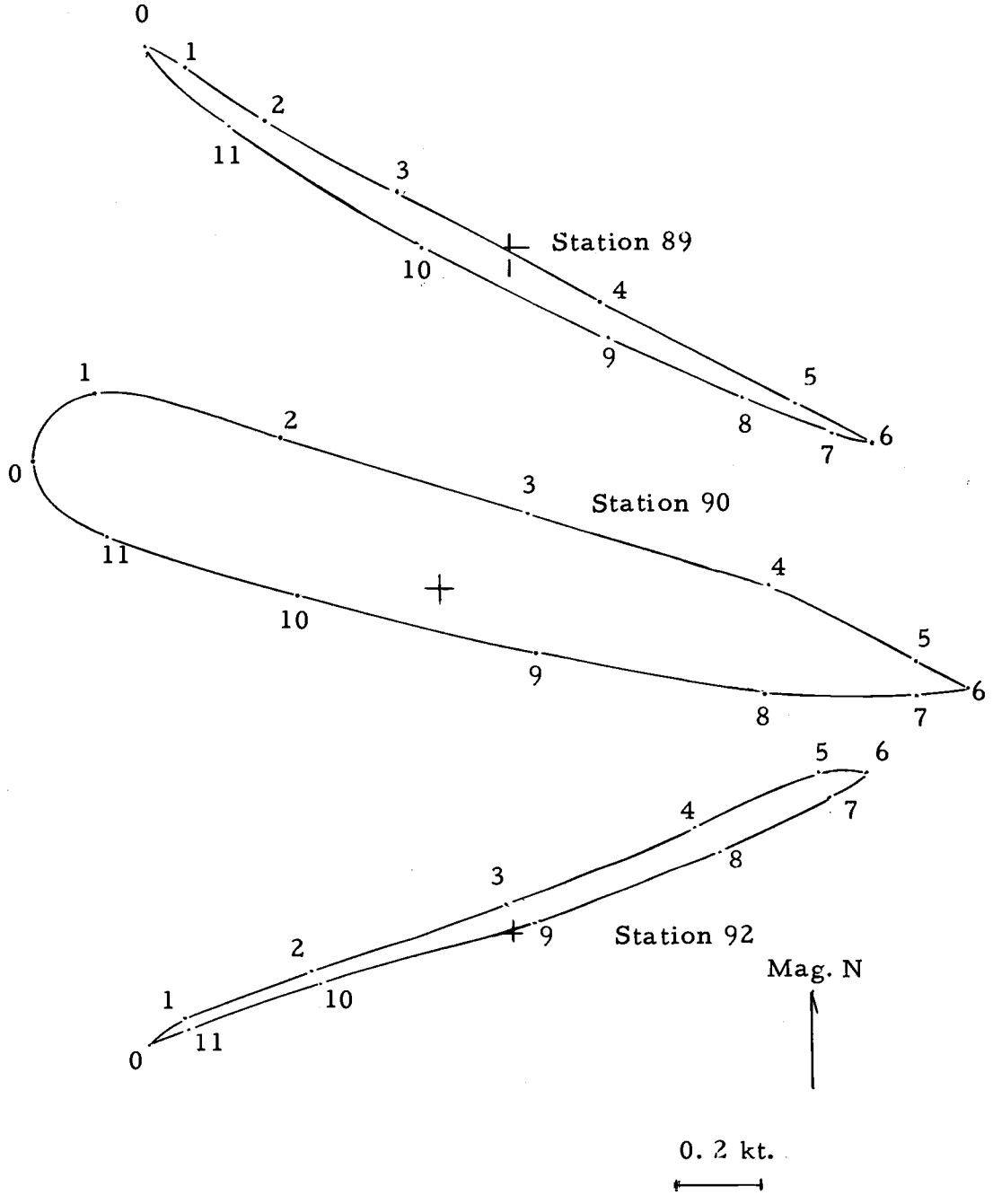

Figure 11. The average tidal current ellipses - stations 89, 90, and 92.

station used by the Coast and Geodetic Survey in its Tidal Current Tables). Maximum flood at 90 occurs 7 minutes before maximum flood at The Race. Maximum ebb at station 89, as determined from this study, occurs 101 minutes before that of The Race, while maximum ebb at 92 precedes The Race by 25 minutes. Maximum flood at 89 and 92 is respectively 78 before and 2 minutes after that at The Race.

Results and Conclusions

The most striking result of the tidal current analysis is the almost complete dominance of the current by the lunar semidiurnal constituent (M_2) at each location. In fact, the ratio of the lunar semidiurnal and solar semidiurnal, (M_2/S_2) the two largest major axes of the constituent tidal ellipses for stations 89, 90, and 92, are respectively 5.54, 4.82, and 6.06.

The form of the tidal current can generally be described by the ratio of K_1+O_1/M_2+S_2 where K_1 is the lunisolar constituent and O_1 is the main lunar diurnal constituent (both being associated with the moon's declination).

Station	$\frac{K_1+O_1}{M_2+S_2}$
89	0.054
90	0.082
92	0.066

If K_1+O_1/M_2+S_2 is between 0.0 and 0.25 the current can be considered as semidiurnal (Defant, 1958). All three cases are strongly semidiurnal. This conclusion was quite evident without the aid of the ratio, but it is interesting to note that even the criteria indicates the very strong semidiurnal characteristic.

The topographic influence on the orientation of the tidal ellipses is quite noticeable. The major axes of the average ellipses are plotted on a chart in Figure 30. The inshore ellipses in shallow water are parallel to the local shoreline.

The tidal ellipses near the coast may be practically thought of as straight lines indicating a reversing current. Station 90 on the other hand is rotary with the minor axis of the M_2 constituent being 15.3% of the major axis.

The times and speeds of maximum current, referenced to The Race, as depicted on the tidal current chart for Long Island Sound, agree with those found for the three stations analyzed in this study. However, the chart does not indicate the rotary nature of the current which is important in the center of the Sound. The chart would have a greater utility if the variation of current direction could be more accurately displayed.

After computation of the tidal current constituents, a predicted series was generated for each directional component of the three stations. In order to test the fit of the generated curves to that of

the original data, the difference between the observed and predicted data series was computed to form a residual series for each directional component. The mean, variance, and maximum error was found. In addition, the percent of variance remaining of the original data series was computed as indicated below.

Percent variance of original data series =

$$\frac{\text{Variance of residual data series}}{\text{Variance of original data series}} \times 100 \qquad (5\text{-}27)$$

A tabulation of these results is contained in Table VI.

The maximum differences between the observed and predicted values for the components of each station also are tabulated in Table VI. These maximum residuals can be attributed to physical processes, measurement errors or both. Are these values or outliers acceptable or should they be rejected? Quantification for the rejection of outliers can be made. The observation X_m should be rejected if

$$|Zm| \geq C\sigma \qquad (5\text{-}28)$$

where Zm represents the residual and σ is the standard deviation. The value of C depends upon the sample size, n, the number of degrees of freedom, ν and the probability that an outlier will not be rejected. Using a 1% probability and ν/n equal to one (n is large) the value of C is 3.37. The appropriate values of C σ are tabulated in Table VI (Anscombe, 1960).

Table VI. Statistics From the Residual Data Series

Sta No.	East Component						North Component					
	Mean (knots)	Vari.	Max Error (knots)	% Var.	Cσ	Wind (knots)	Mean (knots)	Vari.	Max. Error (knots)	% Var	Cσ	Wind (knots)
89	0.000	0.009	0.326	2.26	0.32	N0 E37	0.000	0.004	0.273	3.89	0.21	S19 E0
90	0.000	0.025	0.737	3.93	0.53	S2 W12	0.000	0.027	0.769	28.61	0.55	N8 E4
92	0.000	0.010	0.444	2.66	0.34	N2 W26	0.000	0.006	0.445	10.13	0.26	N26 W20

In each case the maximum residual exceeds $C\sigma$. However, if the dates of maximum errors of stations 89 and 92 are examined it is evident that the times of occurrence are associated with periods of high wind speeds. The maximum error for each component of station 90 is not associated with high winds. The latter are probably due to erroneous directional observations, resulting in poor directional components.

Since the maximum residuals lie just inside the rejection limits for outliers and since the sample size is large, there is little point in throwing the data out. Actually in the case of stations 89 and 92 the maximum residuals could indeed be real.

The percent of the variance remaining from the original data series in the residual indicates some interesting results. For the most part there is very little of the variance remaining. The percent of variance in the northerly component is greater than each of the corresponding percent variances for the easterly components. This is probably because the predicted values for maximum currents are better estimates than for any other portion of the tidal ellipse. The rotation around the compass slows down perceptibly near the major axes. Near the minor axes where the direction is changing rapidly, deviations of the predicted from the observed are quite obvious. A small nontidal current vector superimposed on the maximum tidal current will vectorially add to a resultant that is little different than

the predicted current, whereas the same vector superimposed at a minimum tidal current will cause the resultant current vector to be considerably different from the predicted value. Since the tidal ellipses are situated with the major axes oriented more generally east-west the predicted values have a better fit to the east-west components of the observed data.

Again, the northerly component of station 90 stands out with a percent variance remaining of almost 29%. The first suggestion is that, since station 90 is more characteristic of a rotary current (as opposed to a reversing current) deviations from predicted values are more likely to occur. Prediction for a rotary current must be for two dimensions rather than one dimension which would be more typical of a reversing current near the shore. Secondly, the zero crossings were adjusted assuming that the current was reversing. It is not. Consequently, any north-south movement of the buoy might introduce errors into the adjusted data series used in the tidal analysis. This discussion is pursued in Chapter 6.

In many sections the residual data series is cyclic if plus and minus signs are used as the observations instead of the actual numerical values. This is not surprising since the data series was only fifteen days. It was not possible to separate all potential frequencies occurring in the data. The most conspicuous constituent not used in the tidal analysis was the lunar constituent, due to the monthly

variation of the moon's distance, denoted by the symbol N_2. This particular constituent has a period of 12.66°/solar hour. Rayleigh's criteria indicates that this constituent cannot be separated from the more important M_2 constituent. The period of the plus and minus signs was on the order of twelve hours. Thus, it might be suspected that N_2 is important in tidal currents of Long Island Sound.

By inference the Coast and Geodetic Survey has found that certain relationships generally hold between the amplitude of one constituent and that of another. Such a relationship exists for N_2.

$$\text{Amplitude } N_2 = 0.194 \times \text{Amplitude } M_2 \qquad (5\text{-}29)$$

(Schureman, 1941).

Using this relationship an approximate amplitude for the N_2 constituent can be obtained for each of the three current stations. For stations 89, 90, and 92 the easterly values are 0.160, 0.208, and 0.166 kts. while the northerly values are 0.088, 0.064, and 0.060 kts. If these estimates are anywhere near correct, the effect of N_2 is certainly important. Since N_2 was not used for prediction, a certain amount of the variance in the residual series should be the result of not accounting for this component in the prediction.

An estimate of this variance can be made by assuming that N_2 is a perfect sinusoid with amplitudes as given and a speed of 28.440°/solar hour. The speed at any time can then be found from

the formula

$$\text{speed} = H \cos at$$

where H is the amplitude. As this is only an approximate evaluation, a graph of cos at was constructed using hourly values of t and then values for velocity at ten minute intervals were scaled. Since the function was cyclic only 6 1/3 hours were scaled and the population variance was estimated by the sample variance

$$s^2 = \frac{\Sigma(y-\bar{y})^2}{n-1} = \frac{\Sigma y^2 - \frac{\Sigma y^2}{n}}{n-1} \qquad (5\text{-}30)$$

where y is a ten minute observation, $\bar{y}$ is the mean of the observations over the 6 1/3 hours and n is the number of samples (Li, 1957).

The values computed for Σy, Σy^2 and n were -0.087 kts., 19.9984 $(\text{kts.})^2$, and 39, giving a sample variance of 0.5265 $(\text{kts.})^2$. The variance of the components of N_2 at each station can simply be obtained by multiplying the variance of cos at by the square of the amplitude of the constituent's east and north components. As before, the percent variance can be calculated as a function of the variance of the raw data.

With the exception of the northerly components of stations 90 and 92, the estimated percent variances of N_2 are very close to the percent variance remaining in the corresponding residual. It appears that even the residuals are mostly tidal, but the two large

discrepancies mentioned above certainly deserve some further investigation.

Table VII. Variance Due to the N_2 Constituent

Station No.	Component	Percent of Total Variance in Record To Be Explained	Est. Variance Due to N_2 (kts.)^2	Percent of Total Variance Due to N_2
89	East	2.26	0.013	3.70
	North	3.39	0.004	3.48
90	East	3.93	0.023	3.59
	North	28.61	0.002	2.15
92	East	2.66	0.014	3.59
	North	10.13	0.002	3.57

CHAPTER 6. SPECTRAL ANALYSIS

Technique

To more thoroughly describe the dynamics of Long Island Sound spectral techniques were used in addition to the more traditional tidal current analysis. For the most part the examination of spectra was limited to the power spectrum, cross spectrum, and coherence.

All processes examined by spectral techniques were assumed to be stationary which is to say that the statistical properties such as the mean and the variance would remain unchanged if there was a shift in the time origin of the ensemble of time dependent functions (Blackman and Tukey, 1959).

The above assumption leads to the fact that all stationary processes can be represented by

$$X_t = \int_{-\pi}^{\pi} e^{it\omega}\, dz(\omega) \qquad (6\text{-}1)$$

and that the autocovariance for all stationary random processes is of the form

$$\mu_\tau = \int_{-\pi}^{\pi} e^{it\omega}\, dF(\omega) \qquad (6\text{-}2)$$

where t = time, τ = time lag, $\omega = 2\pi f$ = the angular velocity, $Z(\omega)$ is a complex random function with uncorrelated increments and $F(\omega)$

is the power spectral distribution function.

From the identities

$$\cos \tau\omega = \frac{e^{i\tau\omega} + e^{-i\tau\omega}}{2}$$

and

$$\sin \tau\omega = \frac{e^{i\tau\omega} - e^{-i\tau\omega}}{2i}$$

it can be shown that for a real process $\mu_\tau = \mu_{-\tau}$ and $dF(\omega) = df(-\omega)$ so that the autocovariance can be rewritten as

$$\mu_\tau = 2\int_0^\pi \cos \tau\omega \quad f(\omega)d \tag{6-3}$$

where

$$dF(\omega) = f(\omega)\, d\omega$$

and $f(\omega)$ is called the power spectrum.

The discrete time Fourier inversion μ_τ is

$$f(\omega) = \frac{1}{2\pi}\left(\mu_o + 2\sum_{j=1}^{\infty} \mu_j \cos j\omega\right). \tag{6-4}$$

With a discrete time series of finite length the power spectrum can be estimated by equations of the form

$$\hat{f}(\omega_j) = \frac{1}{2\pi}\lambda_o C_o + \frac{1}{\pi}\sum_{k=1}^{m} \lambda_k C_k \cos \omega_j k$$

$$\omega_j = \frac{\pi j}{m}, \quad j = 0, 1, 2, \text{ ---- } m.$$

The λ_k's are weights which depend upon m, the number of lags.

The covariances are estimated by

$$C_k = \frac{1}{n-k}\left\{\sum_{t=1}^{n-k} X_t X_{t+k} - \frac{1}{n-k}\sum_{t=1+k}^{n} X_t \sum_{t=1}^{n-k} X_t\right\} \qquad (6\text{-}5)$$

with n data points (Granger, 1964).

The physical interpretation of the power spectrum is that it indicates the contribution to the total variance of the process of a given frequency. This is done over the entire frequency domain.

Whereas the power spectrum indicates frequency characteristics of a single series the cross-spectrum relates the characteristics of corresponding frequencies of two series. The analagous frequencies can be anywhere from in phase to completely out of phase (Blackman and Tukey, 1959).

If the power spectra of the time series $\{X_t\}$ and $\{Y_t\}$ are $f_x(\omega)$ and fy(ω) the autocovariances $\mu_{xx}(\tau)$, $\mu_{yy}(\tau)$, and cross covariance $\mu_{xy}(\tau)$ are

$$\mu_{xx}(\tau) = 2\int_o^{\pi} \cos\tau\omega\ fx(\omega)d\omega \qquad (6\text{-}6)$$

$$\mu_{yy}(\tau) = 2\int_o^{\pi} \cos\tau\omega fy(\omega)d\omega \qquad (6\text{-}7)$$

and

$$\mu_{xy}(\tau) = 2\int_o^{\pi} \cos\tau\omega\ c(\omega)d\omega - 2\int_o^{\pi} \sin\tau\omega\ q(\omega)d\omega \qquad (6\text{-}8)$$

where $Cr(\omega) = C(\omega) + iq(\omega).$ (6-9)

is the power cross spectrum of the two series.

The cospectrum and quadrature spectrum are represented by $c(\omega)$ and $q(\omega)$, respectively.

Inversion gives

$$c(\omega) = \frac{1}{2\pi} \mu_{xy}(0) + \frac{1}{\pi} \sum_{\tau=1}^{\infty} (\mu_{xy}(\tau) + \mu_{yx}(\tau)) \cos \tau\omega \qquad (6\text{-}10)$$

$$q(\omega) = \frac{1}{\pi} \sum_{\tau=1}^{\infty} (\mu_{xy}(\tau) - \mu_{yx}(\tau)) \sin \tau\omega. \qquad (6\text{-}11)$$

An estimate of the correlation between the two series at each frequency can be obtained by examination of coherence square and is equal to

$$(CH(\omega))^2 = \frac{C^2(\omega) + q^2(\omega)}{f_x(\omega) f_y(\omega)} . \qquad (6\text{-}12)$$

As coherence approaches one, the more highly correlated the two series are at the given frequency. The limits for coherence are

$$o \leq CH(\omega) \leq 1$$

The description of the relationship of the two series is not complete unless the phase, $\phi(\omega)$, of the two series is known. This relationship is given by

$$\phi(\omega) = \tan^{-1} \left(\frac{q(\omega)}{c(\omega)}\right) \qquad (6\text{-}13)$$

and indicates for two time series $\{Xt\}$ and $\{Yt\}$ the shift in terms of angle of a frequency of series Y to the same frequency of series X (Granger, 1964).

Computations of spectra and related parameters were computed by two different programs. When there were only several hundred data points a program, BMDO2T of the Western Data Processing Center was used (Dixon, 1965). For data in excess of a thousand points a program utilizing the fast Fourier transform was implemented at a considerable saving of time and money.

The fast Fourier transform is an algorithm which rapidly computes the exponential Fourier transform of a complex series of data. It requires a series of data of length $N=2^n$. To compute a discrete Fourier transform

$$\sum_{k=0}^{N-1} X_k e^{-2\pi jrk/N}, \quad r = 1, 2, ---, N-1 \qquad (6\text{-}14)$$

by the direct method requires approximately N^2 multiplications while the fast Fourier transform requires $2N \log_2 N$. where N is the number of data points. If $N = 2^{10} = 1024$ then the ratio of multiplications by the direct method to the fast method is $(1024)^2 : 20480$. Similarly calculation of autocorrelation functions

$$\sum_{k=0}^{N-1-r} X_k X_{r+k}, \quad r = 0, 1, ---, N-1 \qquad (6\text{-}15)$$

requires $\frac{N}{4}(\frac{N}{2}+3)$ multiplications by the direct method and $3N \log_2 N$ by the fast Fourier transform.

The efficiency of the FFT leads to the use of much less computer

time and, consequently, a considerable savings of funds (Cochran et al., 1967).

The Residual Current Series

If a long series of tidal current record could be obtained, it would be possible to fit many tidal frequencies in a harmonic or least squares analysis and, consequently, estimate the observed current series with a high degree of reliability. Fifteen days of record is far from a long series and in fact is about as short as can possibly be used for any sort of harmonic analysis for the tidal constituents. The fit of the predicted series to the observed series therefore could be considerably better in this particular study had a longer series of observations been obtained.

A great deal can be learned, however, if the residual current series (the difference between the observed series and the fitted series) is examined. Motions other than tidal oscillations should be retained in the residual series as well as those tidal oscillations which were not fitted in the tidal analysis. Spectral methods are probably the best means of examining the residual data series.

There are statisticians who object to using spectra on a residual time series such as has been generated here. Harmonic regression and subtraction, however, is an accepted method of detrending when the trend occurs only in the mean. Perhaps one objection to the above

technique is that the spectrum of the residual data series has a tendency to be biased as a function of $o(n^{-1})$. The symbol o is any function such that when the function is multiplied by n (number of data points), letting n go to infinity, the product remains bounded. This is to say that the spectrum of the residual series is negatively biased. Additionally, the variance of the residual series is a function of time. The spectrum of the residual series has a narrow band removed at the zero frequency but the remaining frequencies are not adversely affected (Granger, 1964).

Despite the disadvantages and objections, the use of spectra on a residual series has been made quite extensively by the physical scientist with satisfactory results. For example, see Thomann (1967) and Zetler and Lennon (1967). The spectrum of the residual series in the case of Long Island Sound does have an advantage. Tidal energy in conjunction with the natural period of oscillation is the predominating driving mechanism. There are several tidal frequencies in that portion of the spectrum which lie between one and six cycles per day. These tidal frequencies contain most of the energy. To design a better filter which will remove these predominating frequencies but leave the remainder of the spectrum intact is difficult.

The fast Fourier transform was used to compute the spectral quantities for the three current stations. Each station included a north and east component of current referenced to magnetic north.

The spectrum of each component was computed as well as the co-spectrum, quadrature spectrum, phase and coherence square between the u and v components of each station. The use of the CDC 3300 limited the number of data points for which the calculations could be made to less than 1024 sets. In order to use as much of the fifteen-day series as possible every other residual was used for a total of 1024 or 2^{10} data points. The fast Fourier transform program is limited to the use of 2^n number of points where n is an integer. This meant that the time difference between points was 20 minutes. The spectral values were band averaged over three bands giving six degrees of freedom. Spectral estimates were made for 170 frequencies at an interval of 0.0088 cycles per hour (cy/hr.). The cutoff was the high frequency end of the spectrum which was the Nyquist frequency

$$fn = \frac{1}{2\Delta t}$$

$$= \frac{1}{2(0.333 \text{ hr.})} = 1.5 \text{ cy/hr.}$$

(Blackman and Tukey, 1959).

Unfortunately, the particular program used began at 0.004 cy/hr. instead of a frequency of 0 cy/hr. The spectral estimates for the north and east components are illustrated in Figures 12, 13, and 14 for stations 89, 90, and 92. Coherence square and phase diagrams for cross spectra of the u and v components are shown in Figures 15,

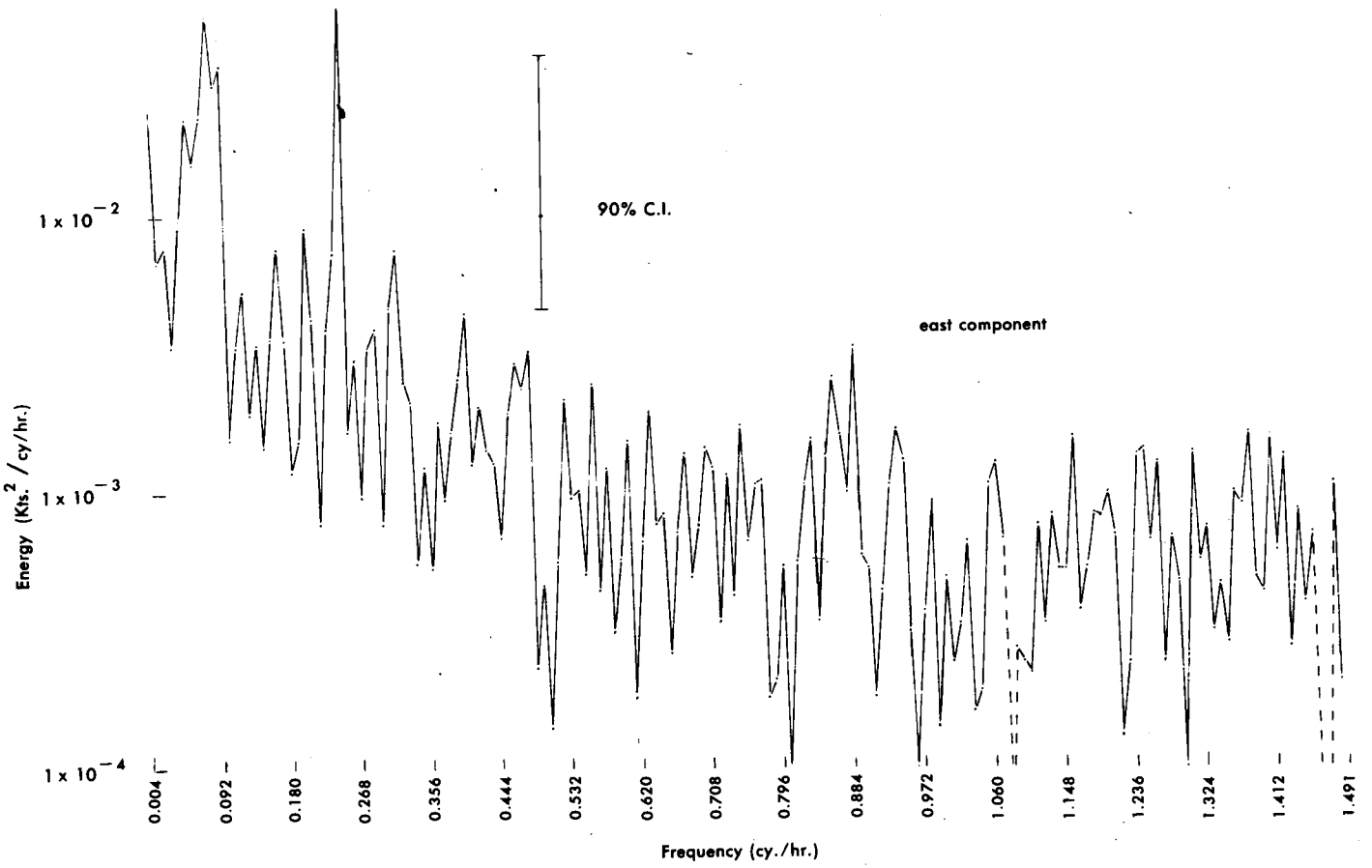

Figure 12. Power spectra – east and north components of residual current series – station 89.

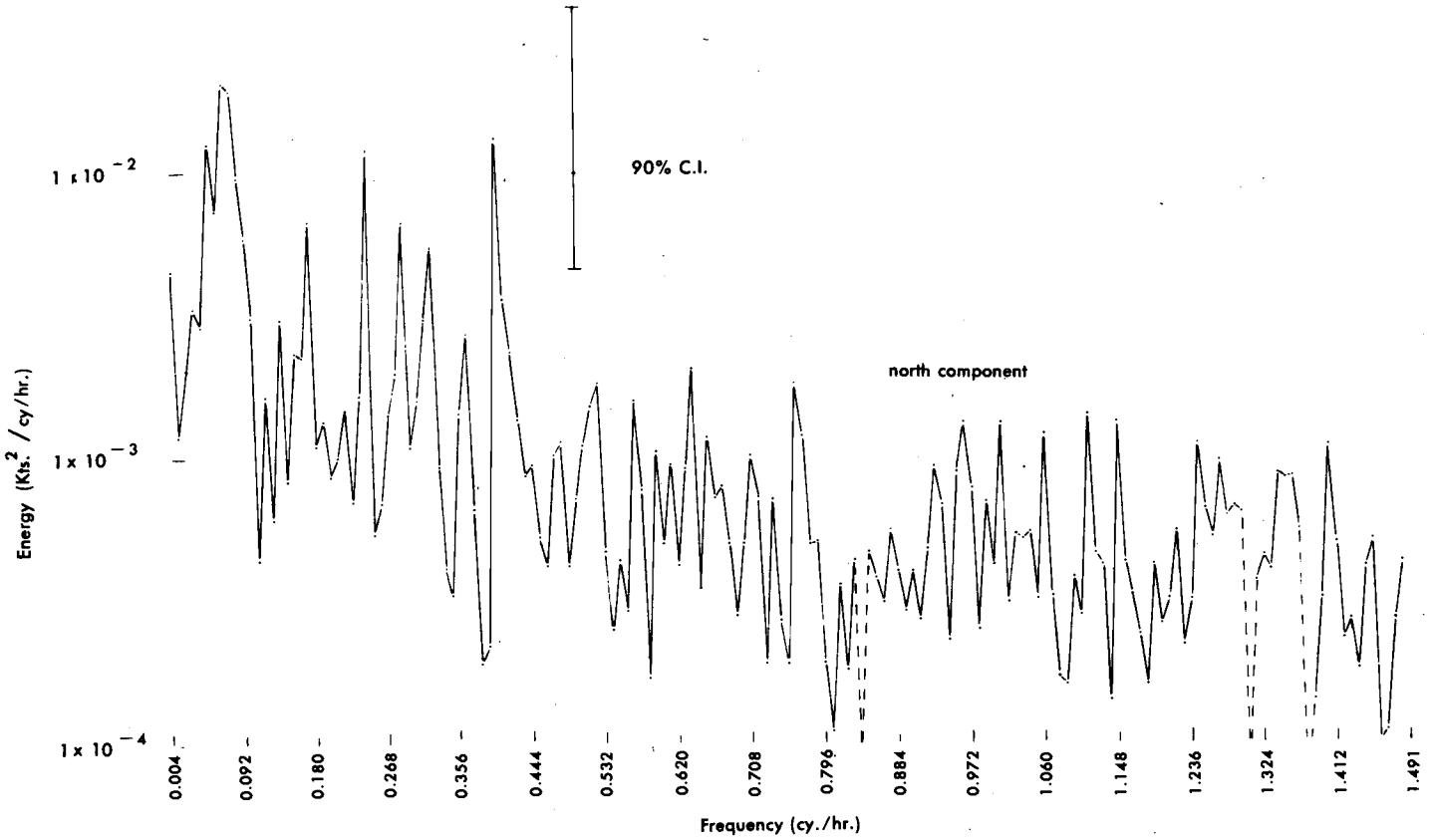

Figure 12, cont. Power spectra – east and north components of residual current series – station 89.

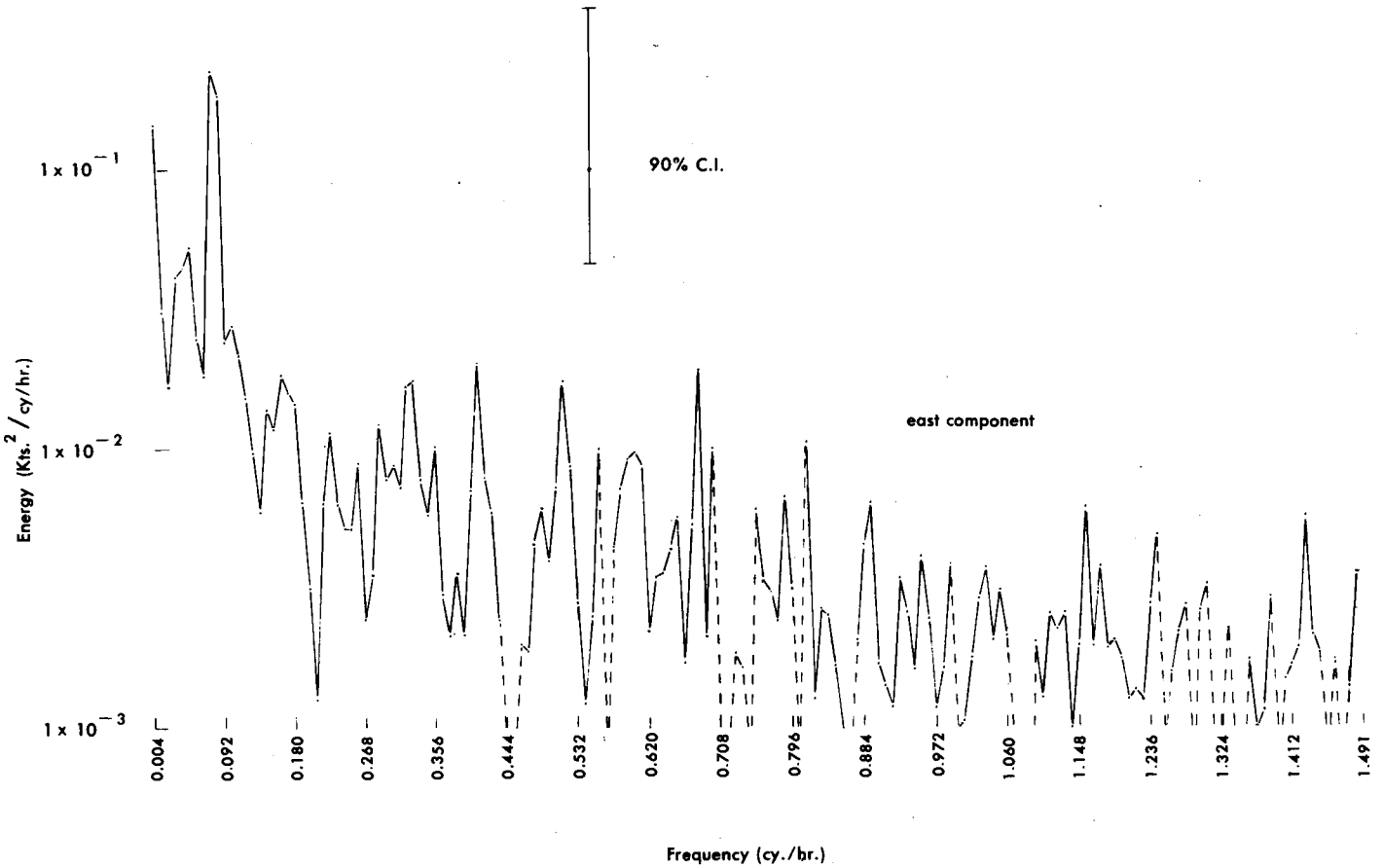

Figure 13. Power spectra – east and north components of residual current series – station 90.

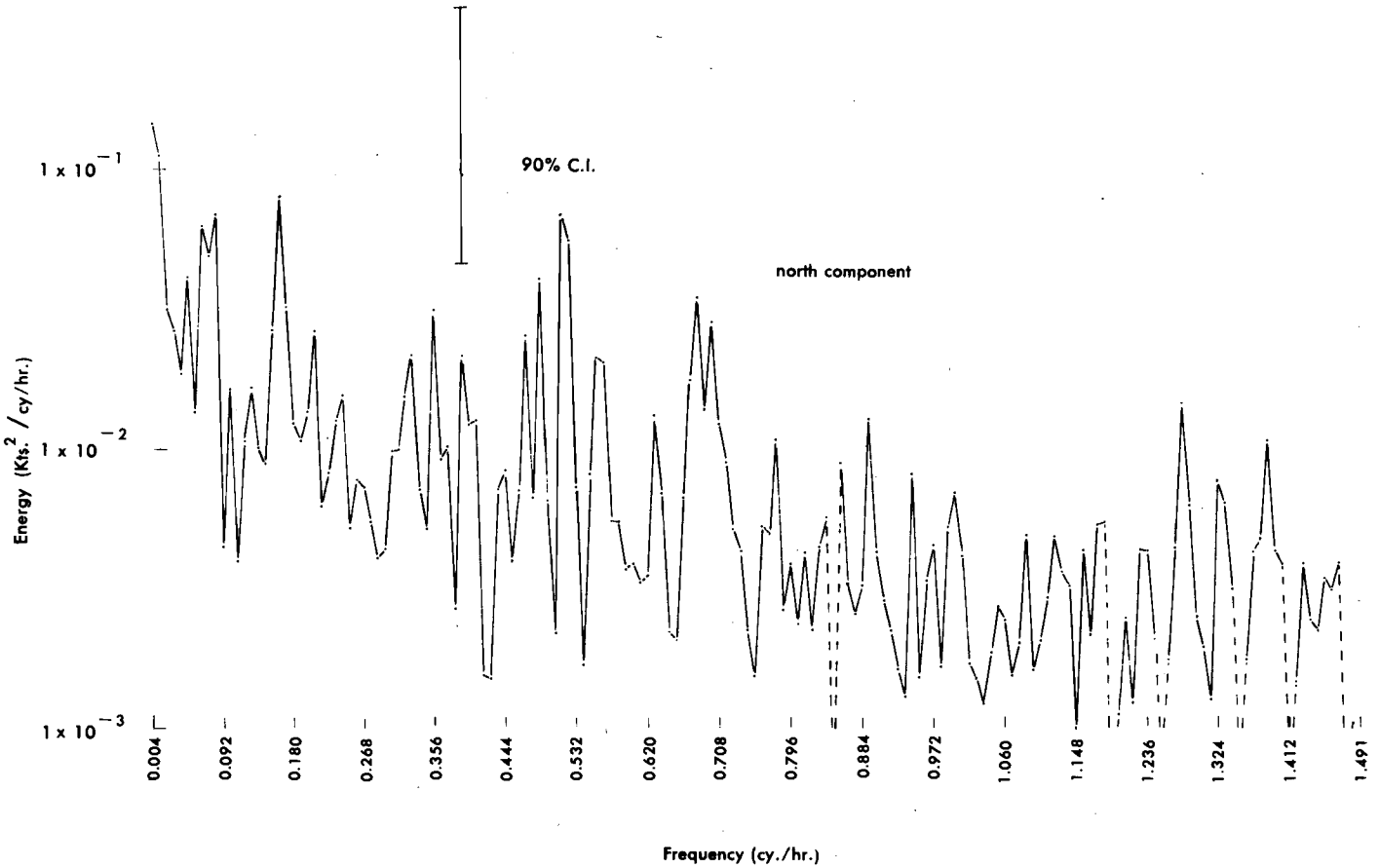

Figure 13, cont. Power spectra – east and north components of residual current series – station 90.

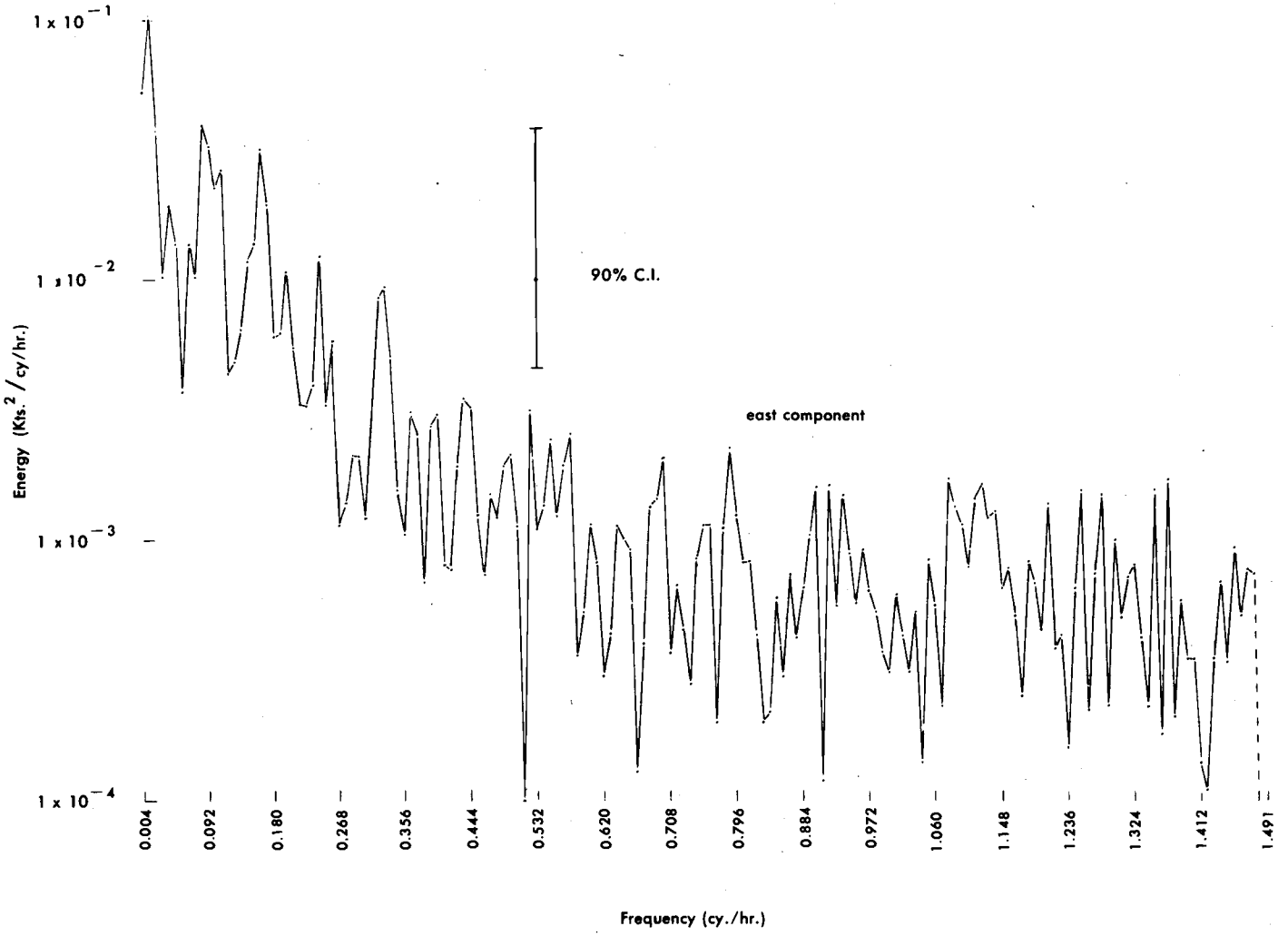

Figure 14. Power spectra – east and north components of residual current series – station 92.

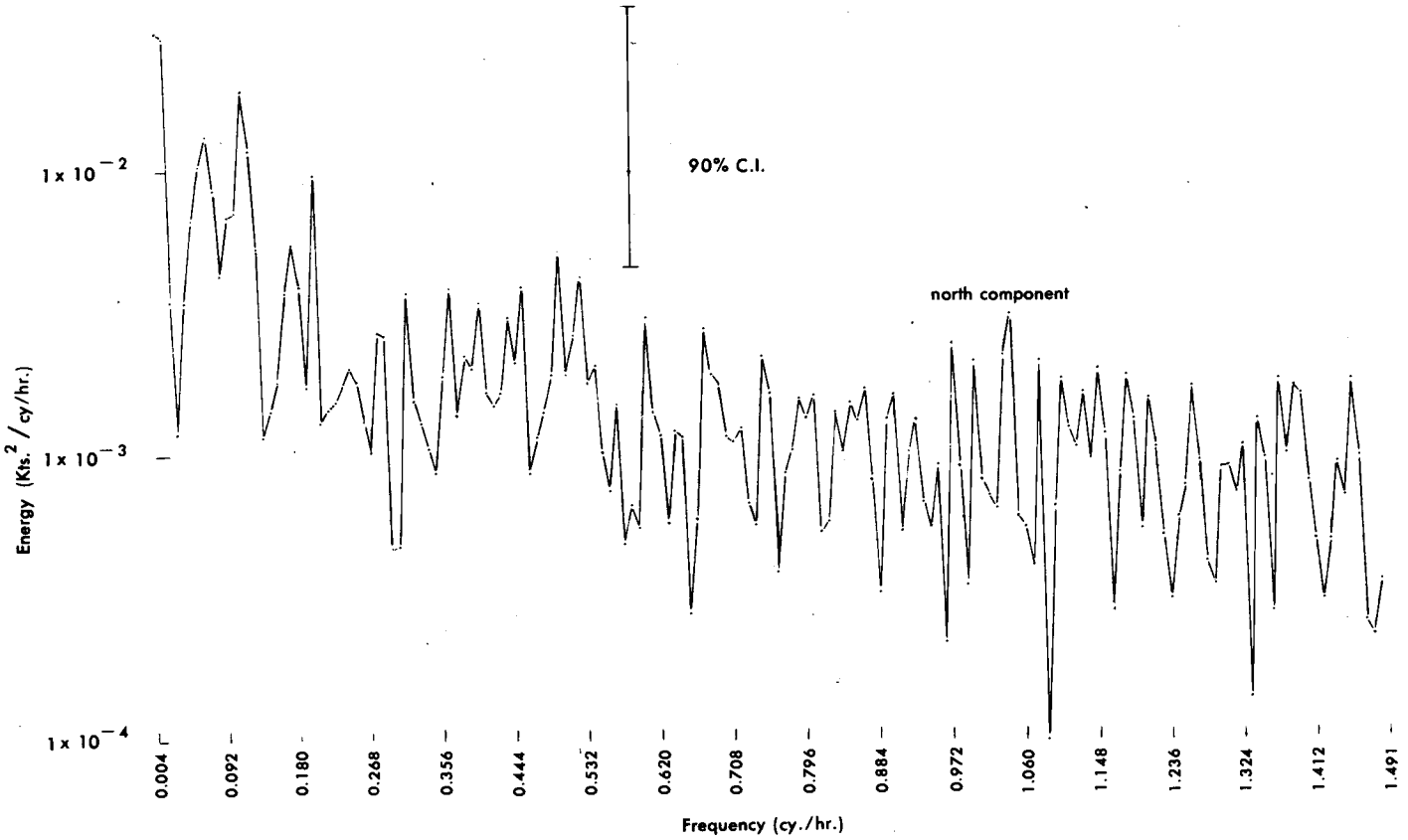

Figure 14, cont. Power spectra – east and north components of residual current series – station 92.

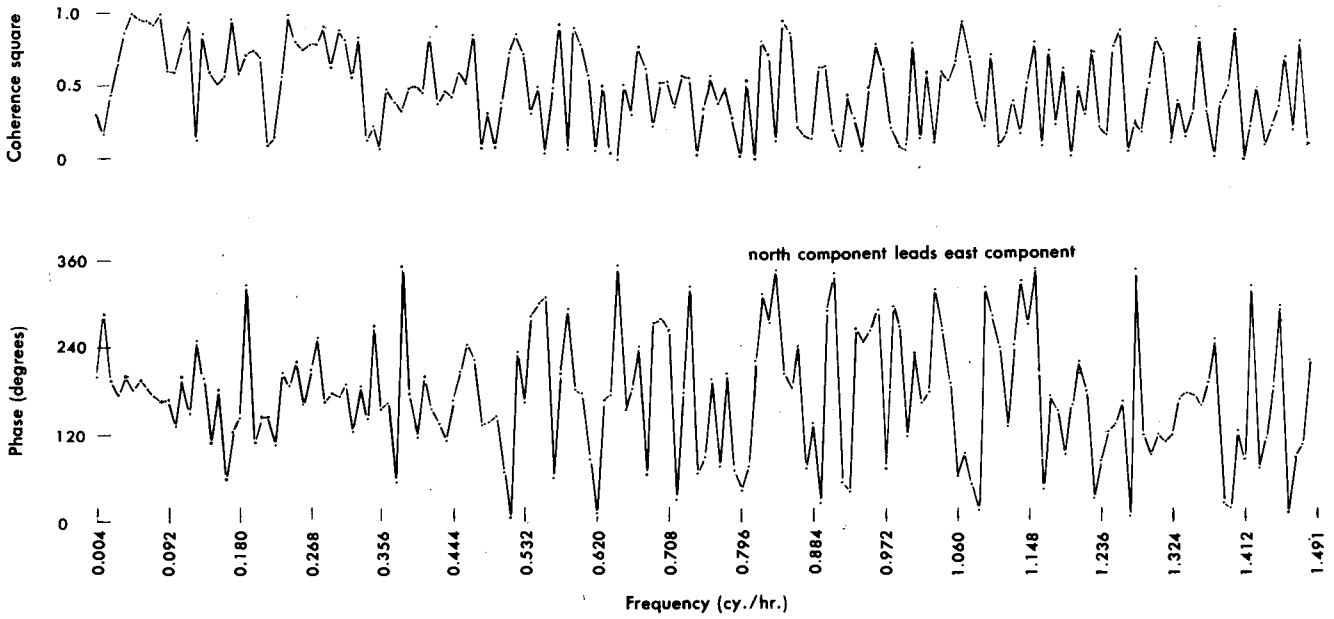

Figure 15. Coherence square and phase of east and north components of residual current series – station 89.

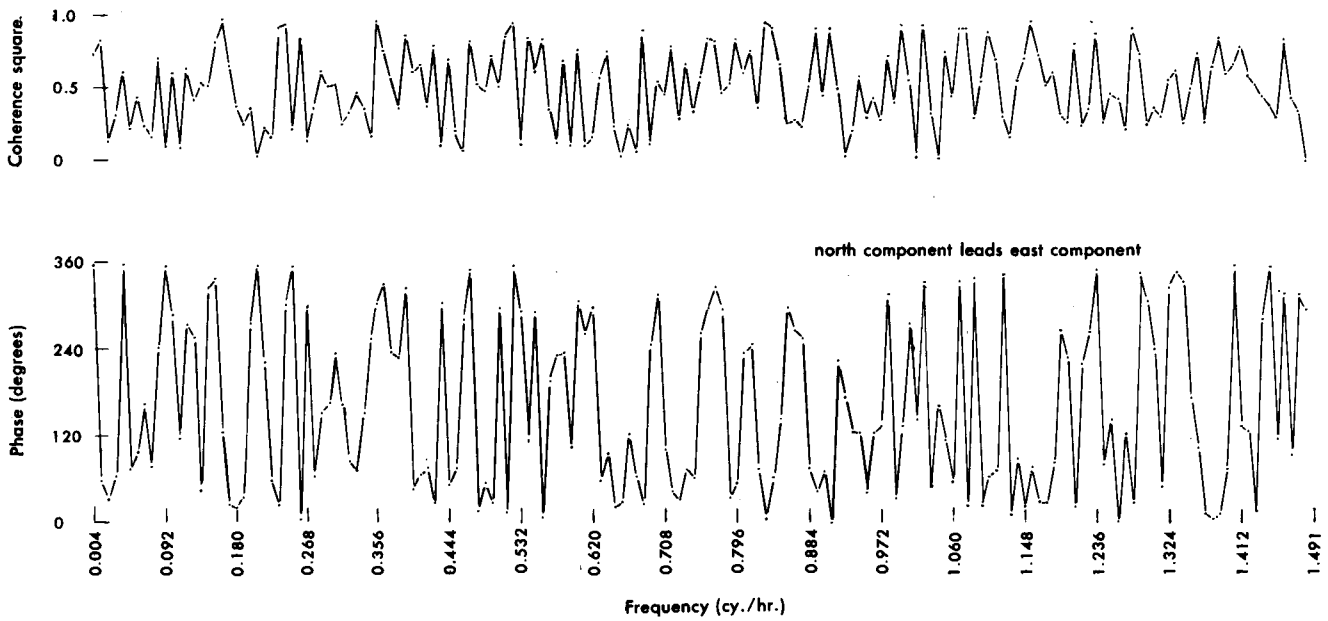

Figure 16. Coherence square and phase of east and north components of residual current series – station 90.

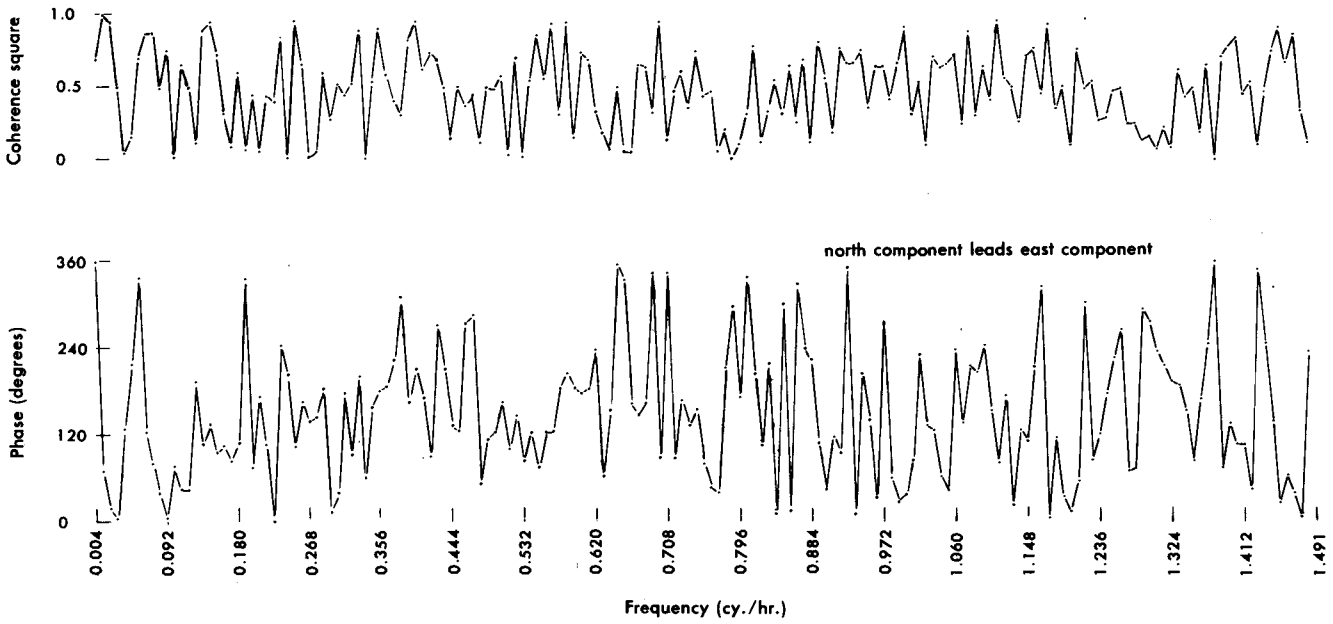

Figure 17. Coherence square and phase of east and north components of residual current series – station 92.

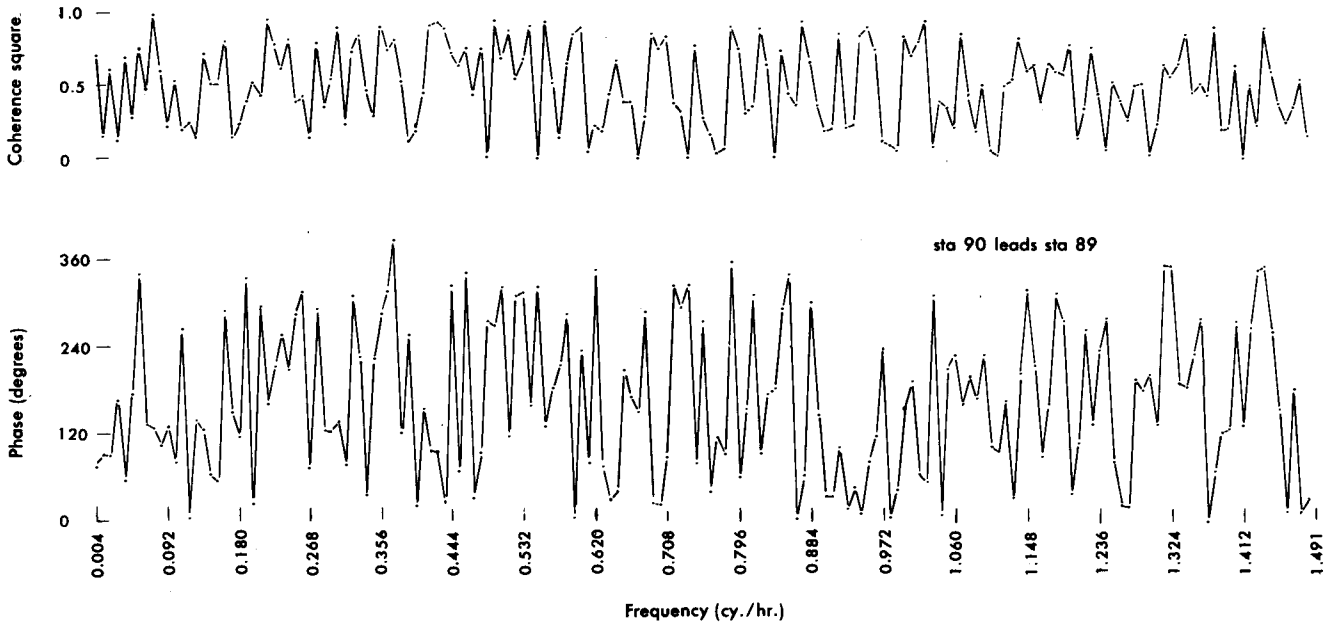

Figure 18. Coherence square and phase of east components of residual current series – station 89 and station 90.

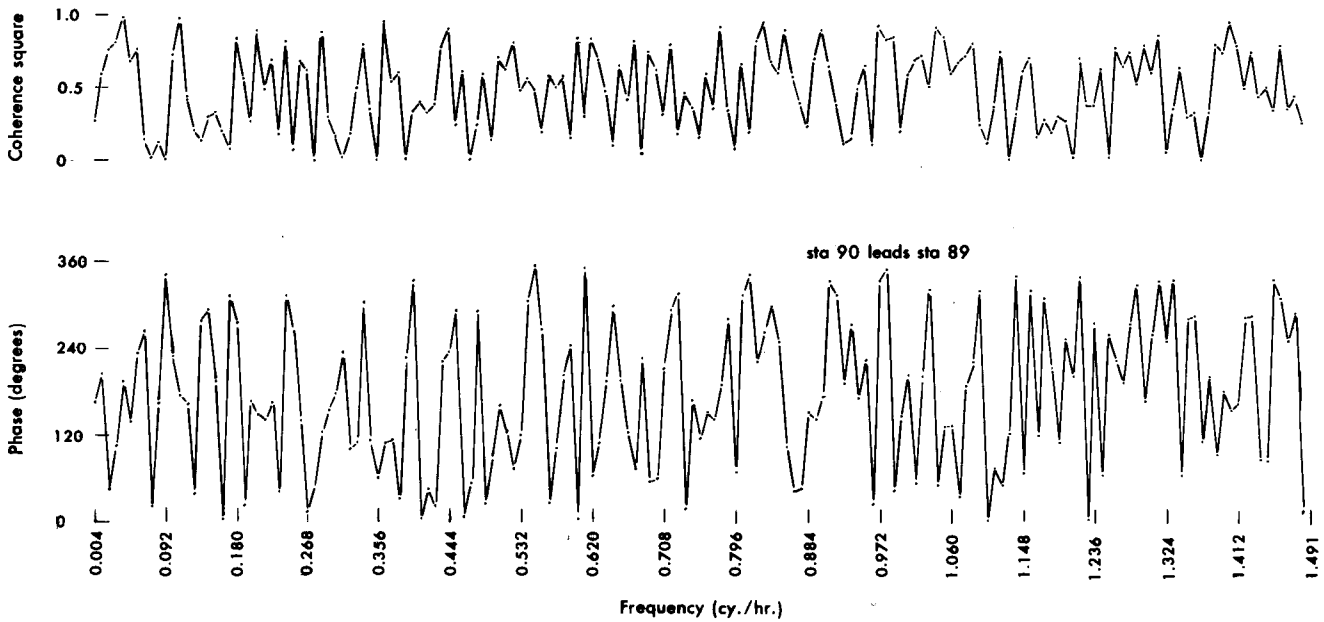

Figure 19. Coherence square and phase of north components of residual current series – station 89 and station 90.

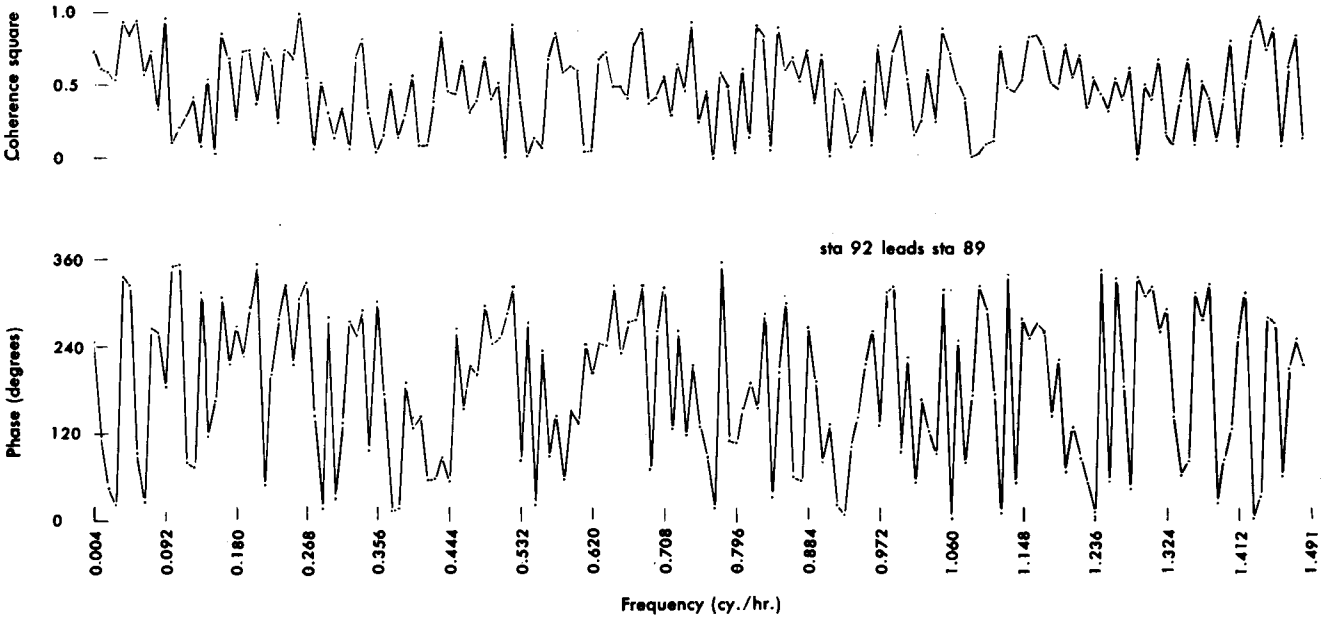

Figure 20. Coherence square and phase of east components of residual current series – station 89 and station 92.

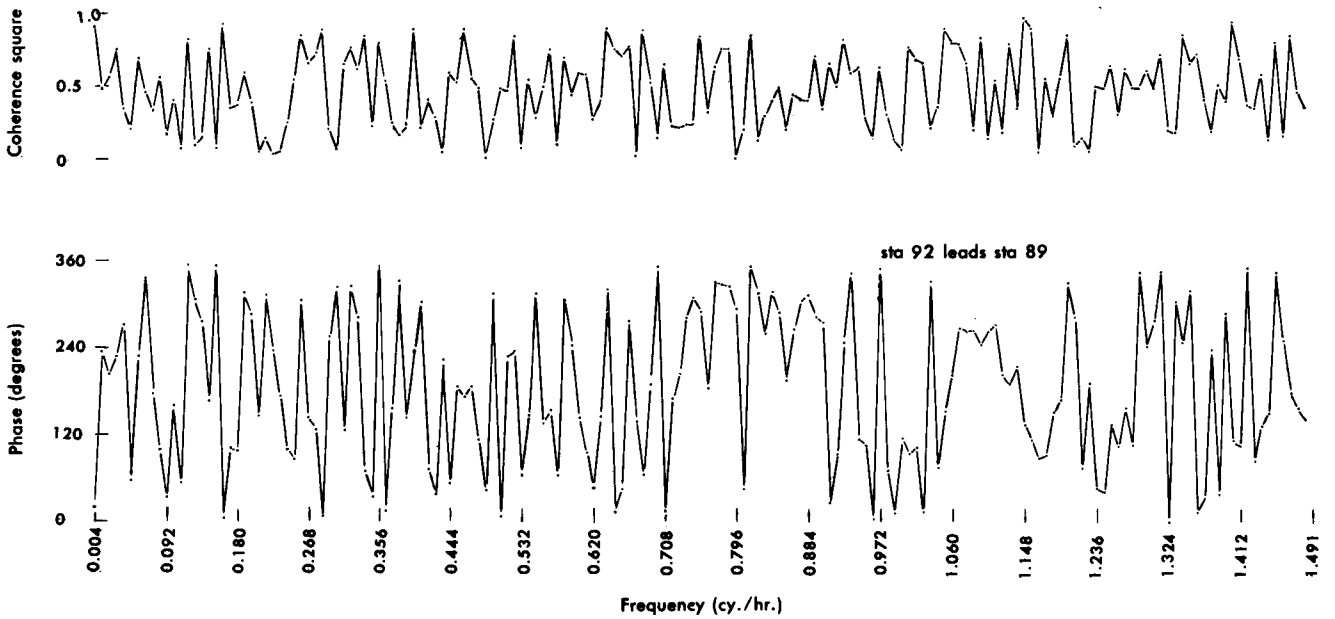

Figure 21. Coherence square and phase of north components of residual current series – station 89 and station 92.

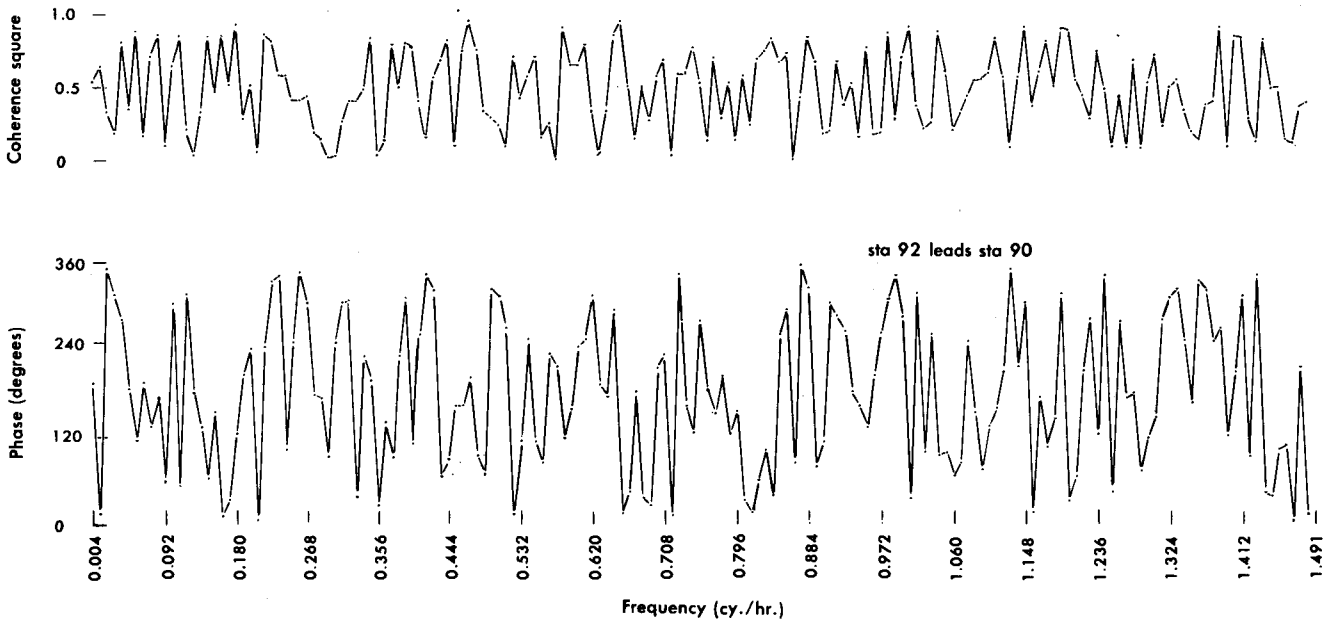

Figure 22. Coherence square and phase of east components of residual current series – station 90 and station 92.

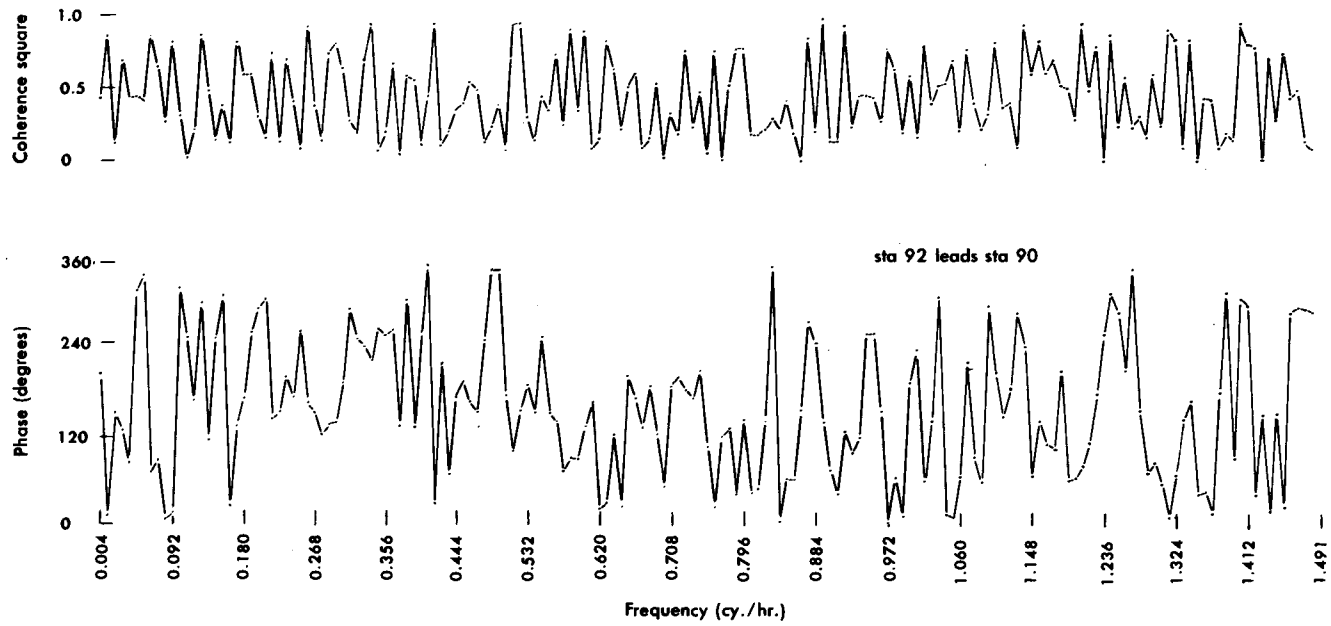

Figure 23. Coherence square and phase of north components of residual current series – station 90 and station 92.

16, and 17. Additional coherence and phase information is presented in Figures 18 through 23 for all possible combinations of the u components for the three sets of data and also for all possible combinations of the v components. The 90% confidence limits for each of the spectral diagrams have been indicated.

In another approach, primarily for the purpose of comparison with wind data, the residual current series was filtered by means of a three hour running average. Using the ten minute spacing of the residual series the spectrum of the series is therefore affected by the power transfer function

$$g(\omega) = \left(\frac{\sin 19\pi\sigma}{19\sin\pi\sigma}\right)^2 \qquad (6\text{-}16)$$

(Hamming, 1962).

This particular filter (Figure 24) accentuates the low frequencies below 1 cycle/day. The average value for every third hour, which corresponded to the period of wind observations, was then used in the BMDO2T spectral analysis program. Results are illustrated in Table VIII.

Results of Spectra on Residual Current Series

In general, the spectra from the fast Fourier transform are unsmooth. It is important to remember, however, that the spectral estimates are plotted on a logarithmic scale. Even so, the almost

Figure 24. Filter resulting from three hour moving average with power transfer function, $g(\omega) = \frac{(\sin 19\pi\sigma)^2}{(19 \sin \pi\sigma)}$.

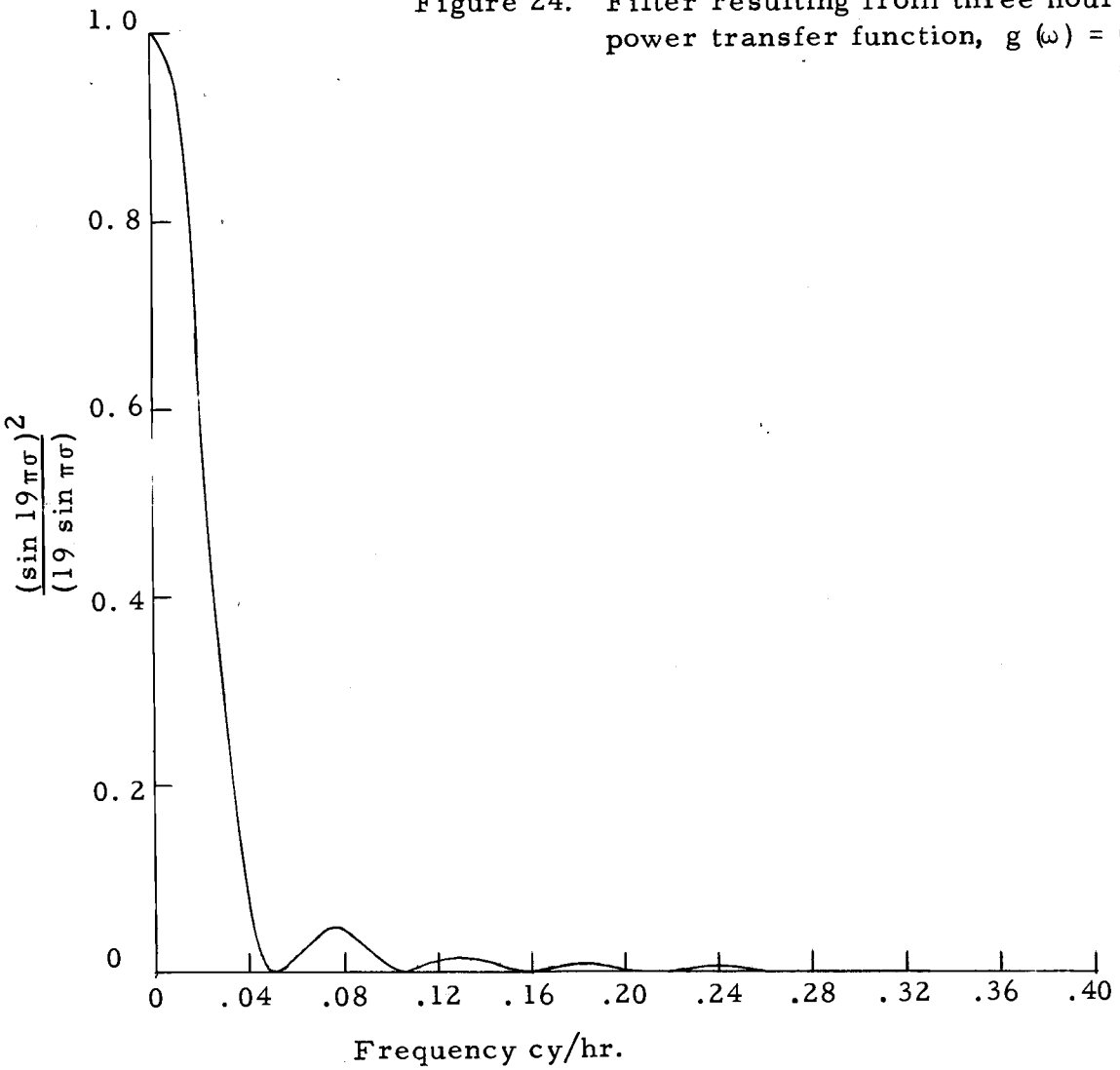

Table VIII. Spectra of Residual Current Series Filtered By a Three Hour Running Average

Frequency cy/hr	Station 89 Energy $kts^2/cy/hr$ x 10^{-2}		Station 90 Energy $kts^2/cy/hr$ x 10^{-2}		Station 92 Energy $kts^2/cy/hr$ x 10^{-2}	
	u	v	u	v	u	v
0	0.737	0.176	12.218	3.916	1.550	0.325
0.008	0.611	0.184	6.470	3.458	1,772	0.459
0.017	0.522	0.168	0.713	1.933	1.642	0.393
0.025	0.343	0.114	0.221	0.981	0.829	0.152
0.033	0.213	0.086	0.777	0.628	0.390	0.092
0.042	0.274	0.103	0.929	0.502	0.301	0.116
0.050	0.328	0.139	0.965	0.687	0.256	0.158
0.058	0.277	0.169	0.802	0.652	0.194	0.144
0.067	0.589	0.356	1.170	1.077	0.318	0.249
0.075	0.909	0.443	2.984	1.169	0.366	0.241
0.083	0.742	0.266	3.148	0.932	0.736	0.125
0.092	0.520	0.141	1.686	0.653	0.976	0.148
0.100	0.228	0.068	0.551	0.386	0.579	0.115
0.108	0.122	0.037	0.318	0.415	0.310	0.196
0.117	0.156	0.038	0.432	0.434	0.124	0.282
0.125	0.143	0.034	0.459	0.427	0.108	0.144
0.133	0.107	0.035	0.178	0.289	0.142	0.057
0.142	0.097	0.044	0.217	0.206	0.124	0.044
0.150	0.076	0.069	0.367	0.457	0.096	0.045
0.158	0.084	0.084	0.311	1.762	0.119	0.051
0.167	0.104	0.053	0.122	2.922	0.094	0.035

cyclic pattern is striking and warrants some discussion.

Echoes in the original data might lead to the cyclic appearance of the spectrum. If an original time series y(t) were multiplied by a constant α and delayed by a time τ, the echo would be $\alpha\, y(t-\tau)$. The combination of the original series and the echo would yield a new time series

$$z(t) = y(t) + \alpha\, y(t-\tau). \tag{6-17}$$

In this simple example a cycle would appear in the spectrum with period τ and amplitude 2α. These are properly called in the literature the quefrency, τ, and gamnitude, 2α, respectively. The problem of echoes has been found to have practical significance in working with seismological data and it is not difficult to imagine that echoes might exist in tidal and tidal current data, particularly in embayments where reflection of the wave can occur (Bogert, Healy, and Tukey, 1963). Only mention of echoes is made here and perhaps further examination of the subject is worthwhile.

It should also be pointed out, however, that many of the peaks contributing to the cyclic appearance of the spectrum might be physically real and resulting from other than echoes. Tides and, consequently, tidal currents are almost unique in the physical world in that the time series generated is for practical purposes stationary. The relationship between the astronomic forces and the resulting vertical

and horizontal motions can be determined quite accurately. The amplitudes and phases of the constituents which contribute to the tidal motions are fixed at a given location. The constituents which can be used for predictors represent lines on the spectral diagram, provided that the analyzed record was of sufficient length to assure separation. However, since a short series was used, and all constituents were not able to be separated, the amplitude and phase of a given constituent is probably contaminated by that of another. An example is that of the M_2 constituent being contaminated by the N_2 in this study. Further, the effect of band averaging in the spectral analysis includes energy of frequencies near that of the specific frequency that was intended for removal in the regression and subtraction routine. The result of the last two statements is that one can probably expect that a given frequency is not solely nor completely removed in the spectrum of the residual series. Peaks in the residual spectrum at or near frequencies supposedly removed will not be surprising. In fact, this has been found in tidal records at San Francisco and Anchorage (Zetler and Cummings, 1967) and (Zetler and Lennon, 1967).

These same investigations also indicated numerous peaks at frequencies greater than two cycles per day, a condition similar to that found in this study. Many of these peaks are apparently real and a result of the non-linear interaction between components which manifest themselves as the so called shallow water constituents.

The spectrum of tidal records exhibit a condition known as a tidal cusp. Comparison of spectra from observed tides and predicted tides have shown that the spectra from observed records contain energy adjacent to the strong tidal lines, which does not appear in the spectra from predicted values. This energy has been attributed to the interaction of the tidal line and the continuum near the zero frequency and has been called the cusp spectrum. Thus, if there is energy at a frequency band $f_o \pm f$, it can be anticipated that energy will also be found symmetrically around f_1 at $(f_1 \pm f_o) \pm f$ (Munk, Zetler, and Groves, 1965). See illustration in Figure 25. This same paper indicates that the cusp spectrum exists not only between species (between the diurnal and semidiurnal for example) but also among the species (components with nearly the same periods, as the semidiurnals for example).

Since interaction occurs between tidal constituents and the variation of mean sea level (Munk, Zetler, and Groves, 1965), it is not unreasonable to expect interaction between the tidal current constituents and the fluctuation of the mean permanent current. These "tidal current cusps" could help to further account for the fact that peaks in the spectra of the residual current series are present even though the specific frequency had been removed.

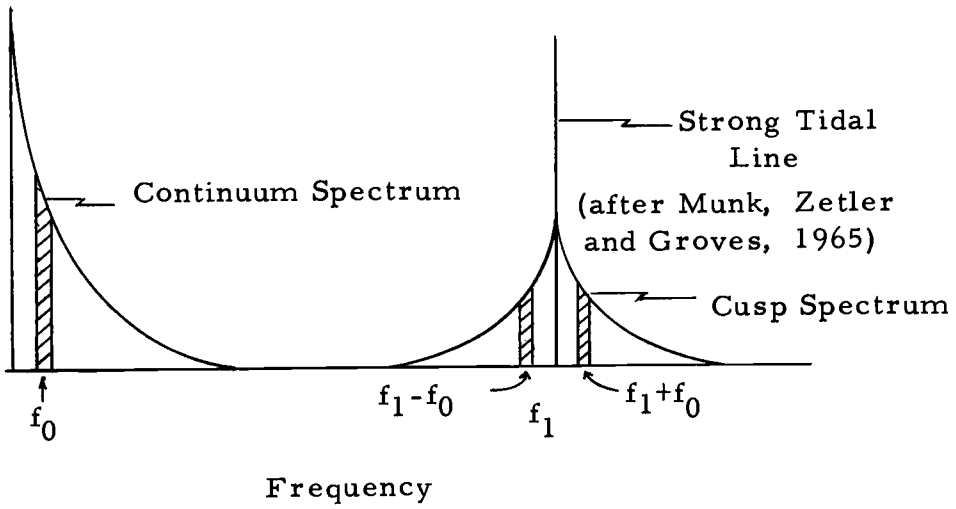

Figure 25. Interaction of a strong tidal line with the continuum near zero frequency.

A. Frequencies Less Than 1.94 Cycles Per Day

In examination of the spectra of the three current stations, one of the peaks that might be expected to be significant is that of the inertial period. The circular motion associated with the inertial period is the result of the centrifugal force of the motion being balanced by the Coriolis force,

$$(2\Omega \sin \phi)c = c^2/r \qquad (6\text{-}18)$$

where Ω is the earth's angular velocity, ϕ is the latitude, c is the horizontal velocity, and r is the effective radius of the inertia circle. In the northern hemisphere the motion is clockwise (Von Arx, 1962).

The driving force for inertial motion is generally the sudden removal of a stress such as wind or barometric pressure. The current then is influenced only by its own inertia and the Coriolis force. In restricted areas the motion will be modified by boundaries and friction resulting in an elliptical path. The period of inertial motion in hours is

$$T = \frac{12 \text{ hr.}}{\sin \phi} \qquad (6\text{-}19)$$

(Wiegel, 1964)

At the mean latitude of Long Island Sound which is $41^{o}06'$N the inertial period is 18.26 hours. The period on the spectral diagram

closest to the inertial period is 17.54 hours corresponding to 0.057 cy/hr. Any energy associated with the inertial frequency should be at the latter frequency as a consequence of the band averaging process.

Examination of the spectra indicates that there is no significant energy at the inertial frequency at any of the current stations. This is somewhat surprising as the mechanism for initiating the motion appears to have occurred during the period of observations. The wind observations at Falkner Island (Appendix II) certainly indicate high speeds. After September 4 and 15 there were periods of relative calm following high easterly and westerly winds, respectively.

One may speculate on the possible existence of some energy at station 90. Coherence square is relatively high at 0.432 while the phase indicates that the v component of the current leads the u component by 97.7^{o}. These conditions certainly are necessary for inertial motion, as it is expected to be orbital in nature. Consequently, for every v component there should be a u component resulting in high coherence square. Also the v component should lead the u by nearly 90^{o} to satisfy the condition that inertial motion is clockwise in the northern hemisphere (Bendat and Piersol, 1966).

The nearshore observations show that any energy associated with the 0.057 cy/hr. frequency has a counterclockwise rotation. The indication certainly is that the inertial currents are unimportant.

There are several possible explanations as to the lack of energy

near the inertial frequency. First, the conditions during the time of observations were not sufficient for initiating the motion. Even though high wind speeds existed there conceivably was not enough time after removal of the stress to permit the current to become established. Any current setup could have been destroyed by initiation of another wind stress shortly after removal of the initiating stress. Second, the physical conditions of the Sound might be such that inertial currents never are significant. Perhaps the tidal motions causing turbulence and friction are such that they have a tendency to destroy any inertial currents.

The complete removal of the semidiurnal tidal frequencies was certainly not accomplished by the methods described in this paper. Significant peaks occur on all components with the exception of the v component of station 92 where the peak actually occurs at 0.066 cy/hr. or 15.16 hr. This peak, as has been previously mentioned, is anticipated as the short length of series did not permit fitting all the major constituents in the analysis. As was pointed out, N_2 with a frequency of 0.079 cy/hr. was found by inference to have enough energy to account for most of the variance of the residual data series. However, the removal of most of the energy at the semidiurnal period as well as some at the diurnal, quarter, sixth and eighth diurnal periods does emphasize some of the lesser oscillations.

B. Frequencies Greater Than 1.94 Cycles Per Day and Less Than 11.9 Cycles Per Day

There are many peaks in the high frequency portion of the spectra of the residual current series which are apparently significant. Most of the peaks can probably be associated with various shallow water tidal constituents. These tides are found in coastal areas and are the result of a distortion of the tidal wave. The effect of the shallow water is to cause a retardation of the trough of a wave with respect to the crest. The cause of this phenomenon can be seen in examination of the shallow water wave equation

$$c = (gh)^{1/2} \tag{6-20}$$

where h is the depth. A decrease in tidal height will cause a decrease in the speed of the wave.

Compound tides (the sums or differences of the angular frequencies of two or more of the principle constituents, see Appendix III) and overtides (angular speed is a multiple of the speed of a principle constituent) make up the various shallow water constituents. The effect of these compound and overtides are described by nonlinear terms in the equations of motion and the equation of continuity (Dronkers, 1964).

Some of these peaks thought to be the result of shallow water tidal constituents will be examined in order of increasing frequency.

0. 163 Cycles Per Hour

Significant peaks might well be expected at this frequency as it is almost exactly twice that of the lunar semidiurnal frequency. There are, however, many compound tides as well as two overtides that would also be concentrated at a period of 6. 144 hours. The overtides of M_4 were removed in the tidal analysis at all stations. In addition, S_4 was removed from station 90. The compound tides of MN_4, $MNKS_4$, SN_4, KN_4, MS_4. MK_4, and SL_4 could also be important. Peaks of significance occur on the easterly component of 92 and also on the northerly component of 90. The easterly component of 89 could also be significant.

It is interesting that drifting of the buoy during slack and at low velocities of a semidiurnal current would contribute energy near this frequency. An attempt was made to compensate for this and was mentioned before. However, the method used assumed the flow to be reversing and not rotary. Station 90 must be considered rotary as the minor axis of the composite tidal ellipse is on the order of 0. 25 kts (Figure 11). The possible result, therefore, is that the peak on the northerly component of 90 conceivably could be the drifting of the surface float. The suggestion is that using the S_4 constituent at station 90 removed enough energy from the east-west component to reduce the peak significantly. Movement of the buoy caused the peak to occur on the north-south component. Apparently S_4 should have

been included in the tidal current analysis of stations 89 and 92. Since the current at 89 and 92 was primarily reversing and mostly in an east-west direction any spurious movement of the buoy in the north-south direction was minimal at these two stations, i. e., the buoy did not move in an elliptical path at 89 and 92 and the linear correction for buoy drift apparently was a reasonable approach.

Examination of the relationships of the three stations is difficult, since significant peaks do not occur on all spectra and since S_4 was removed only from station 90. It is interesting that the u component of 89 leads that of 92 by 20°. Coherence between the same components is very high at 0. 92. These facts, coupled with the clockwise rotation of this frequency (the v component leads the u component by 59° and 104° of stations 89 and 92, respectively), further indicate that this particular frequency band is strongly associated with the overtides and compound tides mentioned previously. The inclusion of the S_4 constituent in the analysis would have improved the results from the two inshore stations.

0. 198 Cycles Per Hour

Several compound tides are found near this frequency and can possibly be associated with the significant peaks on the spectra of the east component of station 89 and the north component of 92. These constituents are MNO_5, $2MO_5$, $3MP_5$, and MNK_5. The presence of

energy at this frequency is apparently isolated as significant peaks occur on only two of the six spectra. Perhaps this frequency is particularly subject to the topographic conditions as neither the significant peaks nor coherency indicate any overall relationships between the three current stations (Dronkers, 1964).

0.242 Cycles Per Hour

This frequency exhibits significant peaks on both components of the spectra of station 89 and on the east component of 92. Similar to 0.163 cy/hr. this frequency is almost an exact multiple of the semidiurnal tidal frequency. The question can be raised as to the validity of these particular peaks. However, their existence is substantiated to some extent by the fact that the 0.198 cy/hr. frequency does not occur on each spectra for which there is a large amount of energy remaining at the semidiurnal frequency. The one overtide near this frequency is M_6 and it was removed at all stations in the tidal analysis. The remaining compound tides possibly contributing energy are in order of increasing frequency $2NM_6$, $2NMKS_6$, $2MN_6$, $2MNKS_6$, MSN_6, MKN_6, $2MS_6$, $2MK_6$, and NSK_6.

Note from the Figure 15 that the east component of 89 leads the north component by 171°, indicating a counterclockwise rotation. Thinking in terms of the motion being represented by two orthogonal sinusoids, one reaches a maximum approximately when the other

reaches a minimum. The result is an ellipse with an almost insignificant semiminor axis and the semimajor axis lying in the northwest and southeast quadrants of the compass. This is the same sort of ellipse found to exist in the tidal analysis. The coherence is 0.999 which for all practical purposes is perfect.

In the case of the u components of stations 89 and 92 the former leads the latter by 36^{o} with a coherence of 0.86.

0.286 Cycles Per Hour

This frequency appeared as a significant peak only on the spectrum of the northern component of station 89. The motion at 89 is clockwise with v leading u by 164^{o} with a coherence of 0.958. The motion at 90, if it exists, is similar with v leading u by 151^{o} and a coherence of 0.791. The energy is possibly the result of the two compound tides $2MSO_7$, and $MSKO_7$.

0.321 Cycles Per Hour

Energy centered on this frequency is found on the easterly components of stations 90 and 92 and the northerly component of station 89. The overtide of M_8 was used in the tidal current analysis. This frequency is a harmonic of the semidiurnal tide as well as the quarter diurnal tide and it could be that the peaks are a result of being such a harmonic. There are, however, numerous compound tides near this frequency such as $2(MN)_8$, $3MN_8$, $3MNKS_8$, $2MSN_8$, $2MNK_8$,

$3MS_8$, and $3MK_8$.

The energy is concentrated on one component of each of the three current stations. The coherence between the north and east components of each are 0. 754, 0. 576, and 0. 720 for stations 89, 90, and 92, respectively. These values are somewhat lower than some of the values cited for other frequencies, possibly a result of the energy being primarily associated with only one component. However, in each case the v component leads the u by 124^{o}, 84^{o}, and 94^{o} for the same station order given above.

Cross spectra of the easterly components of the stations shows that 89 leads 90 by 49^{o} with a coherence of 0. 859, 89 leads 92 by 83^{o} but the coherence is low at 0. 254. Station 90 leads 92 by 50^{o} with a coherence of 0. 642.

0. 330 Cycles Per Hour

There are several more compound tides which possibly are contributing to the energy at this particular frequency. They are $MSNK_8$, $2(MS)_8$, and $2MSK_8$. Only on the easterly components of 90 and 92 do significant peaks appear. At 90 the v component leads the u by 71^{o} with a coherence of 0. 684, which is very close to the results found for the same station at the previously discussed frequency. However, the relationship at 92 is considerably different with u leading v by 158^{o}. The coherence is high at 0. 938.

In addition, the phase relationship of the easterly components are considerably different from the previous frequency band. Here 92 leads 90 by 39^{o}. The coherence is nearly the same being 0. 644 in this case.

0. 356 Cycles Per Hour

A significant peak is found on the northerly component of 90. There is a small peak, although not significant, on the easterly component. The coherence is high at 0. 985 with the u component leading the v by 58^{o}. The rotation is therefore counterclockwise. The compound tide of $2M2NK_9$ lies near this frequency.

0. 400 Cycles Per Hour

Significant peaks are located on the spectra of both components of station 89. Notice that the north component of 89 has considerably more energy than the east component of the same station. The apparent rotation is clockwise. The north component leads the east component by 116^{o}. The coherence is 0. 712.

The constituents $4MN_{10}$, M_{10}, and $3MNS_{10}$, are located near this frequency.

0. 488 Cycles Per Hour

This frequency appeared as significant only on the spectrum of the northern component of station 90. The northerly component leads the easterly by 54^{o} and the two have a coherence of 0. 695.

It is conceivable that the peak is a result of the compound tidal constituents of $4MNS_{12}$, $5MS_{12}$, $3MNK_{12}$, and $4M2S_{12}$.

Conclusions Concerning Compound Tides and Overtides

It is of particular interest that most of the peaks in the spectra below the semidiurnal period can be associated with compound tides or overtides. However, the higher the frequency the more easy it is to obtain an increasing number of possible combinations of the major tidal constituents that might yield a particular frequency (Zetler and Cummings, 1967). It is significant, however, that the existence of many of the frequencies found in current data of Long Island Sound were also found in the tidal records for Anchorage, Alaska. Since Anchorage is located at the head of Cook Inlet, which is similar to Long Island Sound in that it is a cooscillating tidal basin, it is reasonable that similar oscillations might occur.

The ratio of the mean tide ranges of Anchorage and Willets Point, both of which are situated near the heads of their respective basins, is nearly 3. 8 (United States Coast and Geodetic Survey, 1966b). Even though the tidal range is considerably greater at Anchorage, the compound tides and overtides in Long Island Sound might still contribute to the overall circulation of the Sound. The summation of the amplitudes of the minor constituents (the constituents found in the spectra of Long Island Sound) at Anchorage

represents 13.3% of the total of the 114 constituents (Zetler and Cummings, 1967). Obviously, if this percentage is similar in Long Island Sound these constituents are important.

It is noticeable that the energy peaks discussed here are not common to both components of all the stations. In fact, with the exception of the 0.163, 0.242, and 0.321 cy/hr. frequencies, the existence of the others are quite isolated. This might well indicate the importance of the local topographic effects in propagation of shallow water tides (Dronkers, 1964).

Comparison of the spectral and cross spectral results of the 0.163 cy/hr. frequency is somewhat difficult in view of the fact that S_4 was used in the tidal analysis of station 90 but not in 89 and 92.

Because of the high coherences that exist between many of the speed components, it is possible to make some general inferences concerning the 0.242 cy/hr. frequency. The velocity vector rotates in a counterclockwise direction at each observation site. The low coherence between the north and east components of station 92 is most likely the result of the major axis of the ellipse, described by the spectral and cross-spectral quantities, lying in the east-west direction with the eccentricity approaching one.

The square roots of the power spectral estimates have been used as a relative measure of the magnitudes of the speed components at the several locations. These, along with the phase relationships

between the north and east components of each station, and also the phase relationships between the north components of all three stations, can be used to construct a diagram of the relative magnitudes of the vectors in time for this specific frequency. This diagram (Figure 26), of course, represents average conditions and cannot be assumed to hold at any specific instant.

The inshore stations are nearly in phase, while station 90 lags considerably. The topographic effects are noticeable. The Coriolis effect apparently is important, as indicated by the counterclockwise rotation and the overall decrease in the magnitude of the major axis of the elliptic motion from north to south. In a rotating basin, the streams are expected to be greater on the right side as the wave moves into the basin (Proudman, 1925).

The particularly large peak on the spectral diagram for the east component of 89 is one of the most outstanding features of all the spectra. This same situation was observed in the tidal data from Anchorage. The peak at Anchorage was reduced to a comparable level with adjacent frequencies after analysis for 114 constituents was performed (Zetler and Cummings, 1967). Apparently species six is extremely important in shallow water tidal phenomenon.

The spectral results of the 0. 321 cy/hr. frequency were treated similarly to that preceding. The energy is distributed more evenly over the cross section than has been found with many of the other

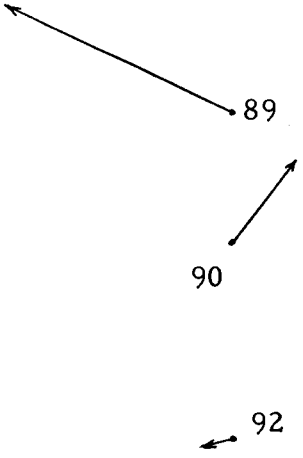

Time = 0

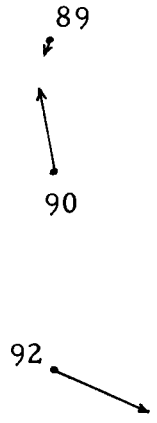

Time = 1/4 constituent period

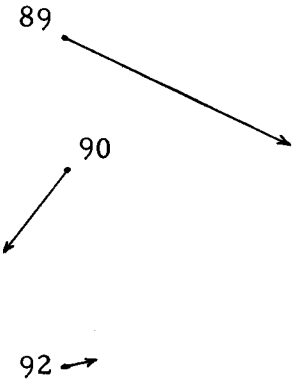

Time = 1/2 constituent period

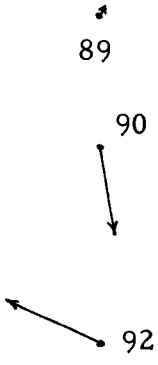

Time = 3/4 constituent period

Figure 26. Relative position and strength of the velocity vector at the 0.242 cy/hr. frequency.

frequencies. In each case, the rotation is in a clockwise direction with 89 and 92 being in phase and 90 lagging slightly (Figure 27).

C. Frequencies Greater Than 12.0 Cycles Per Day

In addition to the free oscillation in the longitudinal axis of Long Island Sound (Chapter 7), there may be a transverse seiche as well. Defining the characteristics of such an oscillation is difficult from current data alone particularly because of the irregular shape of the basin. However, it is possible to estimate roughly the magnitude of such a seiche using Mérian's formula:

$$Tn/n = \frac{2l}{(gh)^{1/2}} \qquad (6\text{-}21)$$

Tn = the period of the n^{th} nodal seiche
l = the width of the basin
g = acceleration of gravity
h = depth of water

(Dietrich, 1963).

The equation applies to a rectangular basin with a uniform depth. However, if the cross section is subdivided into a number of small segments over which the depth is roughly constant and integrated over the width l, the value obtained for the period should be improved somewhat over using the average depth over the entire width. Merian's equation now takes the form of

$$Tn/n = 2\int_0^l \frac{dy}{(gh)^{1/2}} \qquad (6\text{-}22)$$

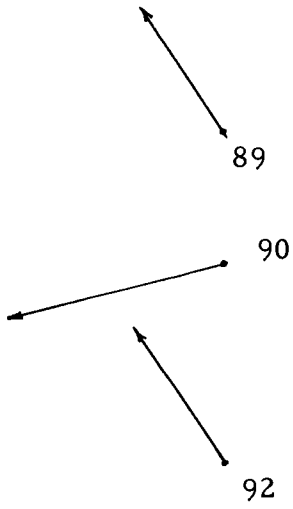

Time = 0

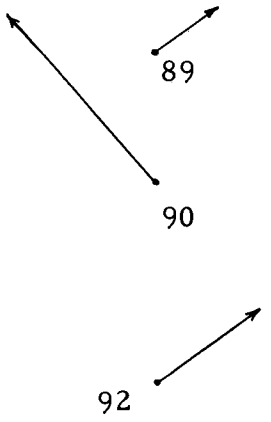

Time = 1/4 constituent period

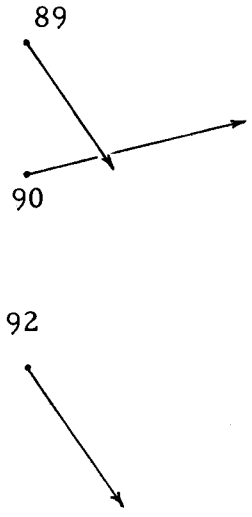

Time = 1/2 constituent period

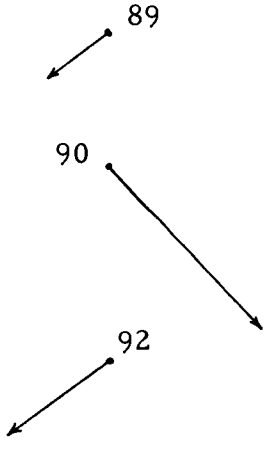

Time = 3/4 constituent period

Figure 27. Relative position and strength of the velocity vector at the 0.321 cy/hr. frequency.

where dy is the segment over which the depth can be assumed constant.

As it is not immediately obvious how a standing wave might be set up in the Sound, a calculation for two different sections was made. The first was a section taken normal to the "Talweg" mentioned in Chapter 7 which passed through the geographic position of station 90. The second was also perpendicular to the "talweg" but it corresponded to section 21 on Figure 30. The latter provides a slightly larger value of 1. The two cross sections are illustrated in Figure 30 with the calculations shown in Table IX and X. A value of three feet was added to the charted depths to approximate a change from mean low water to a value of mean sea level.

The above calculations yielded periods of 1.2 hours and 1.5 hours for the section through 90 and the section corresponding to Section 21. There are several peaks indicated on the spectra of the three stations which correspond to periods between one and two hours. However, the frequencies of 0.515 cy/hr. and 0.682 cy/hr. are perhaps the most suggestive of a transverse seiche. Both frequencies appear extremely strong on the north component of station 90. Station 90 also has the same peaks accentuated on the east component. The u component of both frequencies is highly correlated with the v component of the same frequency and in each case the u and v components of the respective frequencies are nearly in phase. Since the

Table IX. Transverse Seiche - Section Through Station 90

Subsection	Ave. Depth, h feet	Δy n. m.	$(h)^{1/2}$	$\Delta y/(h)^{1/2}$
1	11.5	0.60	3.40	0.176
2	23	0.41	4.80	0.085
3	23	0.11	4.80	0.023
4	28	0.65	5.29	0.123
5	39.5	1.48	6.30	0.235
6	60.5	0.99	7.79	0.127
7	83	1.00	9.11	0.110
8	90.5	0.50	9.53	0.052
9	92	0.60	9.59	0.063
10	82	1.56	9.06	0.172
11	75.5	1.01	8.70	0.116
12	91.5	1.60	9.58	0.167
13	93.5	1.40	9.69	0.144
14	97	0.38	9.85	0.039
15	92	0.47	9.59	0.049
16	71	0.38	8.43	0.045
17	57.5	0.49	7.60	0.064
18	39.5	0.14	6.30	0.022
19	28	0.35	5.29	0.066
20	15.5	0.19	4.06	0.047
21	12	0.46	3.46	0.133
		$\Sigma = 14.77$		$\Sigma = 2.058$

$$T_1 = 2\int_0^1 \frac{dy}{(gh)^{1/2}} = 2\frac{\Sigma \Delta y}{(gh)^{1/2}}$$

$$= 0.59564 \quad \frac{\Delta y}{(h)^{1/2}} = 1.226 \text{ hours}$$

Table X. Transverse Seiche Along Section 20

Subsection	Ave. Depth feet	Δy n. m.	$(h)^{1/2}$	$\Delta y/(h)^{1/2}$
1	7.5	0.40	2.74	0.146
2	19	0.85	4.36	0.195
3	23	0.29	4.80	0.060
4	25	0.60	5.00	0.120
5	32	0.20	5.66	0.035
6	40	1.23	6.32	0.195
7	4.95	0.97	7.05	0.138
8	63.5	0.59	7.98	0.074
9	73.5	0.39	8.59	0.045
10	88.5	1.65	9.43	0.175
11	97.5	2.37	9.89	0.240
12	92	1.51	9.59	0.157
13	83	2.89	9.11	0.317
14	77	0.48	8.78	0.055
15	68.5	1.58	8.29	0.191
16	61	0.58	7.81	0.074
17	47	0.84	6.86	0.122
18	28	0.28	5.29	0.053
19	17	0.12	4.36	0.028
20	5.5	0.22	2.35	0.094
		$\Sigma = 18.04$		$\Sigma = 2.514$

$T_1 = 0.59564$

$= 1.497$ hours

seiche is not expected to be exactly in a north-south direction, energy should be found on both components with the north-south component exhibiting most of the energy. This condition is found.

As current data is being used, little energy should be found at the boundaries with the maximum amount near the center for an uninodal seiche. If the seiche is binodal, energy from the current should be a minimum at the center. Station 90 is not exactly in the center of the channel, so that it should exhibit significant energy if the seiche is uninodal or binodal. The phases for the northerly components of the two frequencies under consideration are plotted below.

A uninodal and a binodal wave are sketched for the 0.515 cy/hr. and 0.682 cy/hr. frequencies, respectively. The phase relationships shown at the three stations approximately fit these two seiches. A perfect fit could hardly be expected when the geographic positions of the observations lie along a true meridian and the suspected transverse seiches lie along a line oriented 334^{o} T. Secondly, the band averaging process would tend to distort the relationships of motions due solely to the natural periods of oscillation.

Mention should also be made that the spectra and cross spectra do not agree closely with theory in that the period of the binodal seiche is not half that of the uninodal seiche. In this regard it might be that the irregularity of the topography is such that several transverse oscillations are set up following independent paths. There also

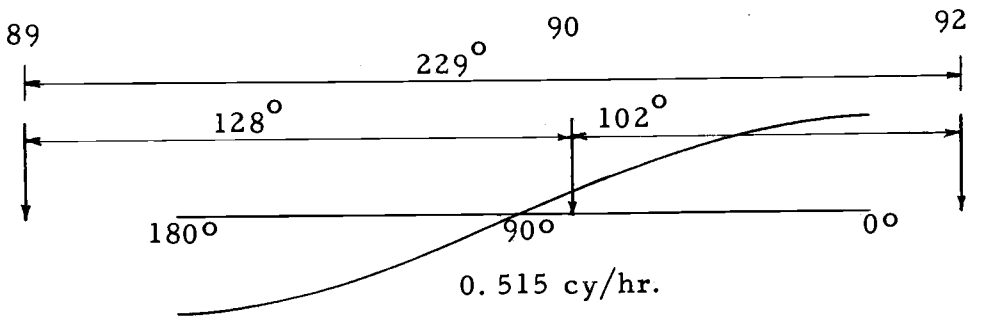

Station 92 considered as leading 89 and 90, and 90 leading 89.

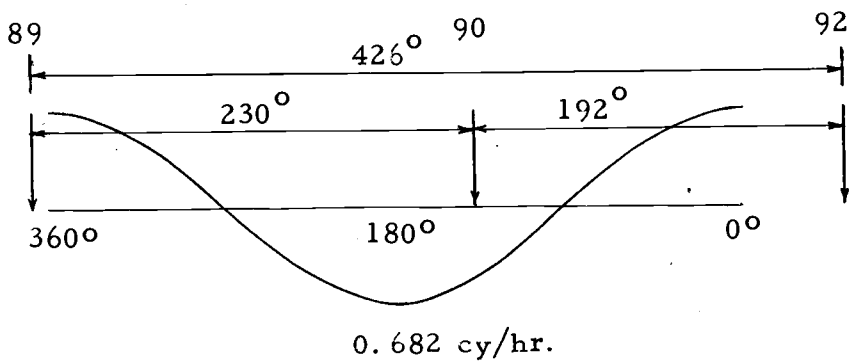

Figure 28. Phase relationships of the northerly component of the 0.515 cy/hr. and 0.682 cy/hr. frequencies.

appears to be little known as to what governs the numbers of nodes in a particular seiche.

At frequencies greater than 1 cy/hr. there is considerable noise in the spectra. In fact, at stations 89 and 92 the fluctuations in the spectra appear to increase after having a tendency to decrease until 1 cy/hr. It is also evident that the inshore stations are more noisy than station 90. Even though there are a few peaks that are significant, such as at 1.280 cy/hr. on 90, there is little indication of any overall relationship between the several sets of observations.

The noise at these high frequencies is undoubtedly due to local variations in the medium.

Results of Spectra on Wind Data

A study of currents is not complete without an investigation of the relationship of the wind field on the currents. The Falkner Island Light Station observed wind data throughout the period of observations at the three current station locations. Data was obtained every three hours throughout the day.

Spectral analysis of the wind data was performed using BMDO2T which had been modified in order to use a Tukey-Hanning spectral window. Two fifteen-day series consisting of 119 data points were run corresponding to 1600 August 30 to 1600 September 14 and 1600 September 2 to 1600 September 17. These periods coincided with

current data at station 90 and stations 89 and 92. Since the data series was short a lag of m = n/6 was chosen which is nearly a value of 20. The effective degrees of freedom is

$$k = \frac{8}{3}\frac{n}{m} \tag{6-23}$$

or 16 (Jenkins and Watts, 1969).

The power spectral estimates of the north and east component of the two series are shown in Table XI. Agreement between the two sets of curves is close as one would expect since the data was identical for 80% of the records. Little power is noticeable above the continuum. There is an indication of a peak at the 0.042 cy/hr. frequency which corresponds to a daily cycle.

Cross spectra between the east components of residual current and the north and east components of wind were run on each current series. The northerly components were treated similarly. Three hour running averages of the residual current data were centered on the time of the wind observations. This approach was used since it would be difficult to select a point to point comparison, due to any possible lag that might occur between the application of the wind stress and reaction by the hydrosphere. The value of these calculations were questionable from the beginning, due to the limited amount of wind data and also because of the location of the current observations.

There were significant peaks in the cross spectral

Table XI. Spectra for North and East Components of Wind - Falkner Island

Frequency cy/hr	In Power Spectral Estimates			
	August 30-September 14		September 2-September 17	
	u	v	u	v
0	6.84	5.75	7.14	6.02
0.008	6.89	5.99	7.21	6.28
0.017	6.41	5.90	6.70	6.03
0.025	5.16	5.04	5.63	4.86
0.033	4.55	4.86	4.86	4.62
0.042	4.77	5.20	4.93	5.17
0.050	4.49	4.55	4.68	4.78
0.058	3.63	4.09	3.98	4.14
0.067	3.68	3.96	4.00	3.99
0.075	3.64	3.68	3.91	3.59
0.083	3.31	3.18	3.44	3.13
0.092	3.13	2.69	3.31	3.05
0.100	3.44	2.67	3.31	2.67
0.108	3.20	2.85	2.94	2.50
0.117	2.34	3.10	2.09	3.18
0.125	2.32	3.24	2.34	3.51
0.133	2.69	3.22	2.74	3.36
0.142	2.23	3.43	2.67	3.34
0.150	2.53	3.28	2.66	3.04
0.158	3.44	2.93	3.31	2.49

representations. However, it was doubtful if these peaks were the result of dependence of current on wind. Coherence square between wind and current was generally quite low. The largest value for coherence square was 0.666 for the 0.0167 cy/hr. frequency of the u component of station 89. The wind in this case led the current by nearly 180^{o}. There is little doubt that wind does have an effect on the current. For example, recall that the maximum residuals for stations 89 and 92 occurred during the times of high wind speeds. Also the high frequency fluctuations in the spectra generated by the FFT are likely associated with the wind. The lack of conclusive evidence from the approach taken in this paper perhaps can be explained by one or a combination of the three following suggestions. First, the wind field as represented by the data collected at Falkner Island does not have an ordered effect on the residual currents at the given locations. Local wind observations might lead to a more appropriate approach. Second, the wind field might have been so variable that three hour wind observations and running averages of the residual currents provide insufficient information for conclusive results. It was noted previously that inertial currents were not in evidence in the spectra of the residual currents. At that time it was suggested that rapid variability in the wind field might prevent the inertial currents from being established. The cross spectra of wind and current seem to further substantiate this point of view. Thirdly, the running average

scheme used on the current data effectively filters out the frequencies much greater than one cycle per day (Figure 24) resulting in a poor input for a cross spectral analysis.

CHAPTER 7. LONG ISLAND SOUND - A COOSCILLATING SYSTEM

Resonance of Long Island Sound

Earlier mention was made of the fact that Long Island Sound is a cooscillating tidal basin. LeLacheur and Sammons (1932) approximated the natural period, assuming that the bay was rectangular with a mean depth of 71 feet. The length of the bay was considered to be the distance between Little Gull Island Light and Throgs Neck, approximately 82 nautical miles (n. m.). Using the formula for the period of a stationary wave in a rectangular bay, where L = length, h = depth, and g = acceleration of gravity,

$$T = \frac{4L}{(gh)^{1/2}} \qquad (7\text{-}1)$$

a value of 11. 6 hours was obtained as the period of oscillation. This is at best a crude approximation.

A much better approximation can be found by using Defant's method for determining the seiche characteristics of an irregularly-shaped lake or bay. In the case of a bay, the seiche is assumed to travel along the "Talweg" or the deepest portions of the basin. Cross sections normal to the "Talweg" can then be constructed. In this manner the bay is divided into small sections such that the equation of continuity can be applied for approximating the change in elevation of the free surface by the gain or loss of the volume of water through

the bounding cross sections. Linear theory with an incompressible fluid is assumed. The boundary conditions are known, or can be assumed to be such that with a trial value for the period of oscillation successive iterations will yield improvements to the initial period (Defant, 1961).

Defant's method for computing the period of oscillation for a bay has been applied to Long Island Sound, using roughly the same boundaries as previously described in this section. The basic equations are:

$$\eta_{n+1} = \eta_n + (\xi_n + \xi_{n+1})\ (\alpha/2) \tag{7-2}$$

$$Q_{n+1} = Q_n + V_{n+1}\ (\eta_n + \eta_{n+1})/2 \tag{7-3}$$

$$\xi_{n+1} = \frac{-1}{(S_{n+1} + \alpha V_{n+1}/4)} \left[Q_n + (\eta_n + \alpha \xi_n/4) V_{n+1}\right] \tag{7-4}$$

where η_n, Q_n and ξ_n represent the vertical displacement of water particles, the volume of water passing and the horizontal displacement of water particles all at the $n^{\underline{th}}$ cross section. The $n^{\underline{th}}$ cross-sectional area and the $n^{\underline{th}}$ surface area of the water body are denoted by S_n and V_n, respectively. The terminology is depicted in Figure 29. Previously, the calculation was tedious and time-consuming, but fortunately a computer program has been developed to assist in finding the solution with relative ease (Fee, 1968). A subdivision of a basin into ten to twenty sections has yielded results for the uninodal

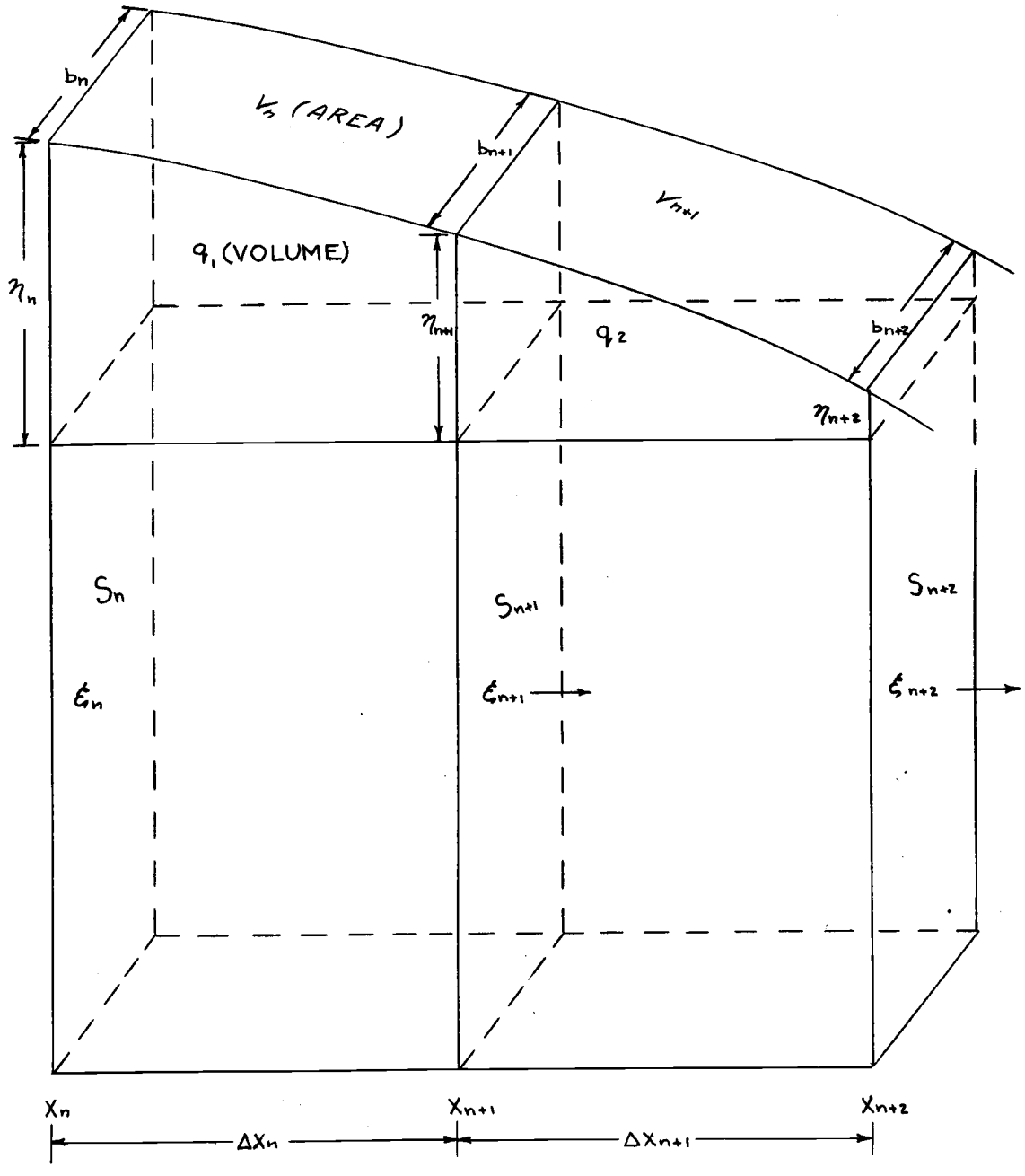

after (Fee, 1968)

Figure 29. Terminology for seiche program.

seiche which was 99% that of the same basin with 160 sections (Fee and Bachmann, 1968). Using this as a basis and also the consideration of the possibility that multinodal conditions might exist, 33 sections were used for Long Island Sound. The program does not allow for a mouth correction in the case of a bay. Using Fee's program and subroutine the first six modes of oscillation were computed (although only the first two were probably meaningful). The subroutine actually is designed for the first five, but for some unknown reason it would only yield results for the second through sixth modes. Consequently, the program for a lake was used assuming that the Sound was a lake, one end of which was a mirror image of the other end. Sixty-five sections were used in this case, where the first, second section, etc., were identical to the sixty-fifth, sixty-fourth, etc. The results seem to be quite satisfactory. The subdivision of Long Island Sound into sections is shown in Figure 30.

Inputs to Fee's program are the number of cross sections used, the area of the cross sections, the surface area of the bay between cross sections, the distance between cross sections and the acceleration due to gravity at the latitude of the lake. All distances and areas were measured from C&GS Chart Numbers 1211, 1212, and 1213. Charted depths were increased by three feet throughout the Sound (a mean value) to approximate mean tide level instead of mean low water. The mean latitude of the Sound was approximated as

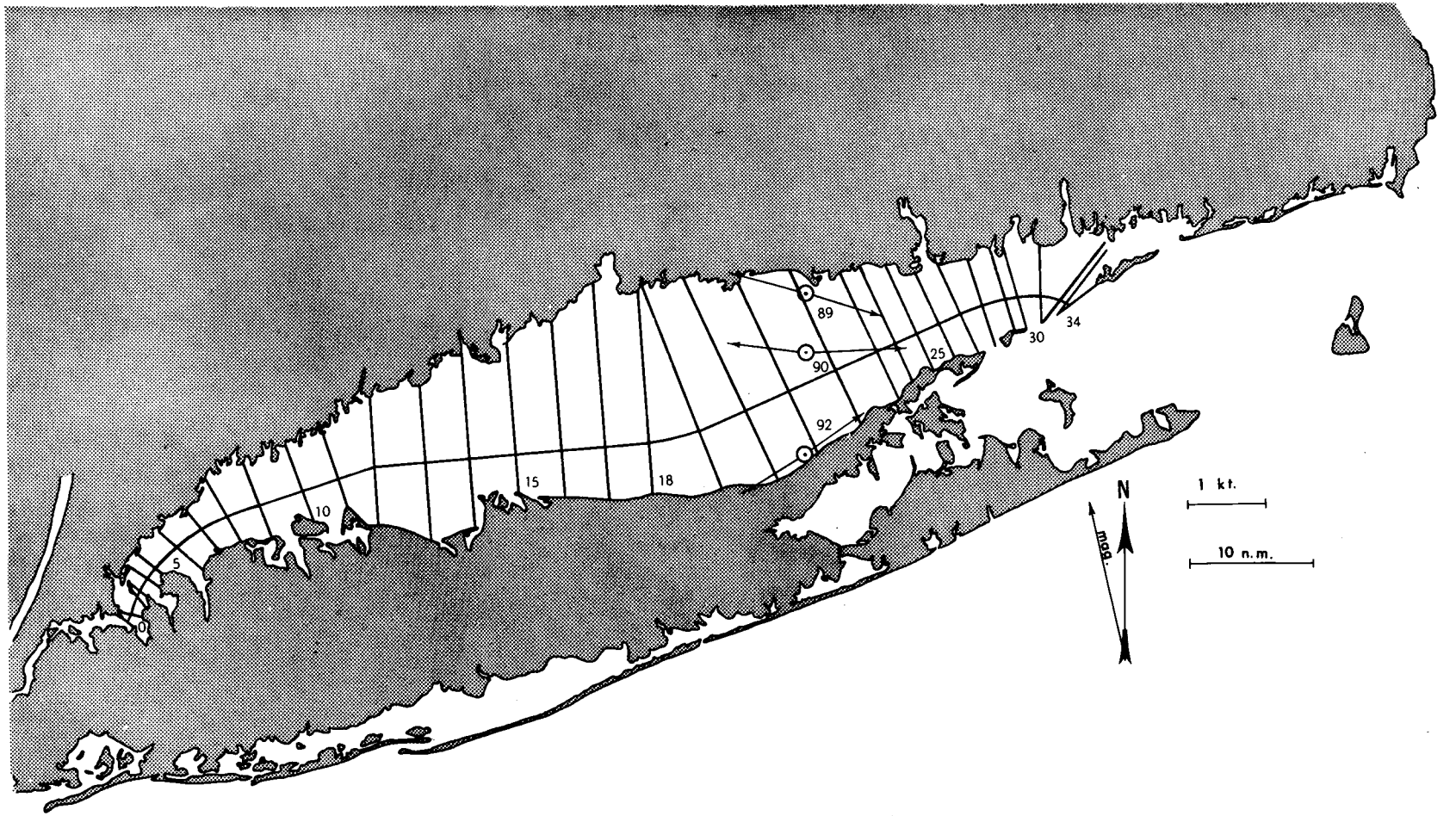

Figure 30. Long Island Sound showing sections used for seiche program — also showing positions of the average maximum vectors relative to the shoreline.

$41^{o}06'$N. The "international gravity formula" was used to compute the value of gravity for this specific latitude (Dobrin, 1960).

$$g = 978.049\ (1+0.0052884\ \sin^2\phi - 0.0000059\ \sin^2 2\phi) \qquad (7\text{-}5)$$

The value of g was found to be 980.201 cm/sec^2.

Output for the Defant method yields the relative vertical displacement, the relative volume of water passing and the relative horizontal displacement of a water particle at each section. In addition, the period of the seiche is approximated. The computed periods for the first three modes of oscillation are 9.77, 3.36, and 2.11 hours.

The first mode of oscillation is near that of the semidiurnal tide. The tidal oscillation and the seiche tend to complement one another in a cooscillating basin and the closer the seiche period approaches that of the tide the greater the tidal height becomes (Defant, 1958).

An estimation of the expected tidal amplitudes can be made by examining the equations of motion. If a long rectangular bay with a constant depth is assumed, the horizontal and vertical displacement of a wave in the bay which satisfies the equations of motion and continuity are respectively:

$$\xi = 2a \sin\frac{\sigma}{c} x \cos(\sigma t+\epsilon) \qquad (7\text{-}6)$$

$$\eta = -2ah\frac{\sigma}{c}\cos\frac{\sigma}{c} x \cos(\sigma t+\epsilon) \qquad (7\text{-}7)$$

Friction and the rotation of the earth have been ignored (Sverdrup, Johnson, and Fleming, 1942). The wave amplitude is "a," depth is h, the angular velocity of the water particle is $\sigma = \frac{2\pi}{T}$ and c is the velocity of propagation of a shallow water wave and is equal to $(gh)^{1/2}$. The boundary conditions for the cooscillating tide are such that the horizontal displacement is zero at the closed end where x = 0; and the vertical displacement at the open end where x = 1 follows that of the tide in the open ocean, $\eta = Z\cos(\sigma t + \epsilon)$. The symbol Z is the amplitude of the tide at the open end.

The value of "a" can be determined using this latter boundary condition

$$= Z\cos(\sigma t+\epsilon) = -2ah\frac{\sigma}{c}\cos\frac{\sigma}{c}1\cos(\sigma t+\epsilon)$$

$$a = \frac{-Zc}{2\sigma h\cos\frac{\sigma 1}{c}} \qquad (7\text{-}8)$$

The period of the seiche can be approximated by $T_f = \frac{41}{C}$ while that of the tide is $T_c = \frac{2\pi}{\sigma}$. The ratio of T_f to T_c is

$$\nu = \frac{T_f}{T_c} = \frac{41/c}{2\pi/\sigma} = \frac{2\sigma 1}{c\pi}$$

so that $$\frac{\sigma}{c} = \frac{\pi\nu}{21}.$$

Also letting y = x/l, these ratios can be substituted into the equations for the horizontal and vertical displacements to give expressions for the cooscillating tide as follows:

$$\xi = -Z \frac{1}{h\pi\nu} \frac{\sin 1/2\pi\nu y}{\cos 1/2\,\pi\nu} \cos(\sigma t+\epsilon) \qquad (7\text{-}9)$$

$$\eta = Z \frac{\cos 1/2\pi\nu y}{\cos 1/2\pi\nu} \cos(\sigma t+\epsilon) \qquad (7\text{-}10)$$

(Sverdrup, 1942).

By knowing the range of tide at the open ocean the expected maximum and minimum tidal heights can be easily found. The mean range at Silver Eel Pond on Fishers Island is 2.3 feet (United States Coast and Geodetic Survey, 1966b). The amplitude Z is therefore 1.15 feet. From examination of the tidal current analysis done previously, it is clear that M_2 is by far the predominating constituent. Consequently, its period of 12.42 hours will be used for that of the tide in computing the cooscillation.

Comparison of Computed and Observed Tidal Amplitudes

Table XII shows the expected tidal heights due to cooscillation at each cross section. These values are plotted in Figure 31. Note that the heights are plotted versus section number so that the shape of the wave appears slightly distorted.

In order to indicate the sensitivity of the equation several points have been plotted on the graph for seiche periods of 9.0 and 11.0 hours giving values of ν of 0.724 and 0.885, respectively. It is apparent that the equation for the cooscillation is very sensitive to changes in the resonance period.

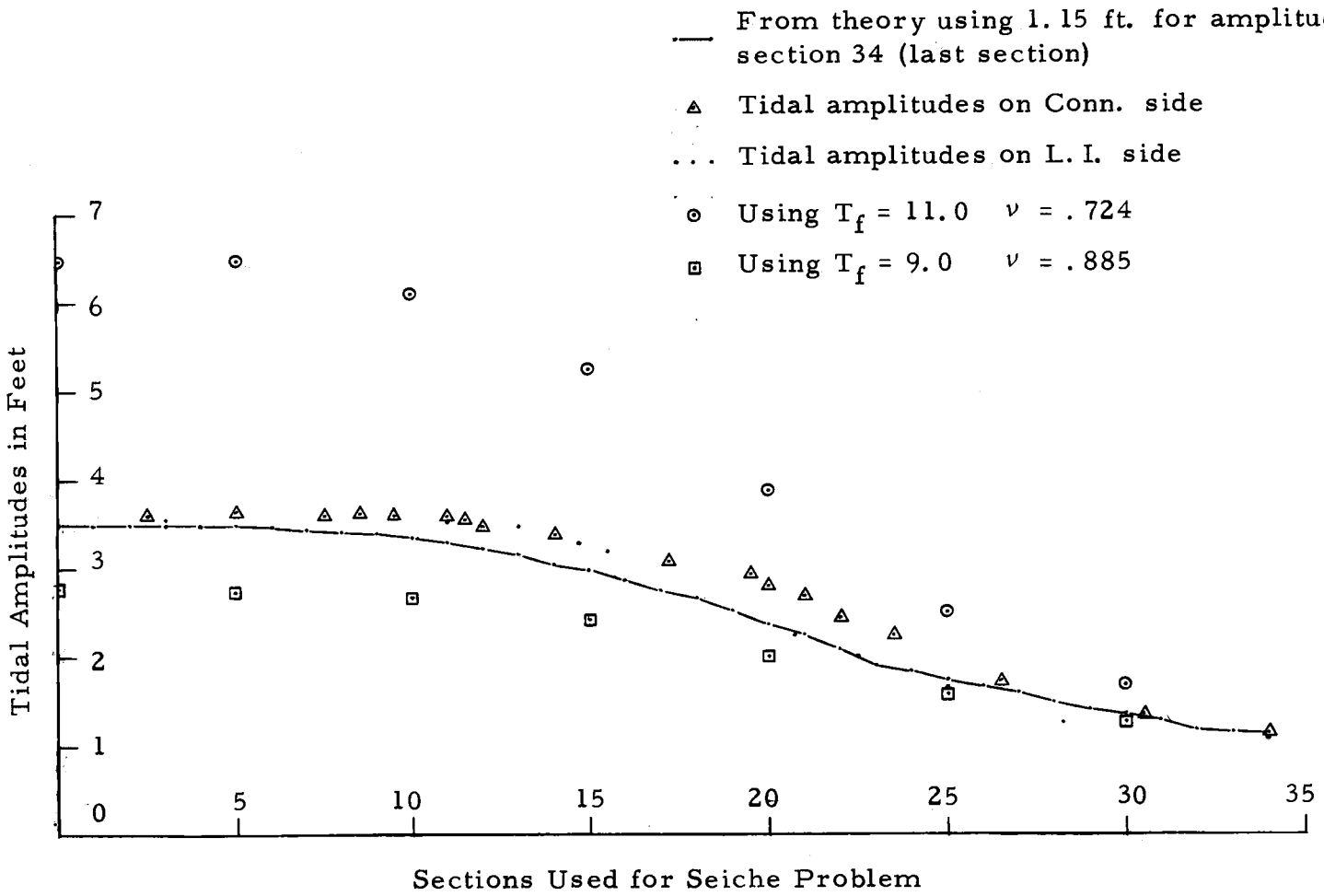

Figure 31. Cooscillating tide in Long Island Sound.

Table XII. Computations for Cooscillating Tide in Long Island Sound

Section	Dist to Section x in n. m.	x/y	$1/2\pi\nu y$	cos $1/2\pi\nu y$	Amplitude of Cooscillation Wave (feet) $Z\frac{\cos 1/2\pi\nu y}{\cos 1/2\pi\nu}$
0	0	0	0	1.000	3.48
1	0.76	0.009	0.637	0.9999	3.48
2	1.89	0.022	1.557	0.9996	3.48
3	2.74	0.032	2.262	0.9992	3.48
4	3.74	0.044	3.112	0.9985	3.48
5	4.85	0.057	4.03	0.9976	3.48
6	7.10	0.083	5.87	0.9947	3.46
7	9.84	0.115	8.13	0.9900	3.45
8	11.95	0.140	9.90	0.9851	3.43
9	14.99	0.176	12.45	0.9767	3.40
10	18.47	0.216	15.29	0.9646	3.36
11	21.57	0.253	17.90	0.9512	3.30
12	25.06	0.294	20.80	0.9348	3.25
13	29.10	0.341	24.13	0.9128	3.17
14	32.89	0.386	27.30	0.8886	3.08
15	36.76	0.431	30.48	0.8616	3.00
16	40.62	0.477	33.78	0.8310	2.88
17	44.47	0.522	36.93	0.7997	2.77
18	48.32	0.566	40.01	0.7660	2.66
19	52.21	0.612	43.3	0.7278	2.53
20	56.07	0.659	46.6	0.6871	2.38
21	59.93	0.696	49.3	0.6521	2.26
22	63.79	0.747	52.9	0.6032	2.10

Table XII. Continued.

Section	Dist to Section x in n. m.	x/y	$1/2\pi\nu y$	$\cos 1/2\pi\nu y$	Amplitude of Cooscillation Wave (feet) $Z \frac{\cos 1/2\pi\nu y}{\cos 1/2\pi\nu}$
23	67.64	0.794	56.2	0.5563	1.93
24	69.62	0.817	57.8	0.5329	1.85
25	71.53	0.840	59.5	0.5075	1.76
26	73.46	0.862	61.0	0.4848	1.69
27	75.39	0.884	62.5	0.4617	1.61
28	77.28	0.906	64.1	0.4384	1.52
29	79.24	0.930	65.8	0.4099	1.42
30	80.34	0.941	66.6	0.3971	1.37
31	82.13	0.963	68.1	0.3730	1.30
32	84.27	0.989	70.0	0.3420	1.19
33	85.02	0.998	70.6	0.3322	1.15
34	85.27	1.000	70.7	0.3305	1.15

$l = 85.27$ n.m.
$\cos 1/2\pi\nu = \cos 1/2(180^{\circ} \times 0.786)$
$= \cos 70.7^{\circ} = 0.3305$
$\cos(\sigma t+\epsilon) = 1.000$

A comparison between the computed cooscillation and the mean tide range as recorded in Table 2 of the Tide Tables can be easily made. Location of the various gauging stations listed in the Tide Tables are referenced to the cross sections used previously. Pertinent information has been tabulated here in Table XIII and also plotted on Figure 31 for comparison purposes.

The fit of the theoretical curve as described by the cooscillation equation is close to the mean amplitudes recorded in the Tide Tables. The mean percentage difference between the latter at 35 locations in the Sound was 7. 1 with a standard deviation of 5. 0%. This is a good check on the assumptions and the computed seiche period.

Comparison of Computed and Observed Currents

Partial differentiation of Equation (7-9) with respect to time leads to an expression describing the horizontal velocity.

$$\xi = -Z\frac{l}{h\pi\nu}\,\frac{\sin 1/2\pi\nu y}{\cos 1/2\pi\nu}\,[\cos\sigma t\cos\epsilon - \sin\sigma t\sin\epsilon]$$

$$u = \frac{\partial\xi}{\partial t} = -Z\,\frac{l}{h\pi\nu}\,\frac{\sin 1/2\pi\nu y}{\cos 1/2\pi\nu}\,[-\sigma\sin\sigma t\cos\epsilon - \sigma\cos\sigma t\sin\epsilon]$$

$$= Z\,\frac{l\sigma}{h\pi\nu}\,\frac{\sin 1/2\pi\nu\, y}{\cos 1/2\pi\nu}\,\sin(\sigma t+\epsilon) \qquad (7\text{-}11)$$

The current will be maximum when $\frac{\partial u}{\partial t} = 0$

$$\frac{\partial u}{\partial t} = Z \frac{1\sigma^2}{h\pi\nu} \frac{\sin 1/2\pi\nu y}{\cos 1/2\pi\nu} \cos(\sigma t+\epsilon)$$

$$= Z \frac{1\sigma^2}{h\pi\nu} \frac{\sin 1/2\pi\nu y}{\cos 1/2\pi\nu} \cos(\sigma t+\epsilon) = 0$$

$$\frac{\partial u}{\partial t} = 0 \text{ when } \cos(\sigma t+\epsilon) = 0$$

or when $\sigma t + \epsilon = 0^{\circ}$.

$$U_{\text{maximum}} = Z \frac{1\sigma}{h\pi\nu} \frac{\sin 1/2\pi\nu y}{\cos 1/2\pi\nu} \tag{7-12}$$

A mean depth in the general vicinity of the observations was estimated to be 68. 3 feet. The value was found by meaning the average depths of sections 21 and 22 as computed by dividing the planimetered areas by the length of the cross sections which were 15, 11 n. m. and 13. 87 n. m., respectively. The distance along the "Talweg" to station 90 was taken to be 62. 2 n. m.

$$U_{\text{maximum}} = 1.15 \text{ ft.} \times \frac{\text{n. m.}}{6080 \text{ ft.}} \times \frac{2\pi}{12.42 \text{ hr.}} \times \frac{85.27 \text{ n. m.}}{68.3 \frac{\text{n. m.}}{6080 \text{ ft.}}} \frac{1}{\pi(0.786)}$$

$$\frac{\sin 1/2\pi\nu y}{\cos 1/2\pi\nu} = 0.294 \frac{\sin 51.6^{\circ}}{\cos 70.7^{\circ}}$$

$$= 0.696 \text{ kts.} \doteq 0.70 \text{ kts.}$$

This maximum current represents the average maximum value for the cross section. If it is assumed that the flow in midchannel is one-third greater than the average, the maximum velocity in midchannel is 0. 93 kts. (Sverdrup, Johnson, and Fleming, 1942).

Table XIII. Mean Tide Range and Amplitude for Selected Locations in Long Island Sound

Location	Pos. Relative to Sections	Mean Range Feet	Mean Amplitude Feet
Willets Point	0	7.1	3.55
Throngs Neck	0	7.0	3.50
City Island	2-1/2	7.2	3.60
Hewlett Point	3	7.1	3.55
Execution Rocks	5	7.3	3.65
Glen Cove, Hempstead Harbor	6*	7.3	3.65
Mamaroneck	6-1/4*	7.3	3.65
Rye Beach	7-1/2	7.2	3.60
Port Chester	8*	7.2	3.60
Great Captain Island	8-1/2	7.3	3.65
Greenwich	8-1/2*	7.4	3.70
Stamford	9-1/2	7.2	3.60
Greens Ledge	11	7.2	3.60
Eatons Point	11	7.1	3.55
South Norwalk	11-1/2	7.1	3.55
Saugatauk River Ent.	12	7.0	3.50
Nissequoque River Ent.	13	7.0	3.50
Bridgeport	14	6.8	3.40
Port Jefferson Harbor Ent.	14-3/4	6.6	3.30
Milford Harbor	15-1/2*	6.6	3.30
Mount Sinai Hbr.	15-1/2	6.4	3.20
New Haven Harbor Ent.	17-1/4	6.2	3.10
Branford Harbor	19-1/2	5.9	2.95
Money Island	20	5.6	2.80
Mattituck Inlet	20-3/4	4.5	2.25
Falkner Island	21	5.4	2.70
Madison	22	4.9	2.45
Horton Point	22-1/2	4.0	2.00
Duck Island	23-1/2	4.5	2.25
Truman Beach	25	3.4	1.70
Saybrook Jetty	26-1/2	3.5	1.75
Plum Gut Harbor, Plum I.	28-1/4	2.5	1.25

Table XII Continued

Location	Pos. Relative to Sections	Mean Range Feet	Mean Amplitude Feet
Millstone Point	30-1/2	2.7	1.35
Silver Eel Pond, Fisher I.	34	2.3	1.15
Little Gull I.	34	2.2	1.10

* Not in Long Island Sound proper

From the tidal ellipse in Figure 11 the maximum flood is 0. 95 kt. while the maximum ebb is somewhat greater at 1. 23 kts. Certainly the maximum flood agrees very well with the value computed above with only a percentage error of 2%. Ebb on the other hand has a percent error of nearly 24%.

The equation for velocity, however, fails to agree with observations at the eastern and western ends of the basin. At the western end the speed does not go to zero as there is communication with the Atlantic Ocean through the East River. Less obvious is the failure of the equation to estimate the speed in the vicinity of The Race.

Topography, however, plays a major role in this regard. If the Sound was a uniform dimension from the meridian of the three stations under examination to The Race, the maximum speed would be

$$U_{\text{maximum}} = 0.294 \frac{\sin 1/2\,\pi\nu y}{\cos 1/2\pi\nu} \text{ kts.}$$

$$= 0.294 \frac{\sin 1/2\pi\nu\,(1)}{\cos 1/2\pi\nu} = 0.84 \text{ kts.}$$

The ratio of the cross sectional areas, however, is:

$$\frac{\text{A Race}}{\text{A Station 90}} \approx \frac{415 \text{ n. m. -ft.}}{990 \text{ n. m. -ft.}} = 0.416$$

As velocity through a cross section is inversely proportional to area the expected speed at The Race should be:

$$U_{Race} = \frac{0.84 \text{ kts.}}{0.416} = 2.02 \text{ kts.}$$

Again, assuming the maximum flow in midchannel to be one-third greater than the average maximum, the maximum midchannel flow should be approximately 2. 7 kts. The average maximum flood and ebb as determined most recently by the Coast and Geodetic Survey was 2. 6 kts. and 3. 5 kts., respectively.

It must be remembered that flow was considered to occur from the surface to the bottom, an assumption that cannot be confirmed by this study as measurements were only obtained at the surface. There is certainly some evidence that a weak two-layered system might exist particularly in the central part of Long Island Sound (Riley, 1967). Inflow might well be greater to the west through The Race along the bottom and outflow greater at the surface. This condition could be expected to be more pronounced during the summer months. If this is the case, then a certain deviation from the above estimated currents is reasonable. In fact the expected result would be that the equations for speed at the surface would overestimate at flood and underestimate on ebb.

Discussion

Redfield (1950) has noted that the stationary wave theory for narrow coastal embayments does not hold up when the times of high,

low, and slack water as determined from theory are compared to the observed times. He has devised a method for determining position and damping of the wave along the channel from observed tidal data. Redfield's examination of Long Island Sound led to the conclusion that the boundary at the western end was in the vicinity of Great Captain Island or near section eight in Figure 30. The nodal line or 90^{o} phase difference from the western boundary lies between Montauk Point and roughly Weekapaug Point, Rhode Island.

The difference in the position of the node between this study and Redfield's leads to some interesting questions. Seemingly the selection of The Race as the approximate location of the node would be more logical considering the topography of the area. Also the location of the western boundary in the vicinity of Great Captain Island is surprising considering the topography, i. e., no physical barrier exists.

Consequently, an additional computation of the seiche program was run using section 6 as the point of reflection which is in the area of Glen Cove. The seiche period is 9.01 hours. This lies close to the curve at 9.0 hours plotted in Figure 31 which was used to indicate the sensitivity of the cooscillation equation. From this it appears that the node could be moved to the east. However, the program is sensitive to large volume changes between sections. East of The Race the width and depth of the basin increases. Therefore, the

node could not be moved a great deal and still obtain the close agreement between the observed tidal elevations and those predicted by the cooscillation equation.

Further, the range of tide east of The Race to a line connecting Montauk Point and Block Island is roughly 2.3 feet. This is indicative of a progressive wave as the range is nearly constant.

At this point it appears that the assumption made originally by LeLacheur and Sammons is correct. That is, the distance between Throgs Neck and The Race represents one-quarter wave length of a standing wave with the node at The Race. The slight decrease in the range of tide found in the western end of Long Island Sound beginning near Execution Rocks is probably the result of a modification of the cooscillation due to the effects of the communication of the Atlantic Ocean through the East River superimposed upon the characteristics of the Sound. This is opposed to the supposition that the point of reflection is near Glen Cove or Great Captain Island.

Certainly the argument concerning the location of the node and antinode for the cooscillating wave needs more documentation to be adequately answered, and I feel that enough evidence has been presented here to reopen the discussion.

CHAPTER 8. SUMMARY

The currents in Long Island Sound are primarily tidal in nature. The major flows are semidiurnal and are greatly influenced by the topography in such a manner that the tidal current ellipses are degenerate resulting in reversing currents along the coasts. The mid-channel flow, however, is definitely rotary. In the central portion of the Sound, the observations indicate that maximum ebb occurs along the shore before it does in mid-channel. The flood, on the other hand, reaches its maximum at station 92 first. There is a very pronounced lead in both the maximum ebb and flood along the Connecticut shoreline, as compared to the southern half of the Sound at this particular cross section.

The inertial frequency did not appear to be significant during the period of observations although conditions possibly existed for initiating the motion. Numerous other frequencies did appear in the spectra of the residual current. For the most part these were compound tides and overtides.

Spectral techniques also indicated that transverse seiches might exist. A uninodal seiche in the area of observations appears possible with a frequency of 0. 515 cy/hr. while a binodal seiche might be present with a frequency of 0. 682 cy/hr.

Correlation of wind and current was attempted but the results

were inconclusive primarily because of insufficient wind observations. However, some of the high frequency noise indicated by the spectra of current data is probably the result of meteorological disturbances.

Tidal heights indicate that Long Island Sound behaves as a co-oscillating tidal system having a minimum range at a nodal point and a maximum tidal range at the head. Obviously, the East River which connects the Sound with the Atlantic Ocean, modifies the ideal characteristics. If the node is considered to occur in the vicinity of The Race, where the tide range is the least and the current speeds the greatest, the observed tidal heights fit well with the cooscillating theory. Observed currents in the central portion of the Sound also agree closely with that which is predicted from theory.

The project was extremely rewarding for me and hopefully will be of value to my sponser, the Coast and Geodetic Survey. As commanding officer of the USC&GSS MARMER in 1966, I participated in the data collection and have since closely followed the reduction and analysis of the data not only in this thesis but for inclusion in the Tidal Current Tables and also in the soon to be published Tidal Current Chart for Eastern Long Island Sound.

Before making further comments, I should again point out that the survey was the most extensive current observation program over such a large area done by the Coast and Geodetic Survey. In fact, it is doubtful that any of this magnitude has been accomplished by any

other organization or institution. Its purpose was to fulfill the needs of the C&GS nautical charting program which is to provide information essential for safe navigation. This the survey did more than adequately.

As an oceanographer, I greatly appreciate the value of the survey. I feel, however, that with a slight change of philosophy within the C&GS, the tidal current program can be modified to meet the needs of a broader spectrum of users.

This thesis points out two distinct areas in which worthwhile changes can be made. First, the data collected can be analyzed more thoroughly for extraction of information beyond that normally done in the traditional reversing current harmonic analysis. Second, collection of additional data in the field could be extremely useful. Vertical sections of current data along with the field of mass and wind would be extremely valuable for the study of coastal dynamics.

The public is becoming aware of the problems that confront humanity in the coastal zone. They are demanding solutions. However, before the solution is possible, there must be understanding of the processes at work in this area in order to provide a mechanism for intelligent management.

The Coast and Geodetic Survey has a nucleus of equipment and experience which can be utilized for more extensive research in the coastal zone. The Federal government could take advantage of this

capability and properly fund a comprehensive program of investigation of our estuarine and nearshore areas.

BIBLIOGRAPHY

1. Anscombe, F. J. Rejection of outliers. Technometrics, 2(2): 123-147. 1960.

2. Bendat, Julius S. and Allen G. Piersol. Measurement and analysis of random data. New York, Wiley, 1966. 390 p.

3. Blackman, R. B. and J. W. Tukey. The measurement of power spectra from the point of view of communications engineering. New York, Dover, 1959. 190 p.

4. Bogert, Bruce P., M. J. R. Healy and John W. Tukey. The quefrency alanysis of time series for echoes: cepstrum, pseudo-autocovariance, cross-cepstrum and saphe cracking. In: The SIAM series in applied mathematics: Proceedings of the symposium on time series analysis, Brown University, 1962, ed. by Murray Rosenblatt. New York, Wiley, 1963. p. 209-243.

5. Cochran, William T., et al. What is a fast fourier transform. IEEE Transactions on audio and electroacoustics AU-15(2): 45-55. 1967.

6. Defant, A. Ebb and flow. Ann Arbor, University of Michigan, 1958. 121 p.

7. Defant, A. Physical oceanography. Vol. 2. New York, Pergamon Press, 1961. 598 p.

8. Dietrich, Gunter. General oceanography, an introduction. New York, Interscience, 1963. 588 p.

9. Dixon, W. J. BMD biomedical computer programs. Los Angeles, University of California, 1965. 620 p.

10. Dobrin, Milton B. Introduction to geophysical prospecting. 2d ed. New York, McGraw-Hill, 1960. 446 p.

11. Doodson, A. T. and H. D. Warburg. Admiralty manual of tides. Corrected reprint. London, Her Majesty's Stationary Office, 1966. 270 p.

12. Dronkers, J. J. Tidal computations in rivers and coastal waters. Amsterdam, North Holland, 1964. 518 p.

13. Fee, Everett J. Digital computer programs for the Defant method of seiche analysis. Milwaukee, 1968. 27 numb. leaves. (The University of Wisconsin. Center for Great Lakes Studies. Special report no. 4)

14. Fee, Everett J. and Roger W. Bachmann. An emperical study of the Defant method of seiche analysis. Limnology and Oceanography, 13(4):665-669. 1968.

15. Geodyne Corporation. Instruction manual 100 DE current meter. Waltham, Mass., n. d., n. p. (TM66-52A)

16. Godin, Gabriel. The analysis of current observations. The International Hydrographic Review 44(1):149-165. January, 1967.

17. Granger, C. W. J. Spectral analysis of economic time series. Princeton, New Jersey, Princeton University Press, 1964. 299 p.

18. Hamming, Richard W. Numerical methods for scientists and engineers. New York, McGraw-Hill, 1962. 411 p.

19. Hogg, Robert V. and Allen T. Craig. Introduction to mathematical statistics. 2d ed. New York, Macmillan, 1965. p. 383.

20. Jenkins, Gwilym M. and Donald G. Watts. Spectral analysis and its applications. San Francisco, Holden-Day, 1969. 525 p.

21. Larkin, Richard R. and Gordon A. Riley. A drift bottle study in Long Island Sound. Bulletin of the Bingham Oceanographic Collection 19(2):62-71. April, 1967.

22. LeLacheur, E. A. and J. C. Sammons. Tides and currents in Long Island and Block Island Sounds. Washington, D. C., United States Government Printing Office, 1932. 184 p. (Special Publication no. 174)

23. Li, Jerome C. R. Introduction to statistical inference. Ann Arbor, Edwards Brothers, 1957. 568 p.

24. Munk, W. H., B. Zetler and G. W. Groves. Tidal cusps. Geophysical Journal, 10(2): 211-219. 1965.

25. Paquette, R. G. Practical problems in the direct measurement of ocean currents. In: Marine Sciences Instrumentation. Vol. 2. New York, Plenum Press, 1963. p. 135-146.

26. Proudman, J. Tides in a channel. Philosophical Magazine, 49: 465-475. 1925.

27. Redfield, A. C. The analysis of tidal phenomena in narrow embayments. Papers in Physical Oceanography and Meteorology, 11(4): 1-36. 1950.

28. Riley, Gordon A. Hydrography of the Long Island and Block Island Sounds. Bulletin of the Bingham Oceanographic Collection, 8(3): 5-39. July, 1952.

29. Riley, Gordon A. Transport and mixing processes in Long Island Sound. Bulletin of the Bingham Oceanographic Collection, 19(2):35-61. April, 1967.

30. Schureman, Paul. Manual of harmonic analysis and prediction of tides. Washington, D. C., United States Government Printing Office, 1941. 317 p.

31. Sverdrup, H. U., Martin W. Johnson and Richard H. Fleming. The Oceans, their physics, chemistry and general biology. Englewood Cliffs, N. J., Prentice-Hall, 1942. 1087 p.

32. Swanson, R. L. and R. H. Kerley. Performance tests of Richardson-type current meters, I. tests 1 through 7. Rockville, Md., 1970. 70 p. (ESSA C&GSTM 8)

33. Thomann, Robert V. Time series analysis of water quality data. Journal of the Sanitary Engineering Division, ASCE, 93(SA 1): 1-23. February, 1967.

34. United States Coast and Geodetic Survey. Manual of current observations. Washington, D. C., United States Government Printing Office, 1950. 87 p. (Special Publication no. 215)

35. United States Coast and Geodetic Survey. Tidal current charts, Long Island Sound and Block Island Sound. 4th ed. Washington, D. C. 1958.

36. United States Coast and Geodetic Survey. Supplement - Tidal current tables, Atlantic coast of North America, Block Island and Long Island Sounds, 1966a. Rockville, Md., 1966 a. n. p.

37. United States Coast and Geodetic Survey. Tide tables: High and low water predictions, east coast of North and South America, including Greenland, 1966. Washington, D. C., United States Government Printing Office, 1966b. 289 p.

38. Von Arx, William S. Introduction to physical oceanography. Reading, Mass., Addison-Wesley, 1962. 422 p.

39. Wiegal, Robert L. Oceanographical engineering. Englewood Cliffs, N. J., Prentice-Hall, 1964. 532 p.

40. Williams, R. G. The physical oceanography of Block Island Sound, A review report. New London, Conn., U. S. Navy Underwater Sound Laboratory, 1967. 15 numb. leaves. (USL Technical Memorandum No. 2213-33-67)

41. Zetler, B. D. and R. A. Cummings. A harmonic method for predicting shallow-water tides. Journal of Marine Research 25(1): 103-114. 1967.

42. Zetler, B. D. and G. W. Lennon. Some comparative tests of tidal analytical processes. The International Hydrographic Review, 44(1):139-147. January, 1967.

43. Zetler, B. D., M. D. Schuldt, R. W. Whipple and S. D. Hicks. Harmonic analysis of tides from data randomly spaced in time. Journal of Geophysical Research 70: 2805-2811. 1965.

APPENDICES

APPENDIX I

Numerical Example for Estimating Zero Crossing of Distorted Tidal Current Time Series

Assume that the anchor cable will form a straight line between anchor and buoy instead of an approximate catenary. For station 89 the sounded depth was 41 feet and the anchor cable was 100 feet.

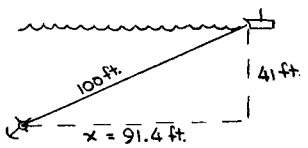

If the zero crossing for a current speed range of 1.9 kts. is desired the acceleration through slack is from Figure A $0.50 \frac{\text{n. m.}}{\text{hr.}^2}$.

horizontal dist. buoy must travel = $x = v_o + 1/2\ at^2$

$91.4 \text{ ft}/6080 \text{ ft/n. m.} = 0 \cdot t + 1/2\ (0.50 \frac{\text{n. m.}}{\text{hr.}^2})t^2$

$t = 0.245 \text{ hr.} = 14.7 \text{ min.}$

Speed at 14.7 minutes

$v = at$

$= .50 \frac{\text{n. m.}}{\text{hr.}^2}\ (.245 \text{ hr.}) = 0.122 \text{ kts.} \simeq 0.12 \text{ kts.}$

Therefore, it takes the buoy about 15 minutes to drift to its maximum position from the anchor at which time the speed of the current will be about 0.12 kts.

By using Figure B these calculations can be found directly by following the four indicated steps, entering the graph with only the

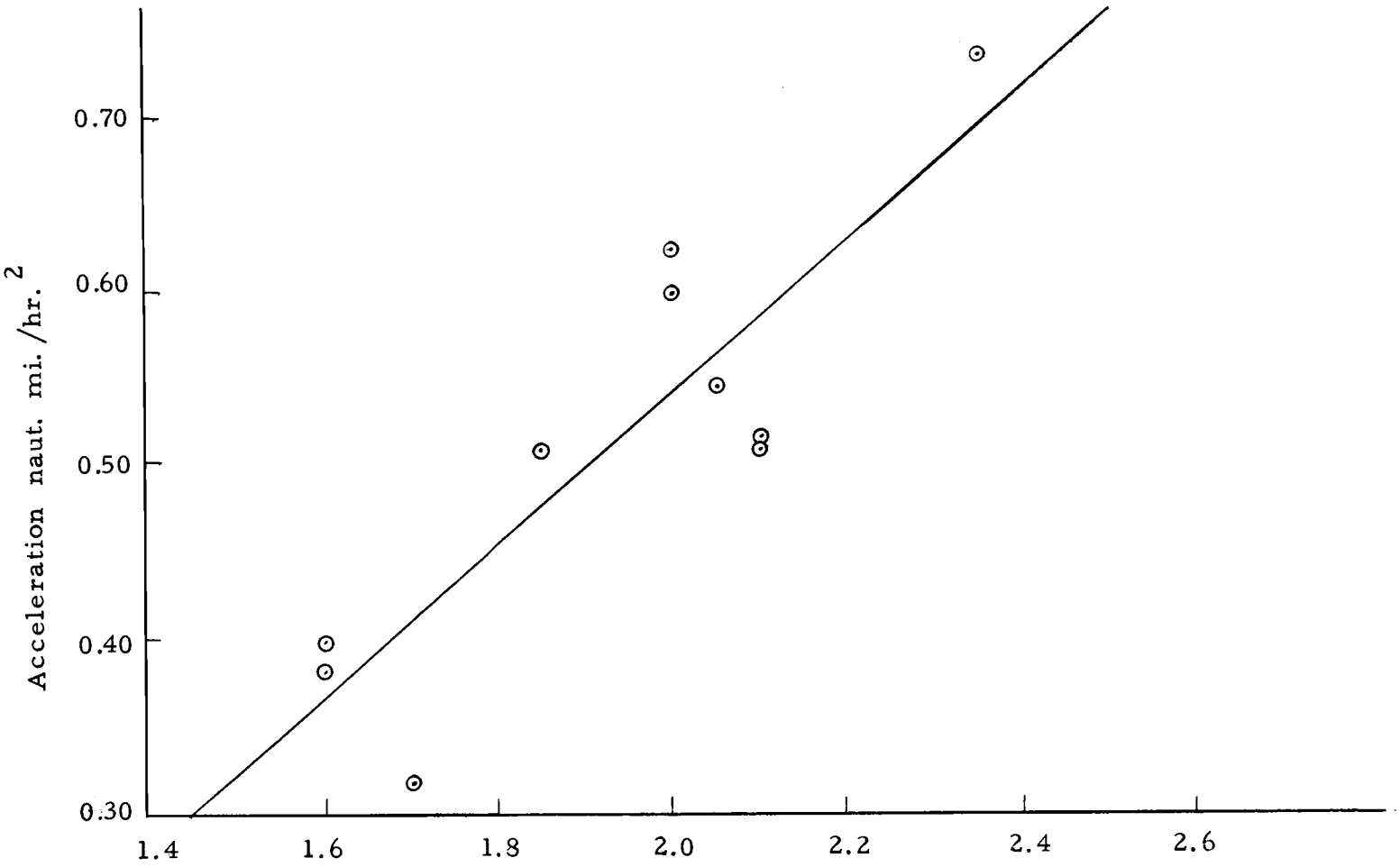

Figure A. Graph of acceleration through slack vs. range in speeds before and after slack for station 89.

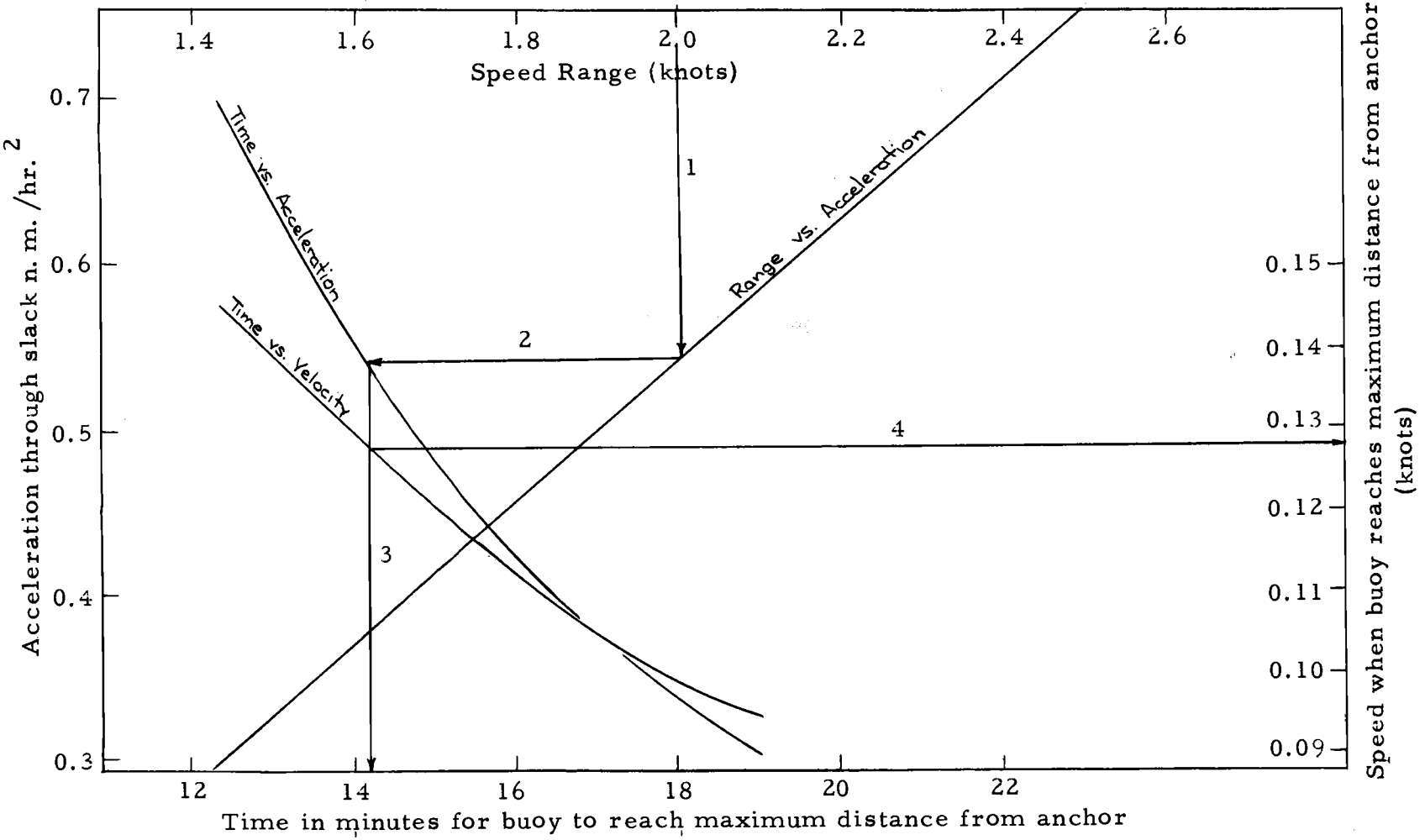

Figure B. Graph for determining time buoy takes to drift to its maximum distance from anchor and the speed of the current at that time.

speed range for the zero crossing in question.

The information can then be plotted by the desired method for selecting the time of slack and the simulated zero crossing is completed.

Figure C shows the actual use of the method for station 89 around 0900 on September 19.

The speed range is -0. 87 to +1. 03 or 1. 90 kts. Enter Figure B with 1. 90.

The time for the buoy to reach its maximum distance from the anchor or when it should begin to read correctly is 14. 7 minutes and the velocity at that time is 0. 122 kts. Plot these values from the selected time of slack. The straight line between the points determines the adjusted values of current speed.

Use the following values:

Time	Speed (kts.)
0840	-0. 13
0850	-0. 04
0910	+0. 04
0920	+0. 13

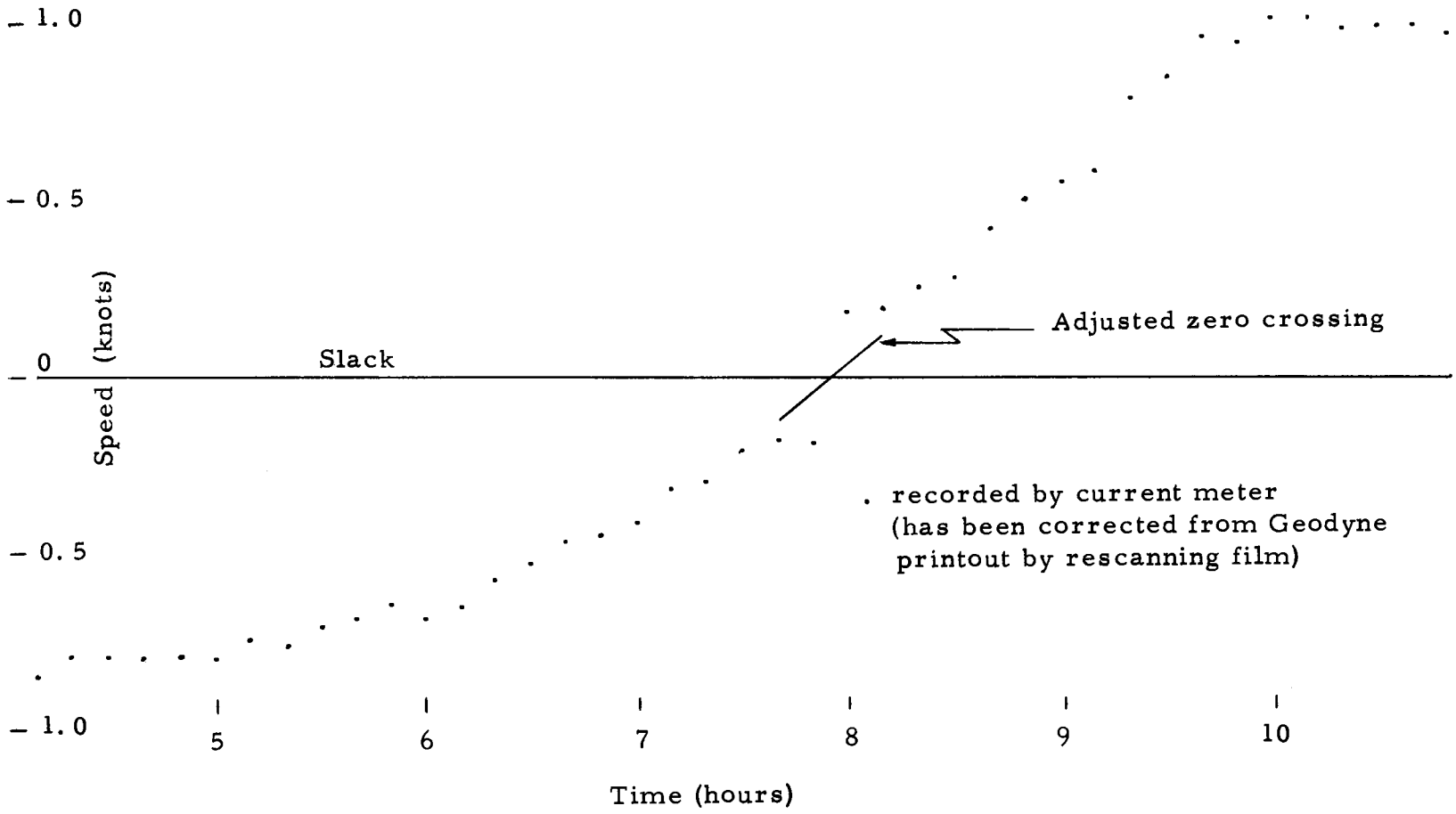

Figure C. Current curve - station 89, Sept. 19, 1968.

APPENDIX II

Observed Wind at Falkner Island

Date	Time (EDT)	Direction (Magnetic)	Speed (knots)	Date	Time (EDT)	Direction (Magnetic)	Speed (knots)
Aug 30	14	SW	10	Sept 2	02	NW	12
	17	SSE	15		05	W	10
	20	S	20		08	WSW	13
	23	S	18		11	W	15
Aug 31	02	SSW	20		14	WSW	12
	05	SW	5		17	SSW	12
	08	SW	10		20	W	12
	11	calm			23	SW	10
	14	SE	10	Sept 3	02	WNW	20
	17	E	5		05	NW	11
	20	NE	15		08	NE	23
	23	NE	20		11	ENE	18
Sept 1	02	NE	10		14	E	18
	05	NNW	12		17	E	22
	02	NE	10		20	E	25
	11	calm			23	NE	18
	14	missing		Sept 4	02	NE	25
	17	E	8		05	E	22
	20	NE	10		08	E	38
	23	NW	5		11	E	36

APPENDIX II Continued

Date	Time (EDT)	Direction (Magnetic)	Speed (knots)	Date	Time (EDT)	Direction (Magnetic)	Speed (knots)
	14	ESE	30				
	17	S	20		08	WNW	10
	20	S	19		11	NW	8
	23	SW	12		14	S	10
Sept 5	02	NW	12		17	SW	10
	05	W	8		20	SW	10
	08	SW	5		23	W	10
	11	SW	16	Sept 8	02	NW	16
	14	SW	20		05	WNW	20
	17	SSW	16		08	N	14
	20	S	14		11	NE	10
	23	SW	16		14	ENE	8
Sept 6	02	calm			17	N	10
	05	WSW	12		20	E	15
	08	SW	8		23	NNE	5
	11	SW	15	Sept 9	02	N	9
	14	SSW	18		05	NW	16
	17	SW	18		08	NW	14
	20	W	12		11	NW	18
	23	W	10		14	ENE	4
Sept 7	02	SW	7		17	SSW	8
	05	NW	8		20	SW	9

APPENDIX II Continued

Date	Time (EDT)	Direction (Magnetic)	Speed (knots)	Date	Time (EDT)	Direction (Magnetic)	Speed (knots)
	23	WSW	18		14	SE	5
Sept 10	02	NNW	16		17	SE	12
	05	W	14		20	SE	12
	08	WNW	18		23	SE	15
	11	WNW	12	Sept 13	02	SE	15
	14	S	15		05	ESE	15
	17	WSW	10		08	SE	20
	20	W	10		11	SE	5
	23	W	20		14	ESE	15
Sept 11	02	W	17		17	ESE	15
	05	W	15		20	ESE	15
	08	WNW	15		23	ESE	17
	11	NW	20	Sept 14	02	ESE	18
	14	NW	24		05	E	14
	17	N	24		08	E	22
	20	N	15		11	NE	19
	23	N	12		14	NE	25
Sept 12	02	N	15		17	NE	30
	05	NNW	15		20	ENE	28
	08	NNW	17		23	ENE	30
	11	ENE	10	Sept 15	02	N	25

APPENDIX II Continued

Date	Time (EDT)	Direction (Magnetic)	Speed (knots)
	05	NNW	30
	08	NW	35
	11	NW	33
	14	W	15
	17	W	22
	20	W	30
	23	W	33
Sept 16	02	WNW	20
	05	W	20
	08	W	18
	11	NW	14
	14	S	8
	17	SSW	7
	20	W	15
	23	NW	10
Sept 17	02	WNW	13
	05	WNW	10
	08	WNW	8
	11	calm	
	14	SSE	10
	17	SSW	10

APPENDIX III

Tidal or Tidal Current Constituents

Constituent	Source
J_1	Smaller lunar elliptic
K_1	Lunisolar diurnal
K_2	Lunisolar semidiurnal
L_2	Smaller lunar elliptic
M_1	Smaller lunar elliptic
M_2	Principal lunar
M_3	Lunar terdiurnal term
M_4	Lunar quarter diur nal term
M_6	Lunar sixth diurnal term
M_8	Lunar eighth diurnal term
N_2	Larger lunar elliptic
$2N_2$	Lunar elliptic second order
O_1	Principal lunar diurnal
OO	Lunar diurnal term
P_1	Principal solar diurnal
Q_1	Larger lunar elliptic
2Q	Lunar diurnal term
R_2	Solar semidiurnal term
S_1	Solar diurnal term
S_2	Principal solar
S_4	Solar quarter diurnal term
S_6	Solar sixth diurnal term
T_2	Larger solar elliptic
λ_2	Smaller lunar evectional
μ_2	Variational
ν_2	Larger lunar evectional
ρ_1	Lunar diurnal term

(Schureman, 1941)
(Defant, 1961)

APPENDIX IV

Source of Overtides

Compound Tidal Constituent	Source
MN_4	M_2+N_2
$MNKS_4$	$M_2+N_2+K_2-S_2$
SN_4	S_2+N_2
KN_4	K_2+N_2
MS_4	M_2+S_2
MK_4	M_2+K_2
SL_4	S_2+L_2
MNO_5	$M_2+N_2+O_1$
$2MO_5$	$2M_2+O_1$
$3MP_5$	$3M_2-P_1$
MNK_5	$M_2+N_2+K_1$
$2NM_6$	$2N_2+M_2$
$2NMKS_6$	$2N_2+M_2+K_2-S_2$
$2MN_6$	$2M_2+N_2$
$2MNKS_6$	$2M_2+N_2+K_2-S_2$
MSN_6	$M_2+S_2+N_2$
MKN_6	$M_2+K_2+N_2$
$2MS_6$	$2M_2+S_2$
$2MK_6$	$2M_2+K_2$
NSK_6	$N_2+S_2+K_2$
$2MSO_7$	$2M_2+S_2+O_1$
$MSKO_7$	$M_2+S_2+K_2+O_1$
$2(MN)_8$	$2M_2+2N_2$
$3MN_8$	$3M_2+N_2$
$3MNKS_8$	$3M_2+N_2+K_2-S_2$
$2MSN_8$	$2M_2+S_2+N_2$
$2MNK_8$	$2M_2+N_2+K_2$
$3MS_8$	$3M_2+S_2$
$3MK_8$	$3M_2+K_2$
$MSNK_8$	$M_2+S_2+N_2+K_2$
$2(MS)_8$	$2M_2+2S_2$
$2MSK_8$	$2M_2+S_2+K_2$
$2M2NK_9$	$2M_2+2N_2+K_1$
$4MN_{10}$	$4M_2+N_2$
$3MNS_{10}$	$3M_2+N_2+S_2$
$4MNS_{12}$	$4M_2+N_2+S_2$
$5MS_{12}$	$5M_2+S_2$
$3MNK_{12}$	$3M_2+N_2+K_2+S_2$
$4M2S_{12}$	$4M_2+2S_2$

(Zetler and Cummings, 1967)